A SYSTEMATIC STUDY OF MATRIX ACIDIZING TREATMENTS USING SKIN MONITORING METHOD

A Thesis

by

NIMISH DINESH PANDYA

Submitted to the Office of Graduate Studies of
Texas A&M University
in partial fulfillment of the requirements for the degree of

MASTER OF SCIENCE

May 2012

Major Subject: Petroleum Engineering

A Systematic Study of Matrix Acidizing Treatments

Using Skin Monitoring Method

A SYSTEMATIC STUDY OF MATRIX ACIDIZING TREATMENTS USING SKIN MONITORING METHOD

A Thesis

by

NIMISH DINESH PANDYA

Submitted to the Office of Graduate Studies of
Texas A&M University
in partial fulfillment of the requirements for the degree of

MASTER OF SCIENCE

Approved by:

Chair of Committee,	Ding Zhu
Committee Members,	A. Daniel Hill
	Yuefeng Sun
Head of Department,	Stephen A. Holditch

May 2012

Major Subject: Petroleum Engineering

ABSTRACT

A Systematic Study of Matrix Acidizing Treatments Using Skin Monitoring Method.

Nimish Dinesh Pandya, B.S., Georgia Institute of Technology

Chair of Advisory Committee: Dr. Ding Zhu

The goal of this work was to evaluate matrix acidizing treatments of vertical and horizontal wells in carbonate reservoirs. Twenty field cases for acidizing treatments were analyzed by evaluating the skin factor evolution from on-site rate/pressure data during the treatment.

A skin monitoring method based on the concept of inverse injectivity (Hill and Zhu, 1996) was used to calculate the skin factor evolution. Viscous diversion techniques were analyzed by using the viscous diversion skin model that accounts for viscosity contrast between the reservoir fluid and the injected fluid. The estimated skin evolution during the treatment was validated using the post-treatment well performance.

From the post-treatment analysis, it was observed that emulsified acid was not an efficient viscous diverter because only 27% of the wells treated with emulsified acid showed evidence of viscous diversion. Therefore, other viscous diversion techniques are needed to ensure uniform acid coverage. In addition, treatments that involved diversion techniques such as foam, associative-polymers, and viscoelastic surfactants were also evaluated. Thus, the post-treatment evaluation was used to improve and optimize the

acid treatment designs. This study was beneficial to diagnose if excess acid volumes were used, or effective diversion was achieved during the acid treatment.

DEDICATION

I dedicate this work to:

My mother for giving me strength and conviction to believe in myself.

My father for inspiring me and being proud of me.

My sister for worrying and caring for me, her little brother.

ACKNOWLEDGMENTS

I would like to thank my advisors Dr. A. Daniel Hill and Dr. Ding Zhu who guided me throughout the course of this research. I am also greatly indebted to them for always being kind and patient with me, especially during difficult times.

Lastly, I would like to thank my colleagues and friends for making me part of their lives and sharing memorable experiences with me at Texas A&M University.

NOMENCLATURE

b	intercept of linear function between flow rate, pressure and time
B	formation volume factor
c_t	total compressibility of reservoir
h_s	coordinate of wellbore location in z-direction
h_x	length of the flow field modeled
h_z	height of the flow field modeled
k_x	permeability in x-direction
k_y	permeability in y-direction
k_z	permeability in z-direction
L_w	length of horizontal well
L_{xd}	left coordinate of wellbore in x-direction
L_{xl}	right coordinate of wellbore in x-direction
m	slope of linear function between flow rate, pressure and time
p_{wf}	bottom flowing pressure
p_i	reservoir pressure
q	flow rate
r_w	wellbore radius
$r_{w'}$	equivalent wellbore radius
s	skin factor
t_D	dimensionless time

Δt_{sup} superposition time function

Φ porosity of formation

μ viscosity of fluid

TABLE OF CONTENTS

Page

Page

LIST OF FIGURES

Page

Page

LIST OF TABLES

Page

1. INTRODUCTION

1.1 Real-Time Skin Monitoring

Matrix acidizing treatment is a complex process involving injection of acid below formation breakdown pressure to remove near wellbore damage. The skin factor value is a quantitative measure of the near wellbore conditions. A positive skin factor is an indication of formation damage, and the objective of the stimulation process is to end the treatment with a negative (or near zero) skin factor.

In order to evaluate the effectiveness of the acidizing treatments, several methods have been developed to monitor the evolution of skin factor. Following is the summary of three approaches which can be used to measure evolution of skin during matrix acidizing treatments.

1.1.1 Steady-State Approach

Paccaloni et al. (1988) introduced a method that used instantaneous pressure and rate to calculate skin factor continuously. This method is based on the concept of finite-radius "acid bank" and steady-state, radial Darcy's flow. Eq. 1 shows the relationship of injection tubing pressure, p_{ti} to injection rate, q_i which is utilized to measure the skin factor, s (Paccaloni et al., 1988),

---

This thesis follows the style of *SPE Journal.*

$$p_{ti} = p_e - p_h + p_{fr} + \frac{141.2 \cdot B \cdot \mu \cdot q_i \cdot \left(\ln \frac{r_b}{r_w} + s \right)}{k \cdot h} \quad \text{.....(1)}$$

In Eq. 1, p_e is the external reservoir pressure, p_h is the hydrostatic pressure, p_{fr} is the friction pressure drop, r_b is the finite-radius of "acid bank", and r_w is the well radius. Also, B, μ, and k are the formation volume factor, viscosity, and permeability respectively. To evaluate the evolving skin factor, Paccaloni constructed a graph of p_{ti} versus q_i with s as a parameter. The skin factor is calculated as

$$s = \frac{0.00708 \cdot k \cdot h \cdot \left[\left(p_w + p_h - p_{fr} \right) - p_e \right]}{B \cdot \mu \cdot q_i} - \ln \frac{r_b}{r_w}, \quad \text{.....(2)}$$

where all variables are in oil field units. **Fig. 1** illustrates skin evaluation for the field case using Paccoloni's method.

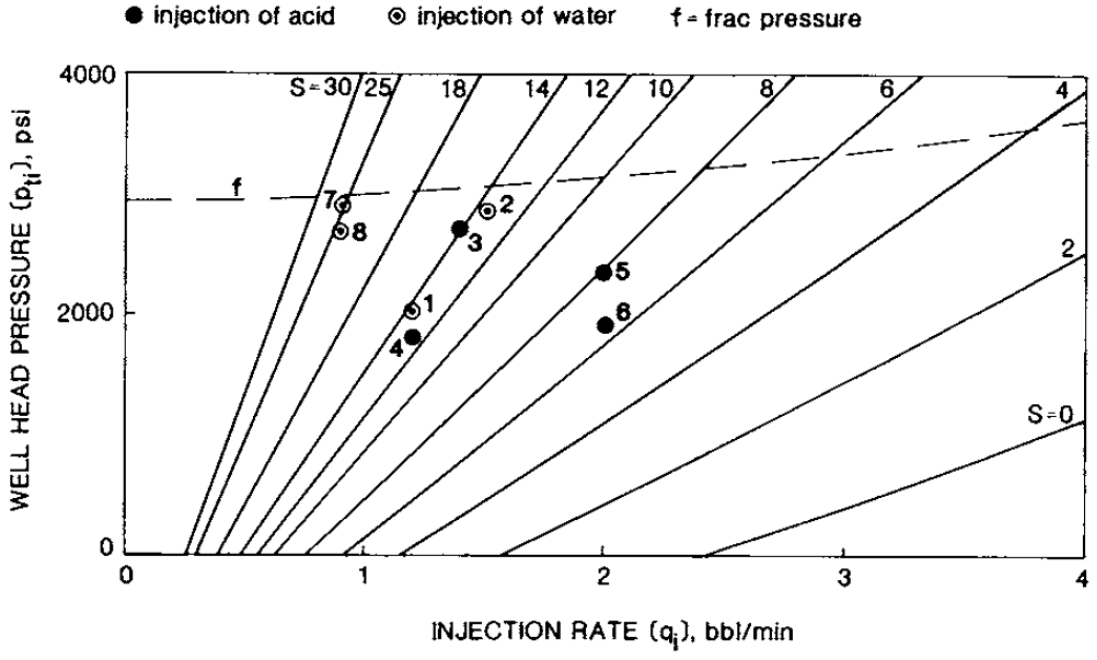

Fig. 1—Field case results (Paccaloni et al., 1988).

In Fig. 1, each point (1 to 8) on the plot represents pressure and rate measurement for an instant of time. The first four points (1 to 4) are for acid injection stage and the point 5 to 8 are for water injection stage. This plot for each treatment is constructed before the treatment. During injection, pressure and injection rate are measured, and marked on the plot to see the evolution of skin factor.

Fig. 1 shows that the skin factor reduced from 14 to 6 during acid injection. Therefore, the acid injection is successful in removing near-wellbore damage. However, the second stage of water injection worsened the damage as indicated by increase in the skin factor from 6 to 25.

1.1.2 Simulated vs. Measured Pressure

Another technique by Prouvost and Economides (1989) proposed to analyze skin evolution by continuous comparison of measured and simulated pressures. The technique requires simulation of the transient pressure response to the injection of inert fluids. The flow rates used for the inert fluids follow the exact injection schedule of the acid treatment. The difference between the actual bottomhole pressure, $p_{meas(t)}$ and simulated bottomhole pressure, $p_{sim(t)}$ is utilized to evaluate the changing skin factor. The skin factor is calculated as

$$s = \frac{k \cdot h \cdot \left(p_{meas(t)} - p_{sim(t)}\right)}{141.2 \cdot B \cdot \mu \cdot q_i}, \quad \text{.....(3)}$$

where s is the skin factor, q_i is the injection rate, B is the formation volume factor, and μ is the viscosity at time t. Fig. 2 illustrates skin evaluation using this method for the field case, where the injection rate of acid was approximately 1 bpm.

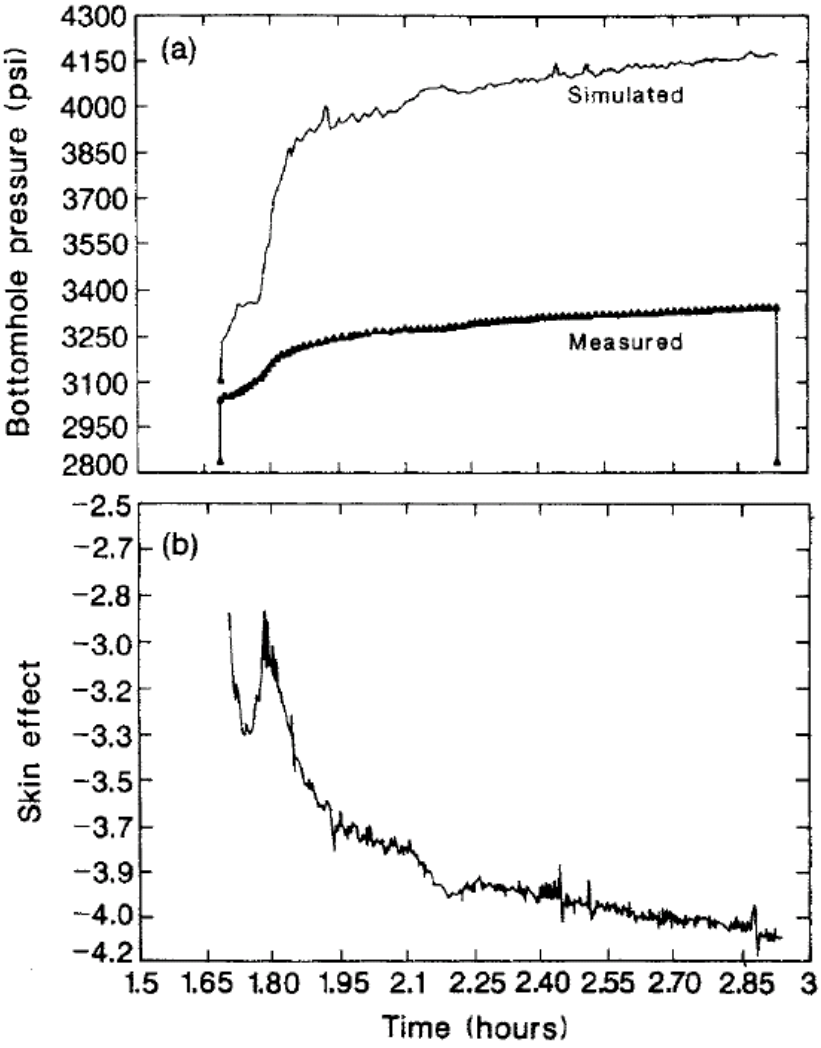

Fig. 2—Field case results (Prouvost and Economides, 1989).

In **Fig. 2,** the simulated pressure response was estimated for injection of an inert fluid. The difference in the simulated and measured pressure was used to calculate the evolving skin effects. Fig. 2 shows that the skin factor reduced from -3 to -4 during acid injection.

1.1.3 Inverse Injectivity Method

Hill and Zhu (1996) proposed a method based on the theory of standard injectivity test using approximate line source solution for transient flow to monitor changing skin during matrix acidizing treatment. The pressure response to multiple injection rates is given by

$$\frac{p_{wf} - p_i}{q_i} = m \cdot \Delta t_{\text{sup}} + b \quad \text{.....(4)}$$

where,

$$m = \frac{162.6 \cdot B \cdot \mu}{k \cdot h} \quad \text{.....(5)}$$

$$b = m \cdot \left[\log\left(\frac{k}{\phi \cdot \mu \cdot c_t \cdot r_w^2} \right) - 3.23 + 0.87 \cdot s \right] \quad \text{.....(6)}$$

$$\Delta t_{\text{sup}} = \sum_{j=1}^{N} \frac{q_j - q_{j-1}}{q_N} \cdot \log\left(t_N - t_{j-1}\right). \quad \text{.....(7)}$$

The slope, *m* (Eq. 5), remains constant as it is based on reservoir parameters that do not change during the acidizing treatment. On the other hand, the only parameter that changes in intercept, *b* (Eq. 6), is the skin factor, *s*. Furthermore, this approach employs a superposition method (Eq. 7 (Earlougher, 1977)) to account for the transient flow effects due to injection of acid at multiple rates and pressures.

Therefore, each point on the inverse injectivity ($\frac{p_{wf} - p_i}{q}$) vs. superposition time ($\Delta t_{\sup}$) plot will lie on a straight line having slope, m, with its intercept depending on the skin factor at time t (Hill and Zhu, 1996).

Using Eqs. 4 to 7, skin factor is calculated in real-time from measured pressure, injection rate, and time during the acid treatment from the equation given below

$$s = \frac{1}{0.868}\left(\frac{b}{m} - \log\left(\frac{k}{\phi \cdot \mu \cdot c_t \cdot r_w^2}\right) + 3.23\right). \quad \text{.....(8)}$$

Fig. 3 illustrates skin evaluation for the field case using the inverse injectivity method. Also, in Fig. 3, the skin factor evolution and the pressure/rate record from the treatment are plotted.

Fig. 3 shows that the skin factor reduced from 100 to 0 during acid injection. It is noticed that the stimulation from HCl pre-flush was more gradual and the most of the stimulation was contributed by the HF/HCl acid system. Thus, the difference between the two pressures yielded the instantaneous change in pressure drop arising from the near-wellbore damage.

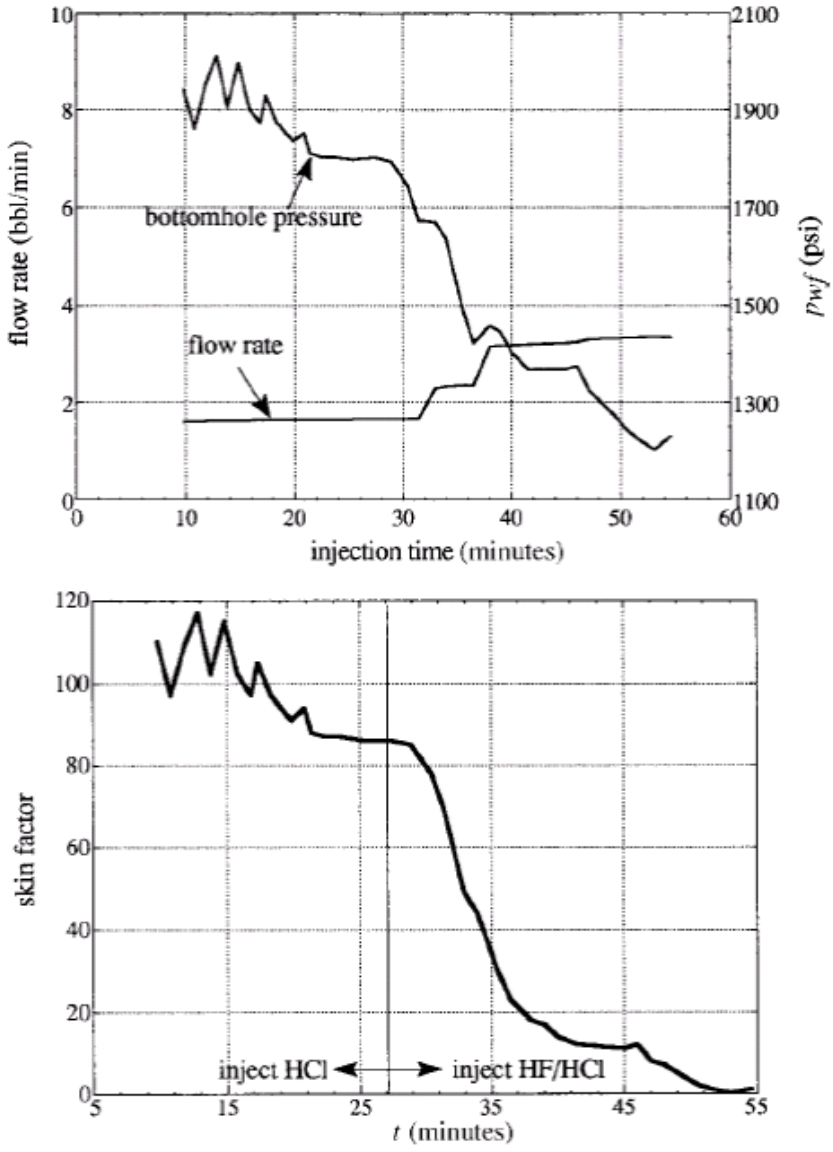

Fig. 3—Field case results (Zhu and Hill, 1998).

1.2 Acid Placement and Diversion

Acid placement is one of the most important concerns during matrix acidizing treatments. A successful treatment design consisting of proper selection of acid types, additives, and volumes may result in inefficient stimulation if the acid does not adequately cover the target interval. Insufficient acid coverage of long target zone or multiple intervals is mainly due to presence of heterogeneities such as presence of a thief zone (high permeability zone), different rock lithology, and varying formation fluid properties (Kalfayan and Martin, 2009).

Diversion techniques are used to ensure proper acid coverage along the target interval. Diversion within the formation may guide acid to the damaged target zone and prevent the acid to run away into high permeability zones. Following is the summary of some of the acid placement and diversion methods.

1.2.1 Coil-Tubing

Using coil-tubing strings is very common for fluid placement in matrix acidizing treatments. Eckerfield et al. (1998) presented a model for fluid placement in horizontal and inclined wells. The fluid placement model tracked multiple interfaces for multiple injections, and handled coil-tubing tail movement during injection. Eckerfield et al. (1998) found that movement of the coil-tubing generally has no effect upon the distribution of fluids to the formation.

Thomas et al. (1998) also conducted computer simulations and found that bullheading of HCl in carbonate reservoirs results in relatively poor acid coverage

compared to acid pumped using coil-tubing. Mitchell et al. (2003) evaluated 19 wells to show that the acid placement through coil-tubing is better than bullheading. **Fig. 4** shows a commonly used placement technique using coil-tubing for stimulation treatments.

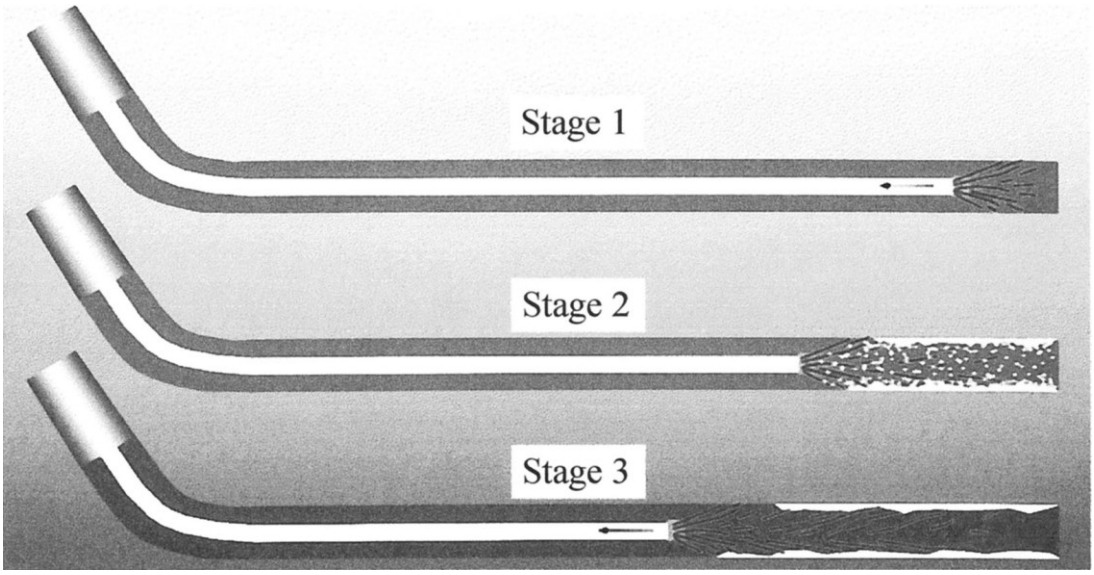

Fig. 4—Commonly used coil-tubing placement technique (Thomas et al., 1998)

Coil-tubing is the ideal placement technique for long horizontal wells because it can be used for selective zone treatment using reduced acid volumes. Although the small diameter of the coil-tubing leads to rate limitations and higher friction pressure, coil-tubing is preferred to pump foam diverter as the small diameter helps maintain the foam quality and increases the chances of achieving diversion. However, particulate diverters and ball sealers are not preferred to be placed using coil-tubing (Kalfayan and Martin, 2009).

1.2.2 Ball Sealers

Ball sealers are small rubber-coated or biopolymer balls that are pumped into the well with the acid system in order to temporary seal perforations. Therefore, this mechanical diversion technique is mainly used for cased and perforated wells.

Ball sealers diversion was first introduced to the oil and gas industry in 1956. Brown et al. (1963) researched on factors such as drag force, inertial force, and holding force affecting the performance of ball sealers. Erbstoesser (1980) later conducted laboratory experiments to find that buoyant ball sealers have higher seating efficiency compared to non-buoyant ball sealers. **Fig. 5** indicates the mechanism of buoyant and non-buoyant ball sealers.

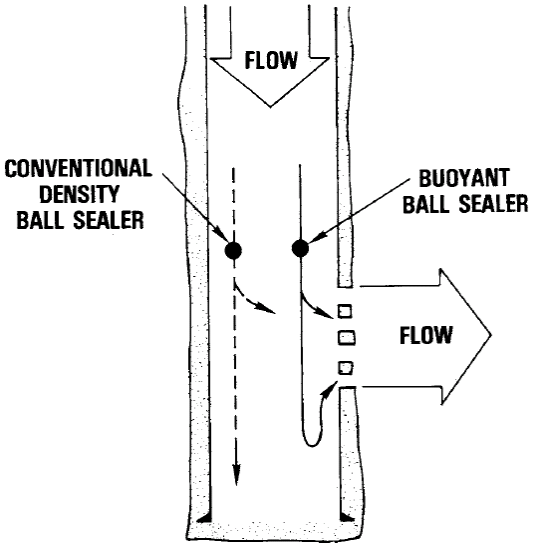

Fig. 5—Ball sealer diversion (Erbstoesser, 1980).

Bale (1984) presented the field case that showed buoyant ball sealers were successfully used as diverting agents in Saudi Arabia. Gabriel and Erbstoesser (1984) optimized the use of buoyant ball sealers by developing field-tested design methodology. Nozaki et al. (2011) showed that the ball sealer seating behavior is statistical in nature by analyzing experiments and one field case.

1.2.3 Foam

Foam diversion is achieved by pumping a gaseous-phase fluid (typically nitrogen) along with a liquid-phase acid during the matrix treatment. This technique is feasible because a two phase system has lower mobility compared to a single phase system in the porous media. Since the foam is created in the formation, it is an in-situ diversion method.

Smith et al. (1969) was the first to conduct laboratory and field tests to show that foam diversion could be applied to wells during acidizing treatments. Burman and Hall (1986) observed that lower quality (volumetric fraction of gas phase) foam yielded more efficient diversion. Thompson and Gdanski (1993) found that highest permeability contrast ratio to expect good foam diversion was about 10, and that diversion lasted longer for higher quality (typically 60% or higher) foams.

Hill and Rossen (1994) found that batch foam diversion followed by acid treatment is not as efficient as the continuous foam diversion. Zerhboub et al. (1994) presented that foam diversion applied should be optimized and adapted to the type of well and addition of surfactant in acid improved diversion. Kibodeaux et al. (1994)

conducted sensitivity study that indicated that foam quality and gas trapping followed by foam injection are the key factors in the success of the foam diversion process.

1.2.4 Viscosified Fluids

This chemical diversion method is based on the mechanism of viscous diversion. Viscous diversion is achieved when the mobility of fluid system decreases in the higher permeability zones due to presence of a bank of viscous fluid. The acid systems are viscosified by adding associative polymers or by creating emulsions (Hill and Rossen, 1994).

In emulsified acids, the internal phase consists of acid and the external phase is made of hydrocarbon (typically diesel). Emulsified acid system results in fluid diversion due to viscosity contrasts and improves acid coverage of the wellbore. The reaction rate of emulsified acid is two orders of magnitude lower than the plain acid. Therefore, the emulsified acid causes deeper acid penetration in the formation (Buijse and Domelen, 2000).

On the other hand, in-situ gelled acid systems are controlled by the pH of the cross-linking polymeric solutions. At low pH values, the acid system has low viscosity and thereby allows high injection rates. As the acid reacts, pH increases and activates the cross-linking polymers. As a result, the viscosity of the system increases leading to viscous diversion. The cross-linking reaction continues until the pH increases to a value which triggers the polymers to break and reduces the system's viscosity. Lynn and Nasr-El-Din (2001) compared emulsified acid and in-situ gelled acids. They found that in-situ gelled acids dissolved higher volume of rock per unit of injected acid. Gomaa et al.

(2010) conducted parallel-core experiments and presented that in-situ gelled acid worked better for low permeability contrast. Disadvantages of in-situ gelled acid are that may lead to precipitation of iron and also leave behind a residue of polymeric material (Lynn and Nasr-El-Din, 2001).

To overcome such shortcomings of polymer-based gelled acids, the viscoelastic surfactant system was introduced. As shown in **Fig. 6,** the mechanism of this system was based on formation of long rod-like micelles and the entanglement of these micelles leads to increase in viscosity of the spent acid (Nasr-El-Din et al., 2006).

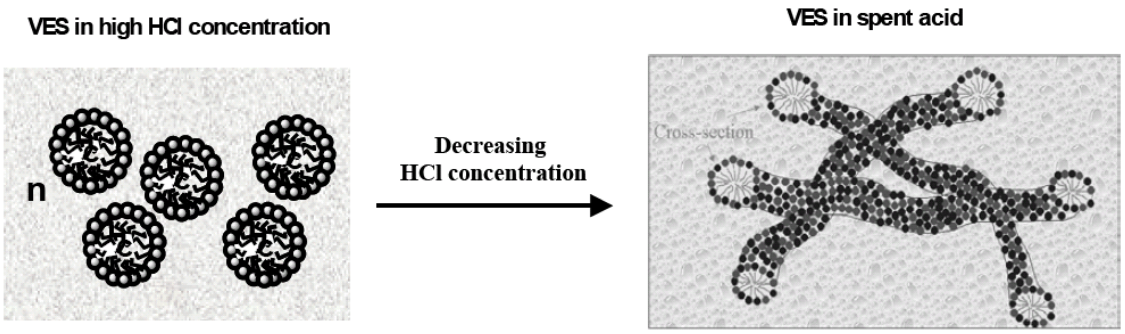

Fig. 6—Mechanism of viscoelastic surfactants (Taylor et al., 2003).

Lungwitz et al. (2007) observed that viscoelastic surfactant systems exhibited similar or better cleanup behavior than polymer based systems, especially in low pressure or depleted reservoirs.

1.3 Statement of Purpose

The objective of this research work is to measure the effectiveness of the acidizing treatment by calculating skin factor evolution. This project involves post-treatment analysis of matrix acidizing treatments in carbonate reservoir. These acid jobs consist of both horizontal and vertical wells. The acid jobs are analyzed by;

1. Validating the trend in the skin evolution during the acid treatment using the well production before and after stimulation.
2. Evaluating the volume of acid that effectively treated the near wellbore damage.
3. Measuring the efficiency of viscous diverters by understanding the effect of each injected fluid.

2. PROCEDURE AND METHODOLOGY

In this section, the approach to achieve the objective of the research is discussed. A skin monitoring method is developed based the concept of inverse injectivity. The aim of the methodology is to analyze skin evolution during acid treatments in both vertical and horizontal wells.

Also, operational concerns such as bottomhole pressure calculations and viscous diversion skin effects are addressed in this approach. The bottomhole pressure is estimated from measured surface pressure on the tubing or the annulus. And, the viscous diversion is modeled by increasing flow resistance in the region affected due to the presence of a bank of viscous fluid. This study conducts the post-treatment skin analysis using the following data;

1. Reservoir properties such as reservoir pressure, permeability, porosity, formation volume factor, viscosity of reservoir fluids, and formation thickness.
2. Wellbore geometry and tubing properties such as total vertical depth (TVD), measured depth (MD), horizontal length (HL), tubing diameter, and roughness.
3. Injection schedule including volume, density, and viscosity of each of the fluids pumped during the treatment.
4. Measured pressure and injection rate at recorded time period.

2.1 Real-Time Skin Monitoring Model

The concept of inverse injectivity is applied to calculate skin evolution using measured rate/pressure data during the matrix acidizing treatment. Several field results for real-time skin monitoring in vertical wells have been presented for the inverse injectivity model (D. Zhu et al., 1999; Zhu and Hill, 1998).

This concept was further extended to horizontal wells (Zhu et al., 1999). The formation contact area is much longer, and acid distribution inside the wellbore is more complex for horizontal wells (Eckerfield et al., 1998). The horizontal well skin model consists of an infinite-conductivity horizontal well located in a semi-infinite homogeneous and anisotropic reservoir of uniform thickness and width (Goode and Thambynayagam, 1987).

Although the analytical solution of the model is more complex, this model makes fewer assumptions in estimating continuous skin factor evolution. **Fig. 7** indicates the schematic of the system for the horizontal skin model.

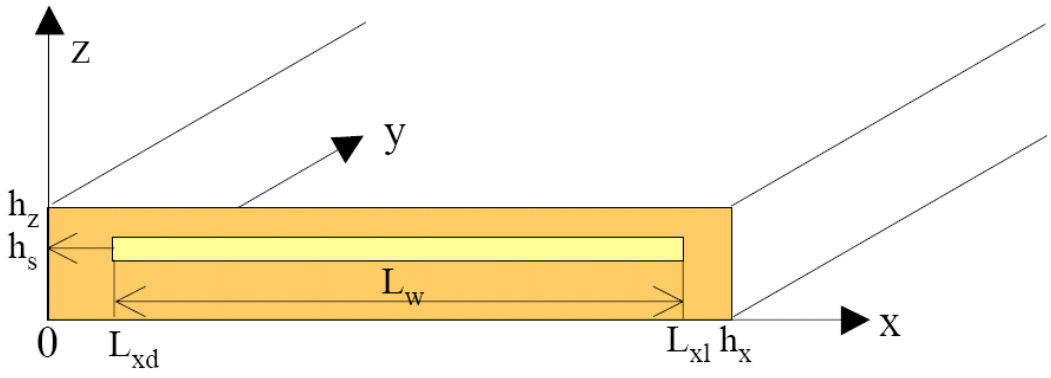

Fig. 7—Schematic for the horizontal well skin model (Zhu et al., 1999).

As seen in Fig. 7, the system consists of a horizontal wellbore that is bounded in x-direction and z-direction. However, the system is not bounded in the y-direction. Therefore, Goode and Thambynayagam, (1987) referred to this model as the semi-infinite slab model.

As discussed in the previous section, the general form of the inverse injectivity equation is given by Eq. 4, which also applies to the horizontal well model. However, the slope, the superposition time function, and the intercept in the equation are defined as following:

$$m = \frac{282.4\mu B r_w'}{h_x h_z k_y}, \quad \text{.....(9)}$$

$$\Delta t_{\sup} = \sum_{j=1}^{N} \frac{q_j - q_{j-1}}{q_N} \sqrt{\pi\left(t_{D,N} - t_{D,j-1}\right)}, \text{ and .....(10)}$$

$$b = m \frac{h_x^2}{\pi^2 v_x} \sum_{j=1}^{N} \frac{q_j - q_{j-1}}{q_N} \Pi + m \frac{hxh_z}{L_w v_z \pi} \sum_{j=1}^{N} \frac{q_j - q_{j-1}}{q_N} \Gamma + \frac{141.2 B\mu}{\sqrt{k_y k_z} L_w} s . \quad \text{.....(11)}$$

In the above equations, the geometry functions and dimensionless groups are (Goode and Thambynayagam, 1987)

$$\Pi = \sum_{n=1}^{\infty} \left[\frac{1}{n} erf\left(v_x \pi n \sqrt{t_D - t_{D,j-1}}\right) \Xi_n^2 \right], \quad \text{.....(12)}$$

$$\Gamma = \sum_{l=1}^{\infty} \left[\frac{1}{m} erf\left(v_z \pi l \sqrt{t_D - t_{D,j-1}}\right) \Xi_l \cos\left(l \pi z_e\right) \right], \quad \text{.....(13)}$$

$$\Xi_n = \frac{1}{nL_w}\left[\sin\left(\frac{n\pi L_{xl}}{h_x}\right) - \sin\left(\frac{n\pi L_{xd}}{h_x}\right)\right], \quad \text{.....(14)}$$

$$\Xi_l = \frac{1}{4lr_w'}\left[\sin\left(\frac{l\pi}{h_z}\left(h_s + 2r_w'\right)\right) - \sin\left(\frac{l\pi}{h_z}\left(h_s - 2r_w'\right)\right)\right], \quad \text{.....(15)}$$

$$z_e = \frac{1}{h_z}\left(h_s + 1.47r_w'\right), \quad \text{.....(16)}$$

$$t_D = \frac{0.000264k_y t}{\phi\mu c_t r_w'}, \quad \text{.....(17)}$$

$$v_x = \frac{r_w'}{h_x}\sqrt{\frac{k_x}{k_y}}, \quad \text{.....(18)}$$

$$v_z = \frac{r_w'}{h_z}\sqrt{\frac{k_z}{k_y}}, \quad \text{.....(19)}$$

$$L_w = \left(L_{xl} - L_{xd}\right), \text{ and} \quad \text{.....(20)}$$

$$r_w' = r_w\left(\frac{k_z}{k_y}\right)^{1/4}. \quad \text{.....(21)}$$

For the above equations, the infinite summation terms are approximated by the first 40 terms for a stable result. The drawback of this skin model is that it does not consider the effect of reservoir heterogeneity. The variation in permeability and skin along the horizontal wellbore is interpreted using three constant values of permeability (k_x, k_y, and k_z) and one skin value. Thus, the horizontal skin model provides a global estimate of skin evolution and will not provide the skin profile along the horizontal length of the wellbore.

2.2 Bottomhole Pressure Calculation

In order to use the concept of inverse injectivity, it is required to calculate bottomhole pressure. In most acid treatments, the bottomhole pressure is not measured and only the surface pressure is recorded at the injection tubing or the annulus. **Fig. 8** shows the schematic of the system for the calculation of bottomhole pressure.

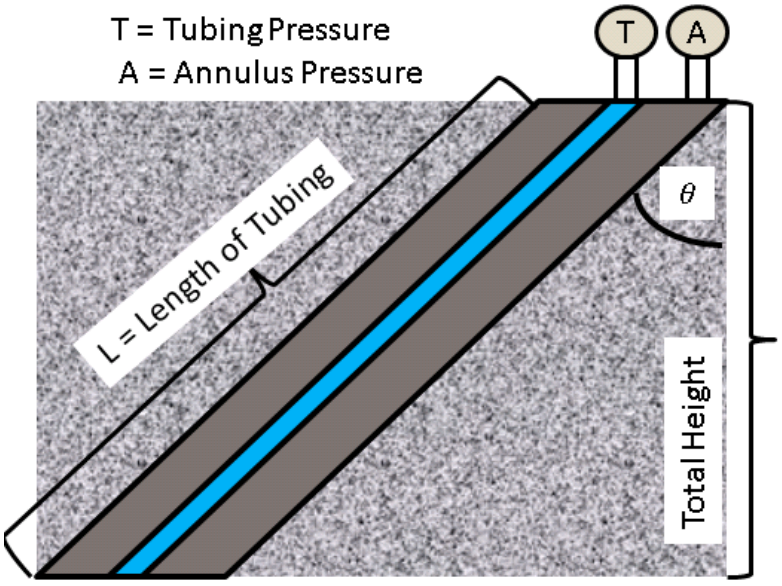

Fig. 8—Schematic of the system for the bottomhole pressure calculation.

The surface pressure can be converted to the bottomhole pressure by

$$p_{wf} = p_{sf} + \Delta p_{PE} - \Delta p_f , \quad \text{.....(22)}$$

where p_{sf} is the surface pressure, p_{wf} is the bottomhole flowing pressure, Δp_{PE} is the hydrostatic pressure drop, and Δp_f is the frictional pressure drop. In case the surface

pressure is measured in the annulus of the well, the frictional pressure drop is zero and only hydrostatic pressure drop is used to calculate the bottomhole pressure.

For single phase liquid, the hydrostatic pressure drop depends only on the density of the fluid and the height of the fluid column. Therefore, the hydrostatic pressure drop changes when a fluid with different density is injected into the tubing. The hydrostatic pressure drop can be calculated by

$$\Delta p_{PE} = \frac{g \cdot \cos\theta}{g_c \cdot A} \sum_{i=1}^{N} \left[\rho_i \left(V_i - q \cdot \Delta t_{new}\right)\right], \quad \text{.....(23)}$$

where A is the cross-sectional area of the tubing, q is the injection rate, θ is the average inclination of the tubing, ρ_{i-1} is the density of the fluid in the tubing, ρ_i is the density of the fluid being pumped, Vi is the cumulative injected volume of the i-th fluid, L is the height of fluid of the tubing, and Δt_{new} is the time increment after start of pumping the new fluid.

Similarly, the frictional pressure drop depends on the injection rate, fluid density, and fluid viscosity, which may vary during an acid treatment. The friction pressure drop is determined from the Fanning equation,

$$\Delta P_f = \frac{2 \cdot f_f \cdot \rho \cdot \left(\frac{q}{A}\right)^2 \cdot L}{g_c \cdot D}, \quad \text{.....(24)}$$

where f_f is the Fanning friction factor, A is the cross-sectional area of the tubing, q is the injection rate, D is the diameter of the tubing, ρ is the density of the fluid, and L is the length of the tubing. In the above equation, the Fanning friction factor depends on the Reynolds number and is explicitly calculated by (Chen, 1979)

$$\frac{1}{f_f} = \frac{16}{N_{RE}} \text{ if } N_{RE} < 2000\text{, or} \quad \ldots\ldots(25)$$

$$\frac{1}{\sqrt{f_f}} = -4\log\left\{\frac{\varepsilon}{3.7065} - \frac{5.0452}{N_{RE}}\log\left[\frac{\varepsilon^{1.1098}}{2.8257} + \left(\frac{7.149}{N_{RE}}\right)^{0.8981}\right]\right\}. \quad \ldots\ldots(26)$$

2.3 Viscous Diversion Skin Model

Hill and Rossen (1994) developed the viscous diversion skin model with the assumption of piston like displacement between fluid banks in the reservoir. Field results for this viscous diversion model in gas reservoir have been presented previously (Fadele et al., 2000; Zhu et al., 1998). Later, Nozaki and Hill (2009) developed a skin model which considered mobility difference between acid and gas and also accounted for damage and wormhole length.

As seen in **Fig. 9,** the viscous diversion model keeps track of the locations of injected fluid banks to account for the viscous skin effect. The viscous skin effect caused by the difference between the viscosities of the fluid banks can be calculated by

$$s_{vis} = \sum_{i=1}^{n} \frac{\mu_i}{\mu_{res}} \ln\left(\frac{r_i}{r_{i-1}}\right) - \ln\left(\frac{r_n}{r_0}\right), \quad \ldots\ldots(27)$$

where s_{vis} is the viscous skin factor, μ_i is the viscosity of the i-th fluid bank, μ_{res} is the viscosity of the reservoir fluid, r_i is the radius of penetration of the i-th fluid bank, and r_0 is the radius of wellbore.

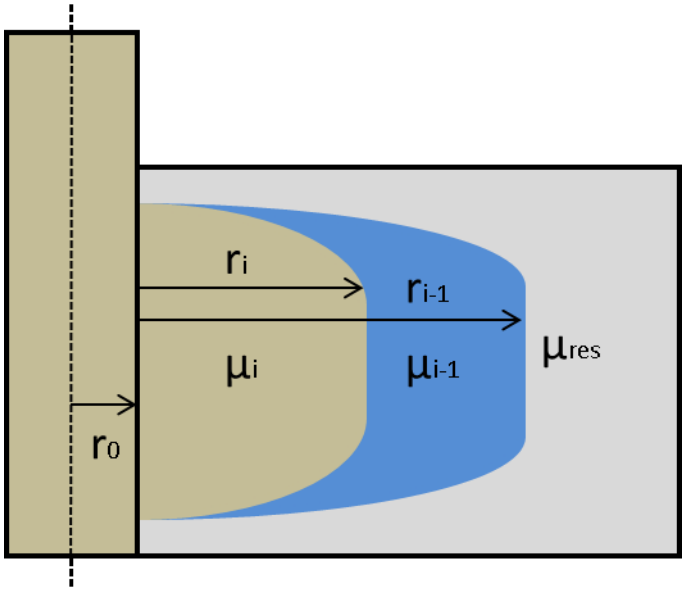

Fig. 9—Schematic of injected fluid banks.

In Eq. 28, the radius of penetration of the i-th fluid bank depends on *Vi*, volume of the i-th fluid injected by

$$r_i = \sqrt{\frac{V_i}{\pi \cdot \phi \cdot h} + r_w^{\,2}} \quad \text{.....(28)}$$

where Φ is the porosity and h is the height of the formation.

Lastly, the damaged skin factor is estimated by subtracting the viscous skin factor from the global (apparent) skin factor from the inverse injectivity model. Thus, the equation for the evolution of the damage skin factor is

$$s_{damage} = s_{apparent} - s_{viscous}. \quad \text{.....(29)}$$

2.4 Skin Calculation Procedure

This section presents the procedure to calculate skin factor as a function of injection time by continuous monitoring of injection rates and pressures;

1. Calculate slope, *m*, using Eq. 5 for vertical wells or Eq. 9 for horizontal wells. The slope, *m*, is constant and depends only on the reservoir parameters such as formation volume factor, permeability, and viscosity of the reservoir fluid.
2. From the measured pressure and injection rate at a desired time interval, calculate superposition time using Eq. 7 for vertical wells or Eq. 10 for horizontal wells.
3. Calculate interception, *b*, using Eq. 4 with the superposition time function.
4. Calculate skin factor using Eq. 8.

3. RESULTS AND DISCUSSION

In this section, the post-treatment analysis using the skin monitoring program for field cases are discussed. In acid treatment analysis, the skin factor is defined for three important time periods: 1) the initial skin factor, 2) the skin evolution during the stimulation process, and 3) the final skin value at the end of the stimulation. Since the actual value of skin factor contains uncertainties, the change in the skin trend during the skin evolution is more important than the absolute value of the skin factor in the evaluation of acid treatments.

The final skin value at the end of the stimulation is an indication of success or failure of the treatment. The initial skin and the final skin can be used to determine the productivity index ratio before and after the treatment. For vertical wells, the productivity index ratio is given by

$$\frac{J_{final}}{J_{initial}} = \frac{\ln\left(\frac{r_e}{r_w}\right) + s_{initial}}{\ln\left(\frac{r_e}{r_w}\right) + s_{final}}, \quad \text{.....(30)}$$

and for horizontal wells, the productivity index ratio is given by

$$\frac{J_{final}}{J_{initial}} = \frac{\ln\left[\frac{hI_{ani}}{r_w(I_{ani}+1)}\right] + \frac{\pi y_b}{hI_{ani}} - 1.224 + s_{initial}}{\ln\left[\frac{hI_{ani}}{r_w(I_{ani}+1)}\right] + \frac{\pi y_b}{hI_{ani}} - 1.224 + s_{final}}, \quad \text{.....(31)}$$

where r_w is the wellbore radius, h is the formation thickness, I_{ani} is the anisotropy ratio,

r_e is the drainage radius of the constant-pressure boundary, and y_b is the drainage length perpendicular to the well in the parrellpiped reservoir (Furui et al., 2002).

These field cases discussed in this section consist of acidizing treatments in both horizontal and vertical wells for carbonate reservoirs in the Middle East. The design for the acidizing treatments consisted of single and multiple stage injection. The two acid systems that were used for the wells were hydrochloric acid and emulsified acid. The acid design for some cases included chemical diverters such as associative-polymer solution, viscoelastic surfactants, and foam.

The cases are discussed in three parts: 1) the treatment description, 2) the skin monitoring results, and 3) the discussion of results. The treatment evaluation helps understand the behavior of each of injected fluids and determine their contribution to the overall skin factor.

3.1 Case 1: Single-Stage Hydrochloric Acid Treatment

3.1.1 Treatment Description

This well is a horizontal well with an open-hole lateral, as seen in **Fig. 10.** The actual acidizing treatment design comprised of treating the target interval with 15% hydrochloric acid (HCl) using coil-tubing.

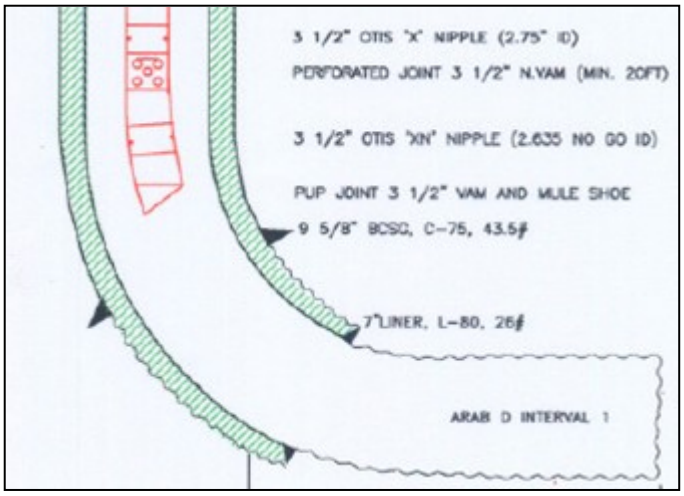

Fig. 10—Well diagram for Case 1.

The data for the reservoir, the wellbore, and the acid injection is shown in **Tables 1 through 3.**

Table 1—Reservoir Properties for Case 1

Initial Reservoir Pressure, psi	2800
Formation Volume Factor	1.397
Porosity	0.17
Total Compressibility, 1/psi	3.50E-06
Formation Thickness, ft	30
Reservoir Fluid Viscosity, cp	0.51
Permeability, md	5.5
k_V/k_H	0.1

Table 2—Wellbore Properties for Case 1

Wellbore Radius, in	3.5
Tubing Diameter, in	1.68
Relative Roughness	0.0001
Vertical Depth, ft	7768
Measured Depth, ft	13934
Horizontal Length, ft	2154
Annulus Fluid Density, lbm/ft3	62.42
Well Fluid Viscosity, cp	0.51

Table 3—Acid Injection Schedule for Case 1

Fluid Name	Volume Used, gal	Density, lb/ft3	Viscosity, cp
HCl	73118	67.11	0.51
Water	1991	62.42	0.51

3.1.2 Skin Monitoring Results

The surface pressure and injection rate data was measured on-site during the acid job. **Fig. 11** plots the measured injection rate, and the measured surface pressure recorded during the acidizing treatment.

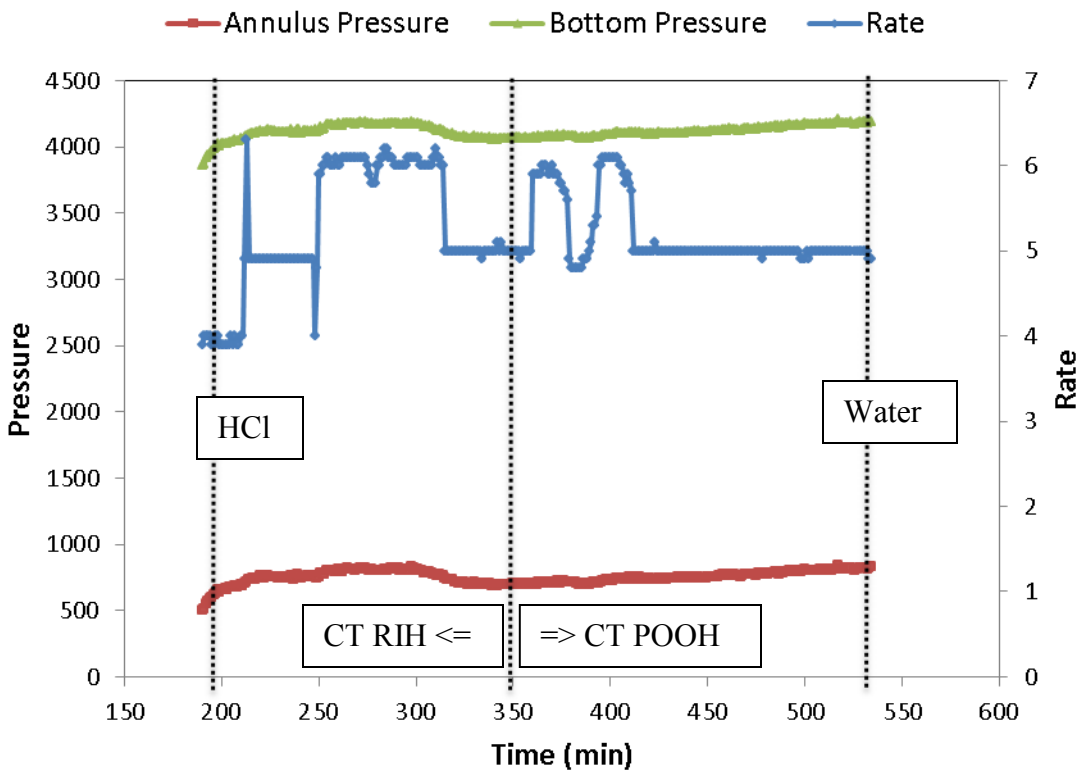

Fig. 11—Treatment data for Case 1.

In Fig. 11, the bottomhole pressure was calculated from the annulus pressure. From the calculated bottomhole pressure and measured injection rate, the skin was calculated at each time step. The skin evolution during the acid job is shown in **Fig. 12.**

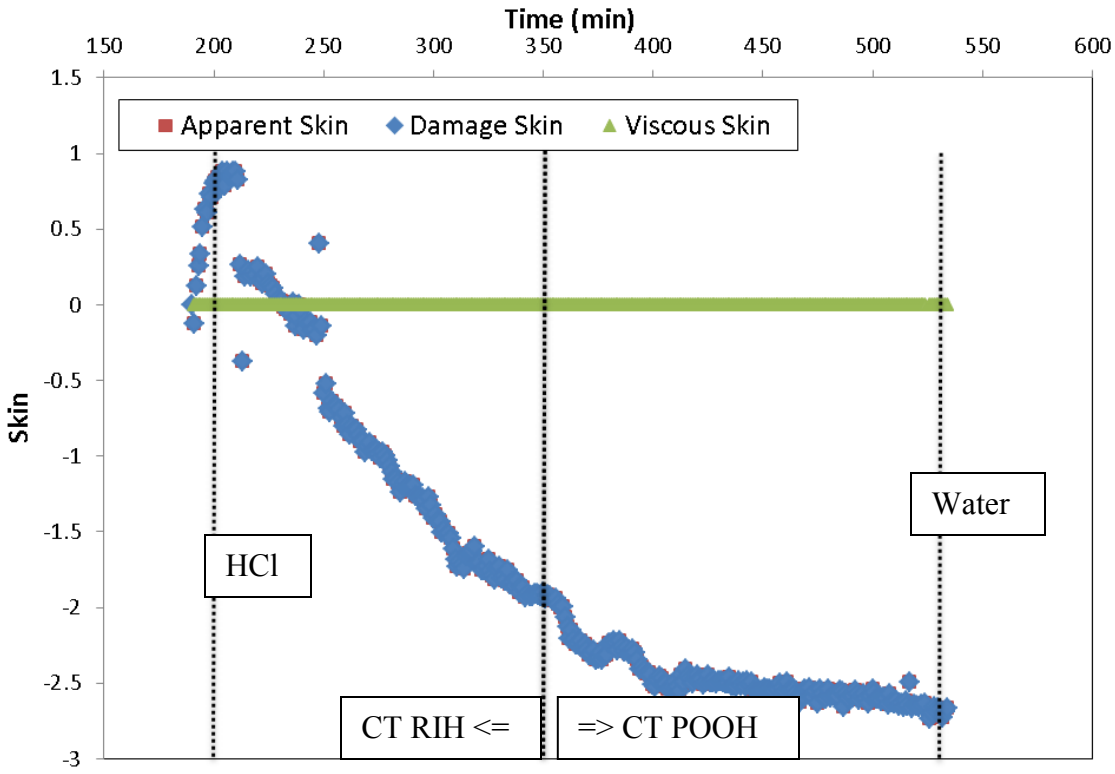

Fig. 12—Skin evolution for Case 1.

3.1.3 Discussion of Results

In Fig. 12, the skin begins to decrease when the acid front enters into the formation, and the skin value decreases from 0 to -2.6 by the end of acid injection. The skin declines for about 220 minutes during acid injection. During the last 100 minutes of acid injection, the skin decreases slightly. This trend indicates that the acid injection was successful in the removal of formation damage. Since the skin continues to decline until the end of the injection, sufficient volume of acid is injected.

Using Eq. 32, the productivity index ratio from the initial and final skin value was estimated as

$$\frac{J_{final}}{J_{initial}} = \frac{\ln\left[\frac{30\times 3.162}{0.258\times(3.162+1)}\right]+\frac{\pi\times 440}{30\times 3.162}-1.224+1}{\ln\left[\frac{30\times 3.162}{0.258\times(3.162+1)}\right]+\frac{\pi\times 440}{30\times 3.162}-1.224-2.5} = 1.23, \quad \text{.....(32)}$$

assuming the drainage length (y_b) of 440 ft. The skin trend was validated using the production test from before and after the stimulation process. In this case, the production rate of liquids from this well after stimulation increased from 2062 barrels/day to 2536 barrels/day. Therefore, the production test confirms the decreasing skin trend.

3.2 Case 2: Single-Stage Emulsified Acid Treatment

3.2.1 Treatment Description

This well is a horizontal well with a cased and perforated completion, as seen in **Fig. 13.** The actual acidizing treatment design comprised of bullheading 22% carbonate emulsion acid (CEA).

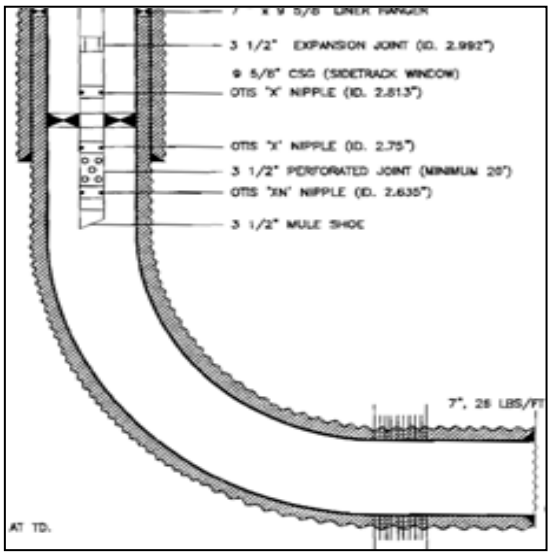

Fig. 13—Well diagram for Case 2.

The data for the reservoir, the wellbore, and the acid injection is shown in **Tables 4 through 6.**

Table 4—Reservoir Properties for Case 2

Initial Reservoir Pressure, psi	2500
Formation Volume Factor	1.35
Porosity	0.12
Total Compressibility, 1/psi	3.50E-06
Formation Thickness, ft	307
Reservoir Fluid Viscosity, cp	0.46
Permeability, md	10
k_V/k_H	0.1

Table 5—Wellbore Properties for Case 2

Wellbore Radius, in	3.092
Tubing Diameter, in	2.992
Relative Roughness	0.0001
Vertical Depth, ft	7560
Measured Depth, ft	9920
Horizontal Length, ft	1796
Well Fluid Density, lbm/ft3	63.58
Well Fluid Viscosity, cp	0.46

Table 6—Acid Injection Schedule for Case 2

Fluid Name	Volume Used, gal	Density, lb/ft3	Viscosity, cp	Friction Reducer
CEA	27007	63.58	0.46	1

3.2.2 Skin Monitoring Results

The surface pressure and injection rate data was measured on-site during the acid job. **Fig. 14** plots the measured injection rate, and the measured surface pressure recorded during the acidizing treatment.

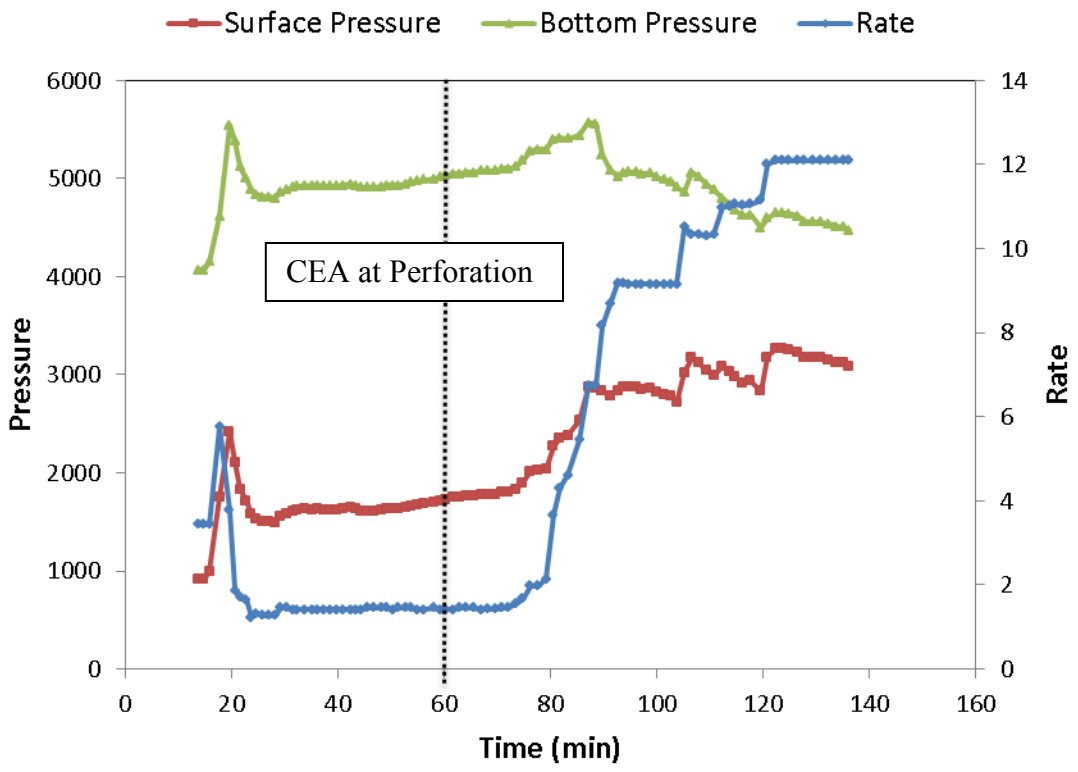

Fig. 14—Treatment data for Case 2.

In Fig. 14, the bottomhole pressure was calculated from the surface pressure. From the calculated bottomhole pressure and measured injection rate, the skin was calculated at each time step. The skin evolution during the acid job is shown in **Fig. 15.**

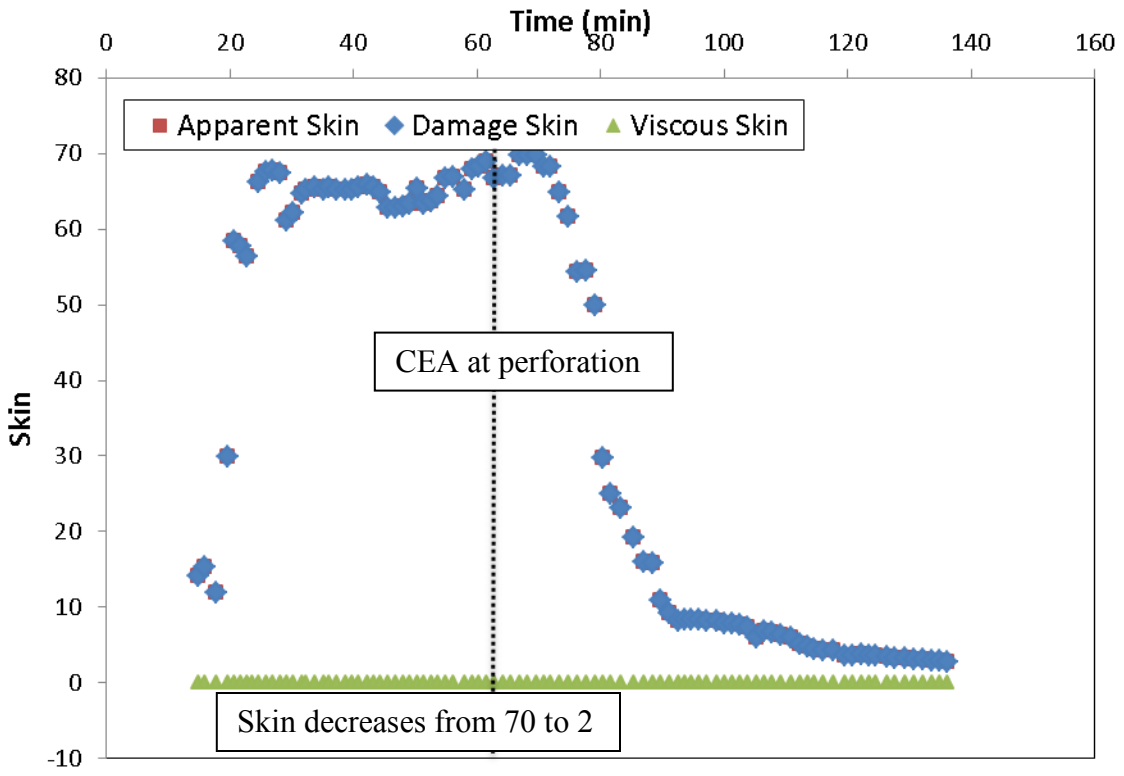

Fig. 15—Skin evolution for Case 2.

3.2.3 Discussion of Results

In Fig. 15, the skin begins to decrease when the acid front enters into the formation, and the skin value decreases from 70 to 2 by the end of acid injection. It is inferred that the volume of acid injected was sufficient as the skin continues to decrease until the end of the injection. However, the skin drops more rapidly initially compared to the later part of the treatment. This rapid decline in skin may be due to high permeability thief zone. The emulsified acid did not show any evidence of viscous diversion because no increasing trend in the skin is noticed.

The productivity index ratio from the initial and final skin value was estimated to be 6, assuming the drainage length (y_b) of 1850 ft. The skin trend was validated using the production test from before and after the stimulation process. In this case, the production rate of liquids from this well after stimulation increased from 805 barrels/day to 4754 barrels/day. Therefore, the production test confirms the decreasing skin trend and it is clear that the acidizing treatment was successful in significantly reducing the near wellbore damage.

3.3 Case 3: Multi-Stage Emulsified Acid and VES Treatment

3.3.1 Treatment Description

This well is a horizontal well with a cased and perforated completion, as seen below in **Fig. 16.** The actual acidizing treatment design comprised of 15% HCl treatment followed by two stages of 2% viscoelastic surfactant (VES), and 22% carbonate emulsion acid (CEA) each.

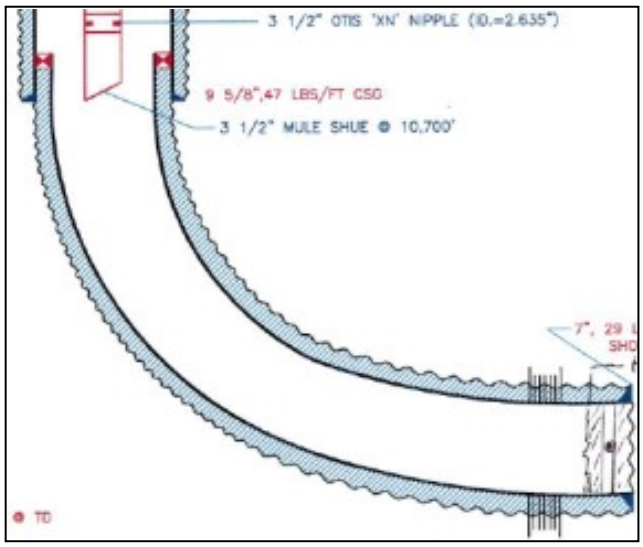

Fig. 16—Well diagram for Case 3.

The data for the reservoir, the wellbore, and the acid injection is shown in **Tables 7 through 9.**

Table 7—Reservoir Properties for Case 3

Initial Reservoir Pressure, psi	2500
Formation Volume Factor	1.397
Porosity	0.22
Total Compressibility, 1/psi	3.50E-06
Formation Thickness, ft	50
Reservoir Fluid Viscosity, cp	0.51
Permeability, md	1
k_V/k_H	0.1

Table 8—Wellbore Properties for Case 3

Wellbore Radius, in	3.5
Tubing Diameter, in	1.5
Relative Roughness	0.0001
Vertical Depth, ft	7737
Measured Depth, ft	14075
Horizontal Length, ft	3179
Well Fluid Density, lbm/ft3	59.84
Well Fluid Viscosity, cp	0.51

Table 9—Acid Injection Schedule for Case 3

Stage	Fluid Name	Volume Used, gal	Density, lb/ft3	Viscosity, cp	Friction Reducer
1	HCl	4416	65.82	1	0.1
2	VES	1598	63.58	1	0.1
3	Water	127	63.58	1	0.1
4	CEA	3244	63.58	3	0.1
5	Water	126	62.83	1	0.1
6	VES	810	63.58	1	0.1
7	Water	127	62.98	1	0.1
8	CEA	5198	63.58	3	0.1
9	Water	4201	62.83	1	0.1

3.3.2 Skin Monitoring Results

Fig. 17 plots the measured injection rate, and the measured surface pressure recorded during the acidizing treatment.

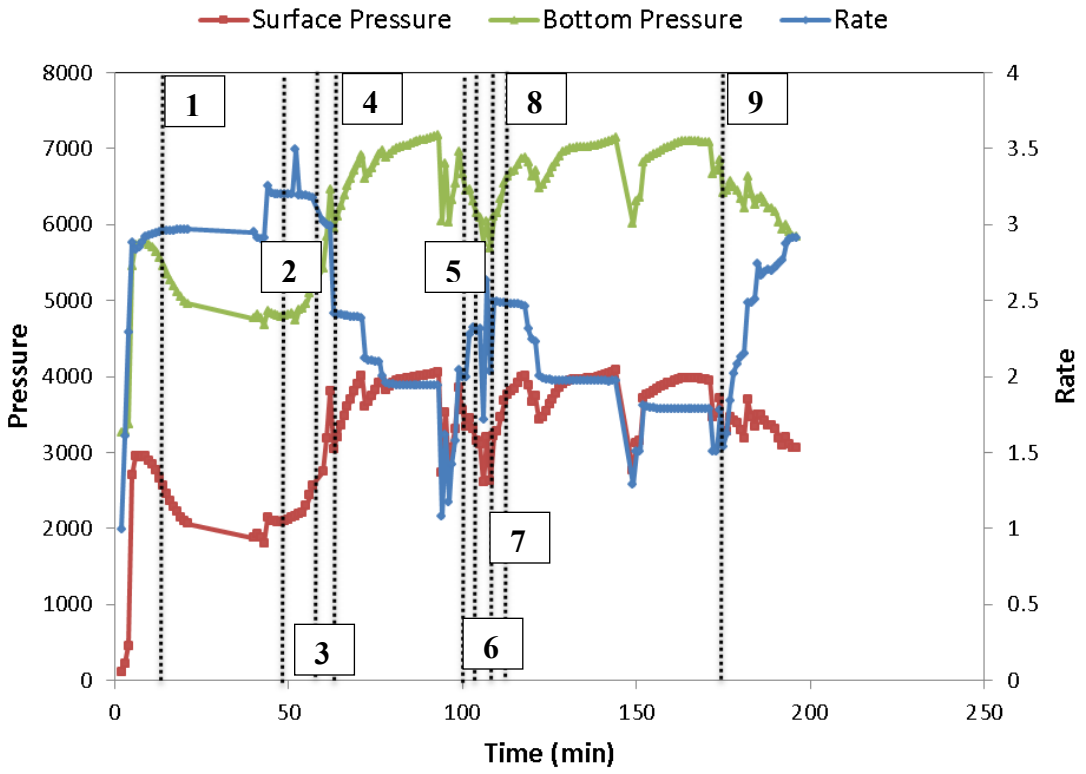

Fig. 17—Treatment data for Case 3.

In Fig. 17, the bottomhole pressure was calculated from the surface pressure. From the calculated bottomhole pressure and measured injection rate, the skin was calculated at each time step. The numbered flags indicate the time when the corresponding stage fluids hit the formation. The skin evolution during the acid job is shown in **Fig. 18.**

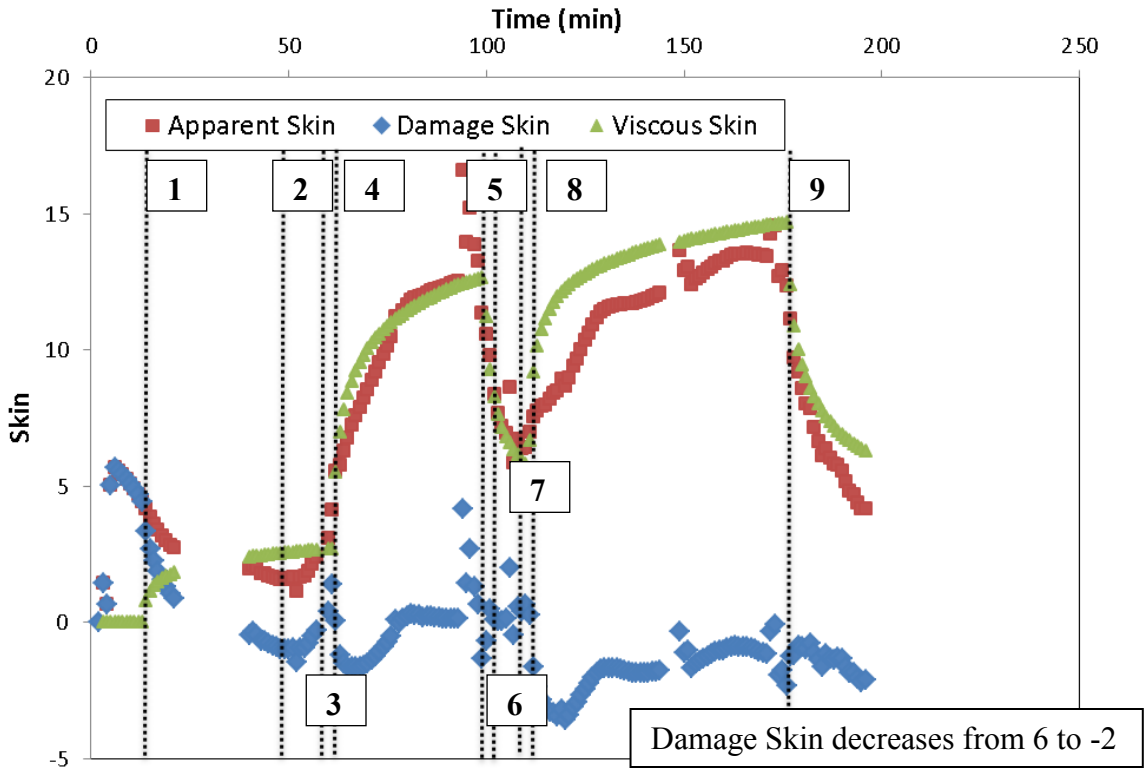

Fig. 18—Skin evolution for Case 3.

3.3.3 Discussion of Results

In Fig. 18, the apparent skin begins to decline when HCl (stage 1) enters the formation. However, the apparent skin remains constant during VES injection (stages 2 and 6) and slightly increases during water injection (stages 3 and 7). Therefore, VES did not lead to in-situ increase in the viscosity. VES forms rod-like micelles at higher pH of the spent acid. Therefore, the volume of VES pumped was not sufficient.

Viscous diversion during emulsified acid injection (stages 4 and 8) is clearly evident because the apparent skin begins to increase when the emulsified acid enters the

formation. During the water injection after the emulsified acid (stages 5 and 9), the apparent skin decreases due to decrease in viscosity of the fluid bank. Therefore, the emulsified acid was more effective as a viscous diverter during the treatment compared to VES.

The viscous skin factor was estimated to develop a decreasing trend in the damage skin factor. It is noticed that the volume of acid injected was sufficient as the damage skin continues to reduce until the end of the treatment.

The productivity index ratio from the initial and final skin value was estimated to be 2, assuming the drainage length (y_b) of 500 ft. The skin trend was validated using the production test from before and after the well is stimulated. In this case, the production rate of liquids from this well after stimulation increased from 1738 barrels/day to 4623 barrels/day. Therefore, the production test confirms that the acidizing treatment was successful in reducing the near wellbore damage.

3.4 Case 4: Multi-Stage Emulsified Acid and Associative-Polymer Treatment

3.4.1 Treatment Description

This well is a vertical well which is cased and perforated, as seen below in **Fig. 19.** The actual acidizing treatment was divided into two parts. The first part consisted of 15% hydrochloric acid flush through coil-tubing, and the second part comprised of alternate stages of bullheading 22% carbonate emulsion acid (CEA) and associative polymer solution.

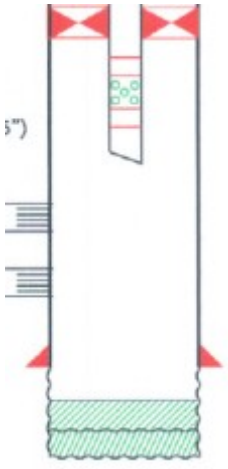

Fig. 19—Well diagram for Case 4.

The data for the reservoir, the wellbore, and the acid injection is shown in **Tables 10 through 12.**

Table 10—Reservoir Properties for Case 4

Initial Reservoir Pressure, psi	2500
Formation Volume Factor	1.397
Porosity	0.12
Total Compressibility, 1/psi	3.50E-06
Formation Thickness, ft	307
Reservoir Fluid Viscosity, cp	0.51
Permeability, md	50

Table 11—Wellbore Properties for Case 4

Wellbore Radius, in	6.125
Tubing Diameter, in	1.844 / 4
Relative Roughness	0.0001
Vertical Depth, ft	7500
Measured Depth, ft	7500
Well Fluid Density, lbm/ft3	63.8
Well Fluid Viscosity, cp	0.51

Table 12—Acid Injection Schedule for Case 4

Stage	Fluid Name	Volume Used, gal	Density, lb/ft3	Viscosity, cp	Friction Reducer
1	15% HCl	2524	66.35	0.51	1
2	Water	4625	61.56	0.51	1
3	CEA 22%	1722	62.83	0.51	1
4	Polymer Diverter	2562	62.83	0.51	1
5	CEA 22%	3444	62.83	0.51	1
6	Polymer Diverter	3444	62.83	0.51	1
7	CEA 22%	3444	62.83	0.51	1
8	Water	9240	61.56	0.51	1

3.4.2 Skin Monitoring Results

Figs. 20 and 21 plot the measured injection rate, and the measured surface pressure recorded during the acidizing treatment.

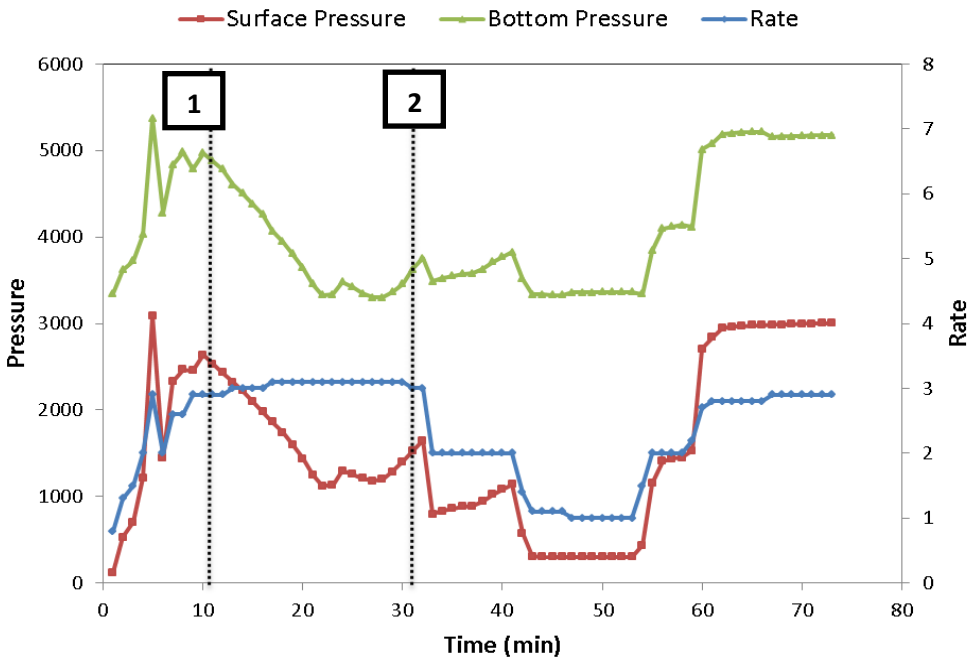

Fig. 20—Treatment data during HCl flush for Case 4.

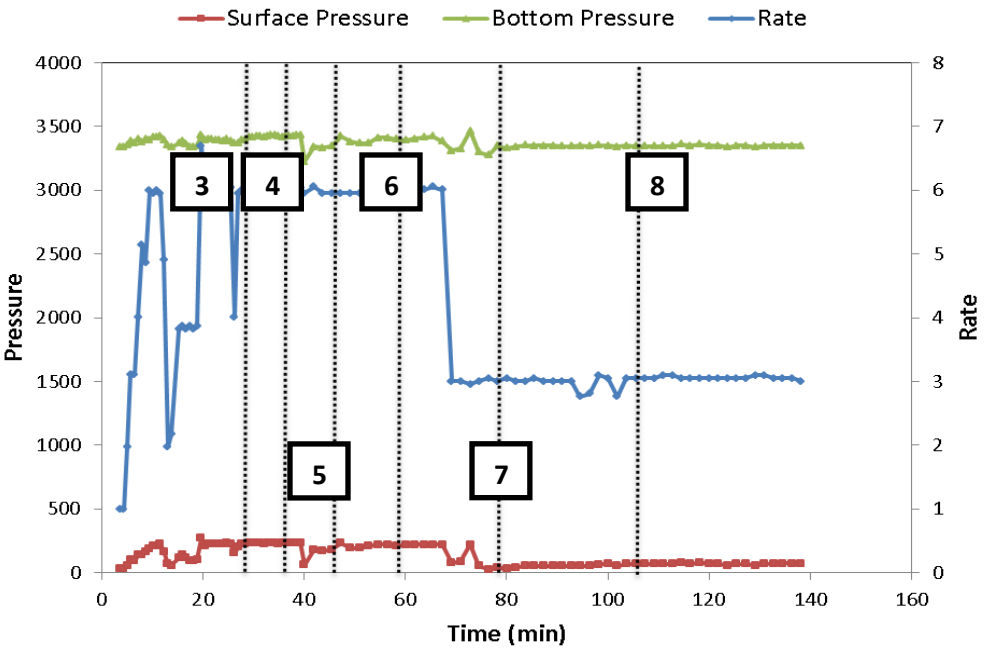

Fig. 21—Treatment data during CEA and polymer diverter injection for Case 4.

The bottomhole pressure was calculated from the surface pressure. The HCl flush was followed by bullheading of CEA and associative polymer diverter after 6 hours of pump shut-in. Also, the numbered flags in the above figure represent the corresponding stage fluid as it enters into the formation. From the calculated bottomhole pressure and measured injection rate, the skin was calculated at each time step. The skin evolution during the acid job is shown in **Figs. 22 and 23.**

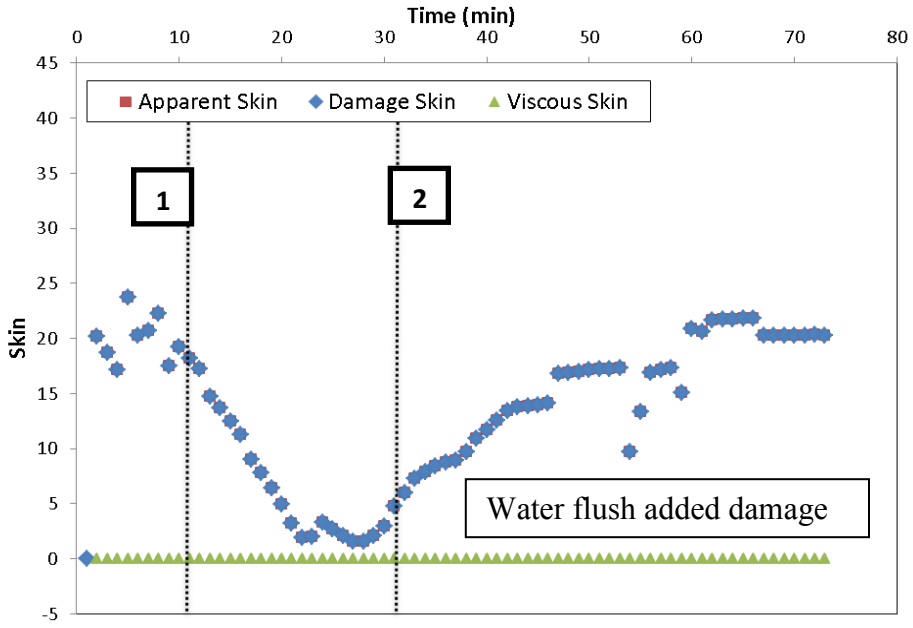

Fig. 22—Skin response during HCl flush for Case 4.

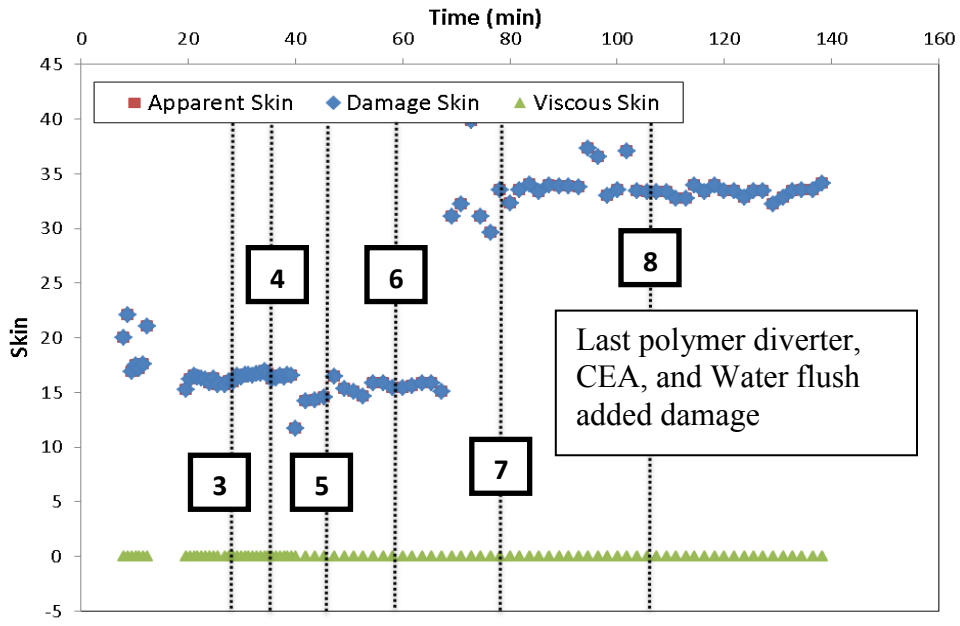

Fig. 23—Skin response during CEA and polymer diverter injection for Case 4.

3.4.3 Discussion of Results

In Figs. 22 and 23, the skin factor fluctuates during the entire acidizing process. For the first part of the treatment, the HCl system resulted in skin decrease from 20 to zero. However, the water injection after the HCl flush resulted in skin increase from zero to 20, thereby, implying addition of further damage to the near-wellbore region.

For the second part of the treatment, it is noticed that injection first round of CEA, polymer diverter, and CEA (stages 3, 4, and 5) did not show evidence of viscous diversion as the skin remained almost constant at 15. However, the second injection of associative polymer diverter (stage 6) indicated increase in the skin. The increasing skin trend continued during next CEA and water injection (stages 7 and 8). Therefore, the

volume of CEA injected was not sufficient to break the viscous polymer. Usually, the displacement stage consists of injection diesel or mutual solvents instead of water. The pressure spikes corresponding to arrival of associative-polymers in the formation were not observed in the pressure response. It is possible that the polymer solution did not behave as expected in the formation.

The productivity index ratio from the initial and final skin value was estimated to be 0.76, assuming the drainage radius (r_e) of 1000 ft. The production rate of liquids from this well after stimulation decreased from 9500 barrels/day to 5635 barrels/day. However, after the stimulation process, the water cut declined from 73% to 66%. Therefore, the skin evolution trend indicates that the associative polymer acid system reduced the well productivity.

3.5 Case 5: Two-Stage Hydrochloric Acid and Foam Treatment

3.5.1 Treatment Description

This well is a horizontal well with an open-hole lateral, as seen below in **Fig. 24.** The actual acidizing treatment design comprised of injection of 15% hydrochloric acid followed by injection of foamed acid through coil-tubing. Foamed acid is made up of hydrochloric acid in liquid phase and nitrogen in gas phase.

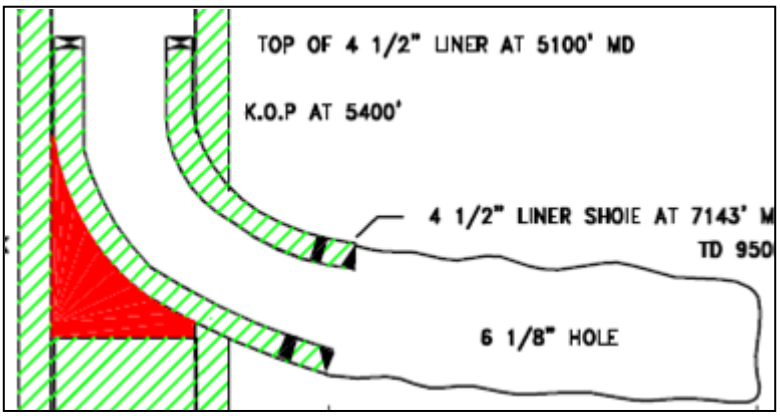

Fig. 24—Well diagram for Case 5.

The data for the reservoir, the wellbore, and the acid injection is shown in **Tables 13 through 15.**

Table 13—Reservoir Properties for Case 5

Initial Reservoir Pressure, psi	2500
Formation Volume Factor	1.405
Porosity	0.16
Total Compressibility, 1/psi	3.50E-06
Formation Thickness, ft	78
Reservoir Fluid Viscosity, cp	0.47
Permeability, md	4
k_V/k_H	0.1

Table 14—Wellbore Properties for Case 5

Wellbore Radius, in	3
Tubing Diameter, in	1.688
Relative Roughness	0.0001
Vertical Depth, ft	6331
Measured Depth, ft	9500
Horizontal Length, ft	2361
Well Fluid Density, lbm/ft3	63.58
Well Fluid Viscosity, cp	0.47

Table 15—Acid Injection Schedule for Case 5

Fluid Name	Volume Used, gal	Density, lb/ft3	Viscosity, cp
15% HCl	43485.44	63.58	0.47
Foamed Acid	54016.27	63.58	0.47
Water	5340.79	63.58	0.47

3.5.2 Skin Monitoring Results

Fig. 25 plots the measured injection rate, and the measured annulus pressure recorded during the acidizing treatment.

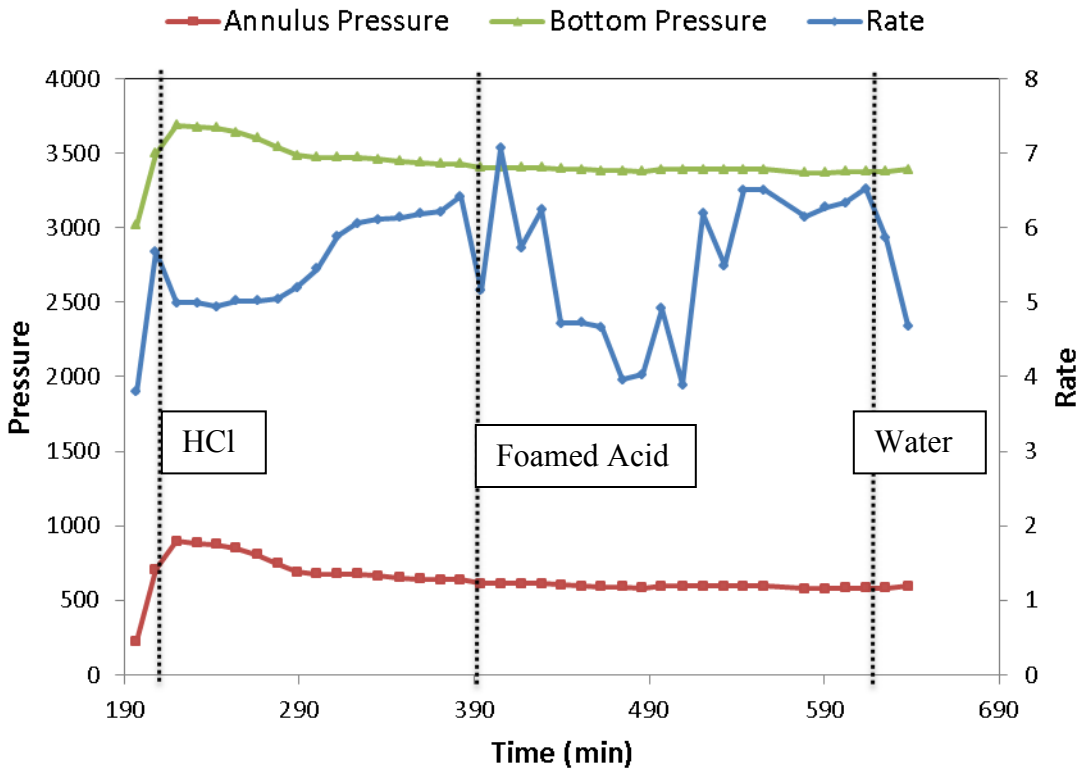

Fig. 25—Treatment data for Case 5.

In Fig. 25, the bottomhole pressure was calculated from the annulus pressure. For the foamed acid, the injection rate is calculated as the sum of liquid acid and nitrogen gas rates. The average foam quality was 40%. From the calculated bottom-hole pressure and injection rate, the skin was calculated at each time step. The skin evolution during the acid job is shown in **Fig. 26.**

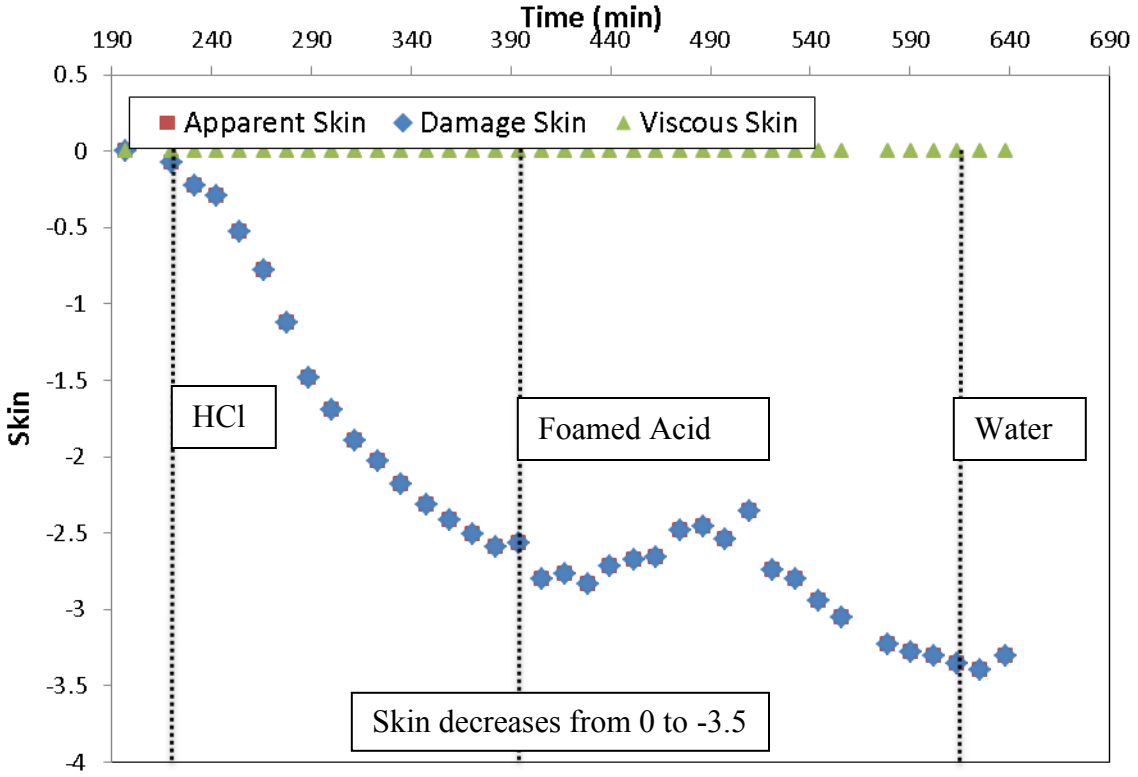

Fig. 26—Skin response for Case 5.

3.5.3 Discussion of Results

In Fig. 26, the skin begins to decrease during the HCl acid injection, and continues to decrease during the foamed acid injection. The skin value decreases from 0 to -3.5 by the end of acid injection. It is noticed that the volume of acid injected was sufficient as the skin continues to decrease until the end of the injection. Although a slight increase in the skin is noticed, the foamed acid did not show strong evidence of viscous diversion.

The productivity index ratio from the initial and final skin value was estimated to be 1.33, assuming the drainage length (y_b) of 500 ft. The skin trend was validated using the production test from before and after the well is stimulated. In this case, the production rate of liquids from this well after stimulation increased 1289 to 1741 barrels/day. Therefore, the production test confirms the decreasing skin trend.

3.6 Case 6: Two-Stage Hydrochloric-Acid and Emulsified Acid Treatment

3.6.1 Treatment Description

This well is a horizontal well with a cased and perforated completion, as seen in **Fig. 27.** The actual acidizing treatment design was divided into two parts: 1) pumping 15% HCl through moving coil-tubing; 2) bullheading 22% carbonate emulsion acid (CEA) through tubing. Each of the two parts of the treatments comprised of the acid stage followed by the fresh water displacement stage.

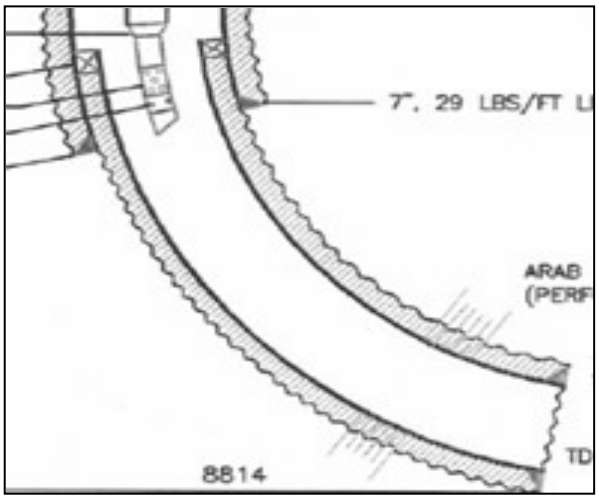

Fig. 27—Well diagram for Case 6.

The data for the reservoir, the wellbore, and the acid injection is shown **Tables 16 through 18.**

Table 16—Reservoir Properties for Case 6

Initial Reservoir Pressure, psi	3650
Formation Volume Factor	1.397
Porosity	0.18
Total Compressibility, 1/psi	3.50E-06
Formation Thickness, ft	30
Reservoir Fluid Viscosity, cp	0.51
Permeability, md	10
k_V/k_H	0.1

Table 17—Wellbore Properties for Case 6

Wellbore Radius, in	2
Tubing Diameter, in	1.5 (CT) / 2.992 (Bullhead)
Relative Roughness	0.0001
Vertical Depth, ft	8340
Measured Depth, ft	9270
Horizontal Length, ft	610
Well Fluid Density, lbm/ft3	64.35
Well Fluid Viscosity, cp	0.51

Table 18—Acid Injection Schedule for Case 6

Fluid Name	Volume Used, gal	Density, lb/ft3	Viscosity, cp	Friction Reducer
15% HCl	2542	66.69	0.51	1
Fresh water	848	63.09	0.51	2
22% CEA	11764	63.92	0.51	1
Fresh water	4202	62.52	0.51	1

3.6.2 Skin Monitoring Results

Fig. 28 plots the measured injection rate, and the measured surface pressure recorded during the acidizing treatment. The given bottomhole pressure is the bottomhole pressure that was calculated on-site during the treatment.

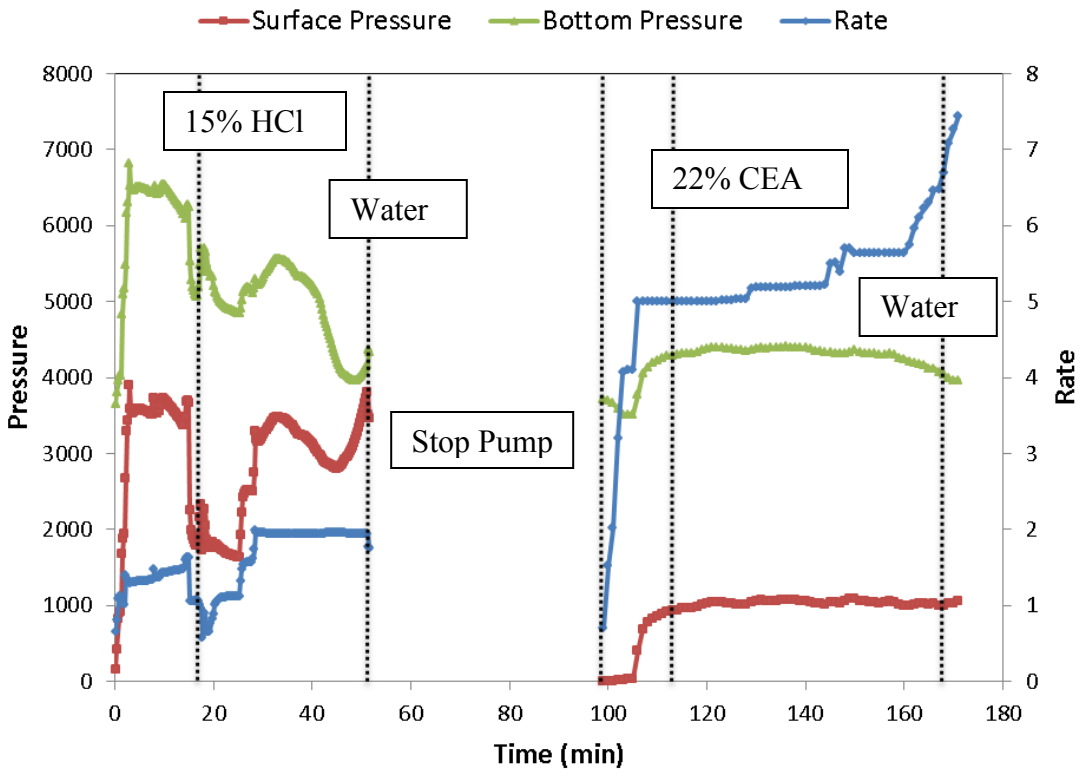

Fig. 28—Treatment data for Case 6.

In Fig. 28, the bottomhole pressure was calculated from the surface pressure. The HCl flush was followed by bullheading of CEA after 50 hours of pump shut-in. Also, the numbered flags represent the corresponding stage fluid as it enters into the formation.

From the calculated bottomhole pressure and measured injection rate, the skin was calculated at each time step. The skin evolution during the acid job is shown in **Fig. 29.**

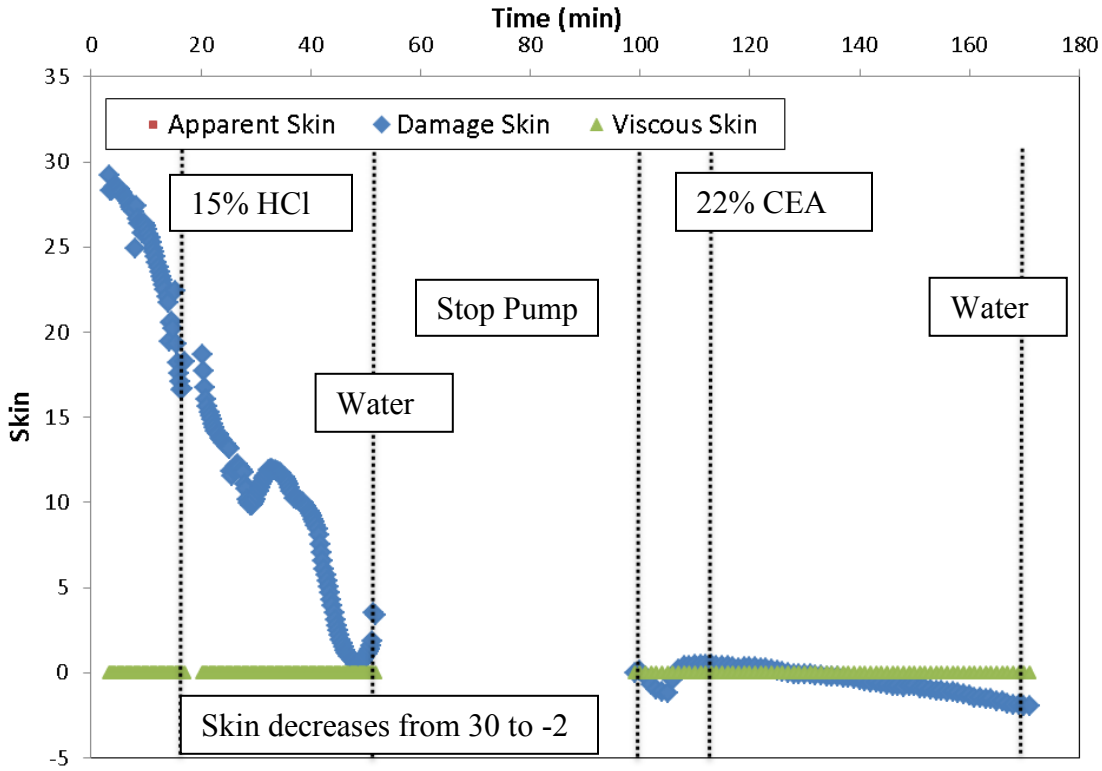

Fig. 29—Skin evolution for Case 6.

3.6.3 Discussion of Results

From Fig. 29, it is inferred that HCl injection reduces the skin factor from 30 to 0. However, the skin factor starts to reduce even before the HCl front comes out of the coil-tubing. This early behavior of skin decline from 30 to 20 may be caused due high bottomhole pressures, resulting in creation of small fractures in the formation. It is

noticed that the volume of acid injected was sufficient as the skin continues to reduce until the end of the acid injection.

The emulsified acid injection reduces the skin factor from 0 to -2. However, the emulsified acid did not show any evidence of increasing viscous diversion skin effects. It is noticed that the 22% CEA system was not an effective diverting agent for this case. From Fig. 29, it is noticed that emulsified acid contributed very little to the well stimulation as compared with normal HCl acid. The treatment with 22% CEA was not beneficial to the well.

The productivity index ratio from the initial and final skin value was estimated to be 3.1, assuming the drainage length (y_b) of 415 ft. The skin trend was validated using the production test from before and after the well is stimulated. In this case, the production rate of liquids from this well after stimulation increased from 641 barrels/day to 1981 barrels/day. Therefore, the production test confirms that the acidizing treatment is successful in reducing the near wellbore damage.

4. CONCLUSIONS AND RECOMMENDATIONS

4.1 Skin Monitoring Method

During this study, the concept of inverse injectivity was successfully applied to evaluate skin evolution during matrix acidizing treatments for horizontal and vertical wells. Some of the key results of the post-treatment analysis are summarized as following:

1. The skin evolution trend helped understand the contribution of each injected fluid to the stimulation process. In other words, the skin trend indicated if the fluid was adding or removing damage.
2. The skin response helped diagnose if effective viscous diversion was achieved, or efficient acid volume were used during the treatment.
3. The production tests before and after acid stimulation validated the skin evolution trend.

Since the objective of the analysis was to estimate an overall skin evolution, the heterogeneities and variations along the length of the target interval were not considered. It is recommended that an acid placement model be used to history match the overall skin trend. The acid placement model may be beneficial in understanding acid injectivity and wormhole length profiles along the length of the target intervals.

4.2 Field Cases

This skin monitoring approach was used for the analysis of acidizing treatments for 20 wells. The design for the acidizing treatments consisted of single and multiple stage injection. The acid systems that were used for were hydrochloric acid and emulsified acid. For some cases, the acid design also included chemical diverters such as associative-polymer solution, viscoelastic surfactants, and foam.

4.2.1 Emulsified Acid

In this study, total of 11 wells treated with emulsified acids were evaluated. The acidizing design for 5 of 11 wells included hydrochloric acid pre-flush followed by main emulsified acid stage. It was observed that the hydrochloric acid pre-flush contributed more than the emulsified acid main stage. Therefore, it is recommended to use milder acid during pre-flush or eliminate the pre-flush to optimize acid injection. The acidizing design may be changed to single acid stage with emulsified acid. Emulsified acid is preferred over normal hydrochloric acid because it's less corrosive leading to lower iron precipitation, and it has slower reaction rates leading to deeper acid penetration.

The one of the objective of using emulsified acid is to provide better acid coverage by viscous diversion. It was observed that only 3 wells (27%) that were treated with emulsified acid showed strong indication of viscous diversion. Therefore, the emulsified acid was not an efficient viscous diverter and should be used with additional diversion techniques.

4.2.2 Associative-Polymer Diverter

Two wells were treated with associative-polymers as viscous diverters along with the emulsified acid. The purpose of the associative-polymers was to divert acid and control water production. The pressure spikes corresponding to associative-polymers arrival in the formation were not observed in the pressure response. These acid treatments were unsuccessful as it resulted in reduced oil and water production.

The treatment design for associative-polymer may be flawed. The design did not include a correct pre-flush and displacement stage. It is recommended that a pre-flush stage should comprise of injection of diesel followed by the associative-polymer. The pre-flush should be followed by alternate emulsified acid and associative-polymer injection stages. Finally, the displacement stage should comprise of injection of diesel. The acid treatments with this sequence of stages have been proven successful in the field (Al-Taq et al., 2007).

4.2.3 Foamed Acid

Foamed acid system was used for diversion during acid treatments of five wells. The skin analysis did not indicate any strong evidence of viscous diversion for any of the wells. Although no viscous diversion was noticed, all the stimulation treatments were successful in increasing the well performance. Therefore, the volume of acid injected with or without the gas-phase contributed in removing formation damage.

The average quality of foam estimated for the five treatments was approximately 46% (standard deviation of 9%). This foam quality is lower than the recommended foam

quality, which is 60% or higher (Thompson and Gdanski, 1993). Therefore, higher injection rates of nitrogen (gas phase) may help achieve viscous diversion. Nasr-El-Din et al. (2006) also found that injection of viscoelastic surfactant as a foaming additive in fresh water to achieve effective diversion.

4.2.4 Viscoelastic Surfactants

Viscoelastic surfactants (VES) were used as viscous diversion in two wells. The pressure spikes due to viscous diversion due to injection of VES were noticed for only one case. The similar behavior was not noticed when alternate stages of VES and acid (emulsified or normal) were pumped. It can be speculated that inadequate volumes of aqueous spacer (HCl or water) and VES were injected. Although diversion due to VES was not efficient, the acid treatments were successful in improving well performance. Therefore, the volume of acid injected contributed in removing formation damage.

The treatment design involving VES may be optimized. It is recommended that a pre-flush stage should comprise of injection of diesel or mutual solvent to push oil from the formation. The pre-flush should be followed by sequence of stages which include injection of normal HCl, emulsified acid, normal HCl, and VES. The two stages of normal HCl and one stage of emulsified acid will ensure that sufficient concentration of spent acid is available for VES to create a viscosified fluid. Finally, the displacement stage should comprise of injection of diesel or mutual solvent to break the viscosified fluid. The acid treatments with this sequence of stages have been proven successful in the field (Nasr-El-Din et al., 2006).

REFERENCES

Al-Taq, A.A., Nasr-El-Din, H.A., Lajami, R., and Sirra, L. 2007. Effective Acid Diversion and Water Control in Carbonate Reservoirs Using an Associative Polymer Treatment: Case Histories from Saudi Arabia. Paper SPE 109714 presented at the SPE Annual Technical Conference and Exhibition, Anaheim, California.

Bale, G.E. 1984. Matrix Acidizing in Saudi Arabia Using Buoyant Ball Sealers. *Journal of Petroleum Technolog,* **36** (10): 1748-1752. SPE-11500-PA

Brown, R.W., Neill, G.H., and Loper, R.G. 1963. Factors Influencing Optimum Ball Sealer Performance. *Journal of Petroleum Technology* **15** (4): 450-454. SPE-553-PA

Buijse, M.A. and Domelen, M.S.v. 2000. Novel Application of Emulsified Acids to Matrix Stimulation of Heterogeneous Formations. *SPE Production & Operations* **15** (8): 208-213. SPE-65355-PA

Burman, J.W. and Hall, B.E. 1986. Foam as a Diverting Technique for Matrix Sandstone Stimulation. Paper SPE 15575 presented at the SPE Annual Technical Conference and Exhibition, New Orleans, Louisiana.

Chen, N.H. 1979. An Explicit Equation for Friction Factor in Pipe. *Industrial & Engineering Chemistry Fundamentals* **18** (3): 296-297.

Earlougher, R.C. 1977. *Advances in Well Test Analysis*. Monograph Series. Dallas: SPE.

Eckerfield, L.D., Zhu, D., Hill, A.D. et al. 1998. Fluid Placement Model for Stimulation of Horizontal or Variable Inclination Wells. Paper SPE 49103 presented at the SPE Annual Technical Conference and Exhibition, New Orleans, Louisiana.

Economides, M.J., Hill, A.D., and Ehlig-Economides, C. 1994. *Petroleum Production Systems*. 1st edition. Upper Saddle River, New Jersey: Prentice Hall, Inc.

Erbstoesser, S.R. 1980. Improved Ball Sealer Diversion. *Journal of Petroleum Technology* **32** (11): 1903-1910. SPE-8401-PA

Fadele, O., Zhu, D., and Hill, A.D. 2000. Matrix Acidizing in Gas Wells. Paper SPE 59771 presented at the SPE/CERI Gas Technology Symposium, Calgary, Alberta, Canada.

Furui, K., Zhu, D., and Hill, A.D. 2002. A Rigorous Formation Damage Skin Factor and Reservoir Inflow Model for a Horizontal Well. Paper SPE 74698 presented at the International Symposium and Exhibition on Formation Damage Control, Lafayette, Louisiana.

Gabriel, G.A. and Erbstoesser, S.R. 1984. The Design of Buoyant Ball Sealer Treatments. Paper SPE 13085 presented at the SPE Annual Technical Conference and Exhibition, Houston, Texas.

Gomaa, A.M., Mahmoud, M.A., and Nasr-El-Din, H. 2010. A Study of Diversion Using Polymer-Based in-Situ-Gelled Acids Systems. Paper SPE 132535 presented at the Trinidad and Tobago Energy Resources Conference, Port of Spain, Trinidad.

Goode, P.A. 1987. Pressure Drawdown and Buildup Analysis of Horizontal Wells in Anisotropic Media. *SPE Formation Evaluation* **2** (4): 683-697. SPE-14250-PA

Hill, A.D. and Rossen, W.R. 1994. Fluid Placement and Diversion in Matrix Acidizing. Paper SPE 27982 presented at the University of Tulsa Centennial Petroleum Engineering Symposium, Tulsa, Oklahoma.

Hill, A.D. and Zhu, D. 1996. Real-Time Monitoring of Matrix Acidizing Including the Effects of Diverting Agents. *SPE Production & Operations* **11** (2): 95-101. SPE-28548-PA

Kibodeaux, K.R., Zeilinger, S.C., and Rossen, W.R. 1994. Sensitivity Study of Foam Diversion Processes for Matrix Acidization. Paper SPE 28550 presented at the SPE Annual Technical Conference and Exhibition, New Orleans, Louisiana.

Lungwitz, B.R., Fredd, C.N., Brady, M.E., Miller, M., Ali, S. et al. 2007. Diversion and Cleanup Studies of Viscoelastic Surfactant-Based Self-Diverting Acid. *SPE Production & Operations* **22** (1): 121-127. SPE-86504-PA

Lynn, J.D. and Nasr-El-Din, H.A. 2001. A Core Based Comparison of the Reaction Characteristics of Emulsified and in-Situ Gelled Acids in Low Permeability, High Temperature, Gas Bearing Carbonates. Paper SPE 65386 presented at the SPE International Symposium on Oilfield Chemistry, Houston, Texas.

Mitchell, W.P., Stemberger, D., and Martin, A.N. 2003. Is Acid Placement through Coiled Tubing Better Than Bullheading? Paper SPE 81731 presented at the SPE/ICoTA Coiled Tubing Conference and Exhibition, Houston, Texas.

Montgomery, C.T., Jan, Y.-M., and Niemeyer, B.L. 1995. Development of a Matrix-Acidizing Stimulation Treatment Evaluation and Recording System. *SPE Production & Operations* **10** (4): 219-224. SPE-26579-PA

Nasr-El-Din, H.A., Chesson, J.B., Cawiezel, K.E. et al. 2006. Lessons Learned and Guidelines for Matrix Acidizing with Viscoelastic Surfactant Diversion in Carbonate Formations. Paper SPE 102468 presented at the SPE Annual Technical Conference and Exhibition, San Antonio, Texas, USA.

Nasr-El-Din, H.A., Chesson, J.B., Cawiezel, K.E. et al. 2006. Investigation and Field Evaluation of Foamed Viscoelastic Surfactant Diversion Fluid Applied During Coiled-Tubing Matrix-Acid Treatment. Paper SPE 99651 presented at the SPE/ICoTA Coiled Tubing Conference & Exhibition, The Woodlands, Texas, USA.

Nozaki, M. and Hill, A.D. 2009. A Placement Model for Matrix Acidizing of Vertically Extensive, Heterogeneous Gas Reservoirs. Paper SPE 124881 presented at the SPE Annual Technical Conference and Exhibition, New Orleans, Louisiana.

Nozaki, M., Zhu, D., and Hill, A.D. 2011. Experimental and Field Data Analyses of Ball Sealer Diversion. Paper SPE 147632 presented at the SPE Annual Technical Conference and Exhibition, Denver, Colorado, USA.

Paccaloni, G., Tambini, M., and Galoppini, M. 1988. Key Factors for Enhanced Results of Matrix Stimulation Treatments. Paper SPE 17154 presented at the SPE Formation Damage Control Symposium, Bakersfield, California.

Prouvost, L.P. and Economides, M.J. 1989. Applications of Real-Time Matrix-Acidizing Evaluation Method. *SPE Production Engineering* **4** (4): 401-407. SPE-17156-PA

Smith, C.L., Anderson, J.L., and Roberts, P.G. 1969. New Diverting Techniques for Acidizing and Fracturing and Fracturing. Paper SPE 2751 presented at the SPE California Regional Meeting, San Francisco, California.

Taylor, D., Kumar, P.S., Fu, D. et al. 2003. Viscoelastic Surfactant Based Self-Diverting Acid for Enhanced Stimulation in Carbonate Reservoirs. Paper SPE 82263 presented at the SPE European Formation Damage Conference, The Hague, Netherlands.

Thomas, R.L., Saxon, A., and Milne, A.W. 1998. The Use of Coiled Tubing During Matrix Acidizing of Carbonate Reservoirs Completed in Horizontal, Deviated, and Vertical Wells. *SPE Production & Operations* **13** (3): 147-162. SPE-50964-PA

Thompson, K.E. and Gdanski, R.D. 1993. Laboratory Study Provides Guidelines for Diverting Acid with Foam. *SPE Production & Operations* **8** (4): 285-290. SPE-23436-PA

Zerhboub, M., Touboul, E., Ben-Naceur, K. et al. 1994. Matrix Acidizing: A Novel Approach to Foam Diversion. *SPE Production & Operations* **9** (2): 121-126. SPE-22854-PA

Zhu, D. and Hill, A.D. 1998. Field Results Demonstrate Enhanced Matrix Acidizing through Real-Time Monitoring. *SPE Production & Operations* **13** (4): 279-284. SPE-52400-PA

Zhu, D., Hill, A.D., and Looney, M.D. 1999. Evaluation of Acid Treatments in Horizontal Wells. Paper SPE 56782 presented at the SPE Annual Technical Conference and Exhibition, Houston, Texas.

Zhu, D., Hill, A.D., and Morgenthaler, L.N. 1999. Assessment of Matrix Acidizing Treatment Responses in Gulf of Mexico Wells. Paper SPE 52166 presented at the SPE Mid-Continent Operations Symposium, Oklahoma City, Oklahoma.

Zhu, D., Hill, A.D., and Motta, E.P.d. 1998. On-Site Evaluation of Acidizing Treatment of a Gas Reservoir. Paper SPE 39421 presented at the SPE Formation Damage Control Conference, Lafayette, Louisiana.

APPENDIX A

SKIN MONITORING PROGRAM

In this section, all the components of the skin monitoring program are discussed. The skin monitoring program is a software package written in Visual Basic for Applications (VBA). VBA is an object-oriented programming language used to build applications in Microsoft Excel. The program is divided into three main parts:

1. Pre-treatment test to obtain reservoir information such as permeability and initial skin factor when that information is unavailable. A pre-treatment test comprises of a pressure transient analysis for a constant rate injection of an inert fluid.
2. Real-time monitoring to process real time field data and calculate skin factor at current monitoring time. The pressure and rate data are input for a desired time interval and the skin is calculated automatically for each time interval.
3. Post-treatment study to evaluate the effectiveness of an already completed acidizing treatment.

A1. Start Panel

This panel introduces the skin monitoring program to the users. It describes the key components of the program and explains the purpose of the program. **Fig. A1** below shows the START button which is used to navigate to the Input panel.

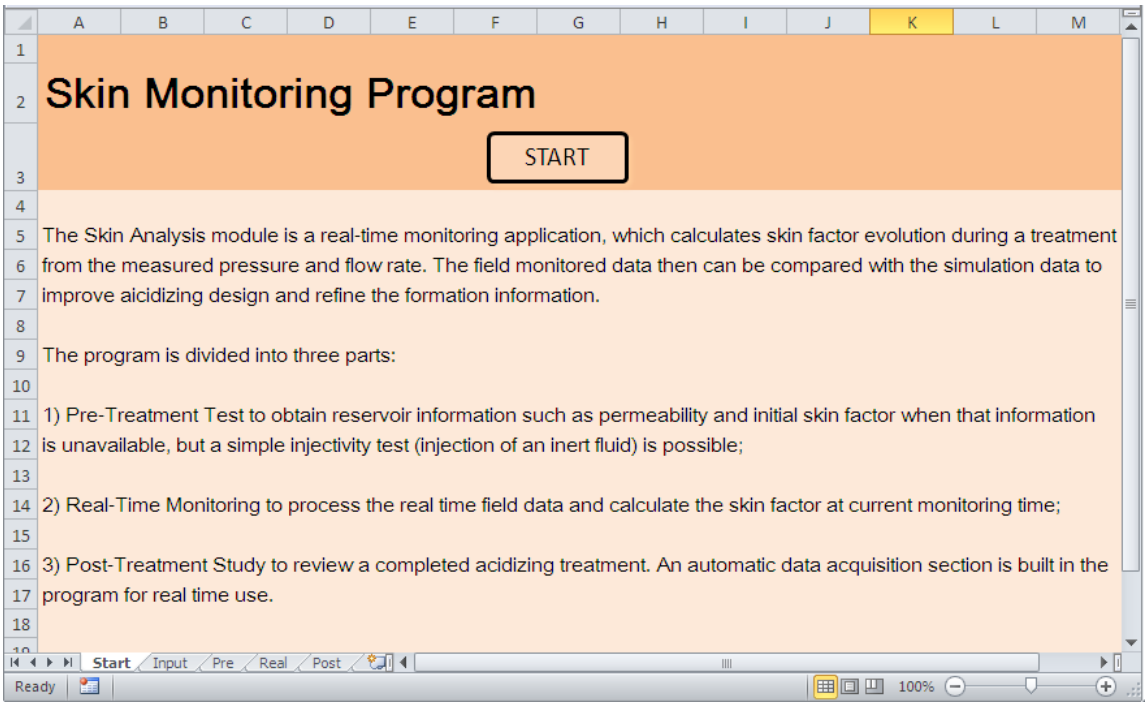

Fig. A1—Start panel for the skin monitoring program.

A2. Input Panel

The Input panel consists of six buttons as shown in **Fig. A2.** Five of the buttons represent sub-categories of input information. The Next button is used to navigate to another panel.

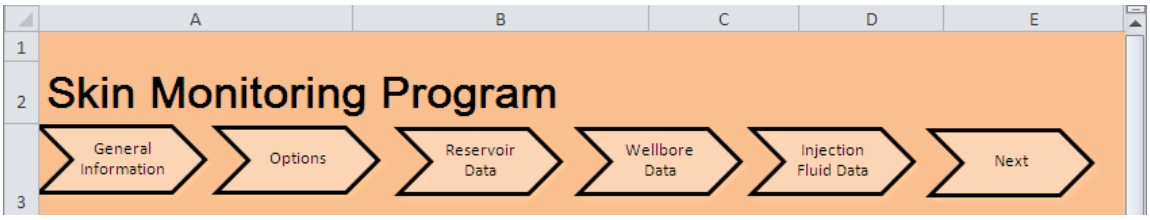

Fig. A2—Buttons for the Input panel.

The General Information button is used to enter information such as the company's name, the field's name and the location, the service company's name and the date which the treatment is done. This panel is shown in **Fig. A3.**

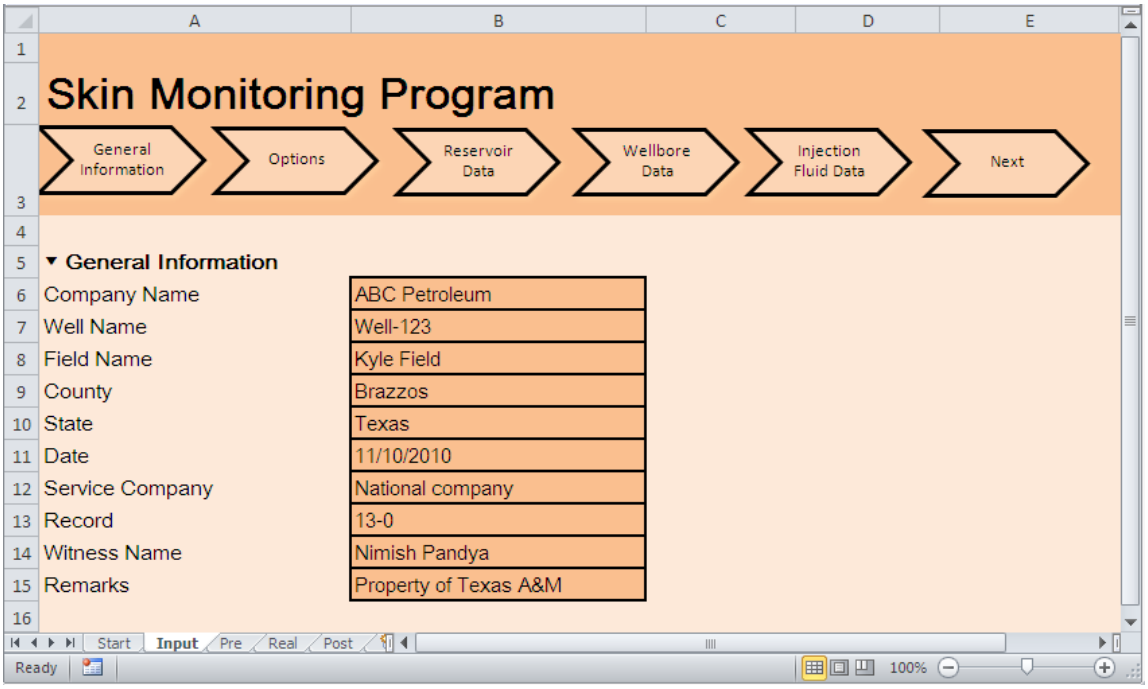

Fig. A3—The general information input panel.

The Options button is used to decide the type of analysis to be conducted, to select the well type (vertical or horizontal), to choose if the pressure is recorded at the bottomhole, the surface (tubing) or the annulus, to pick the type of reservoir fluid (oil or gas), and to elect the time format for the recorded time. **Fig. A4** below shows this panel. A drop-down menu is designed to make the selection process convenient for the user as shown in **Fig. A5.**

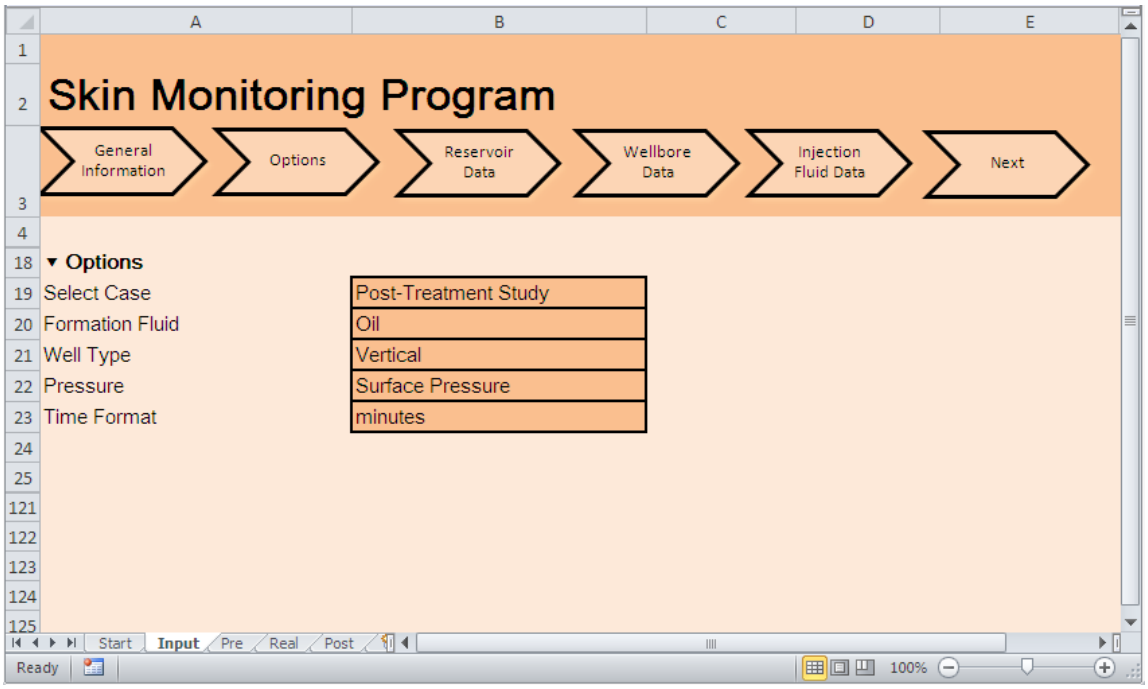

Fig. A4—The options input panel.

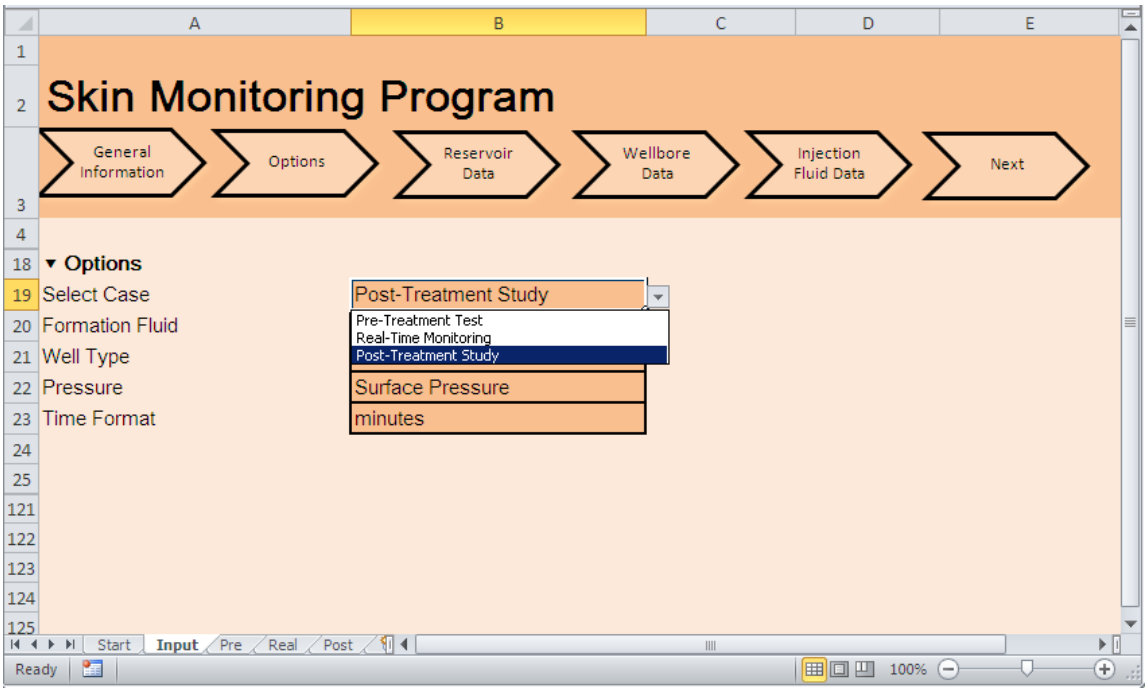

Fig. A5—The options input panel with drop-down menu.

Next, the Reservoir button and Wellbore button are used to input data for the reservoir/wellbore system. The input panel for these buttons depends on the type of well selected previously in the options input panel.

Figs. A6 and A7 represent the input panels if Vertical Well option is selected.

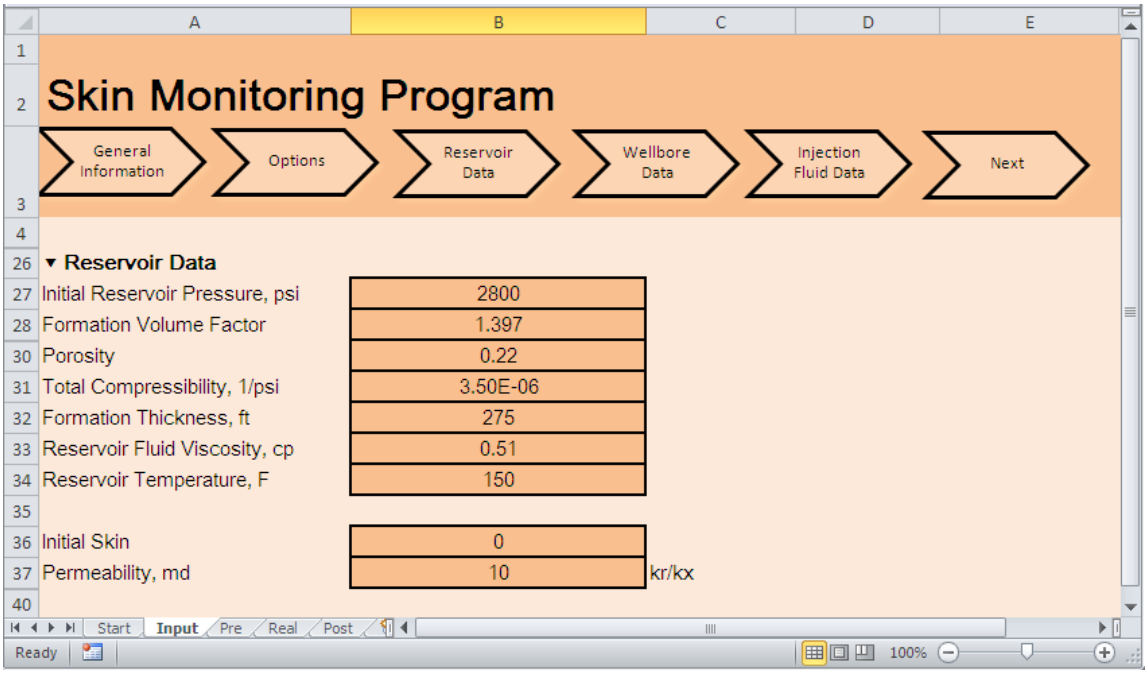

Fig. A6—The reservoir data input panel for vertical wells.

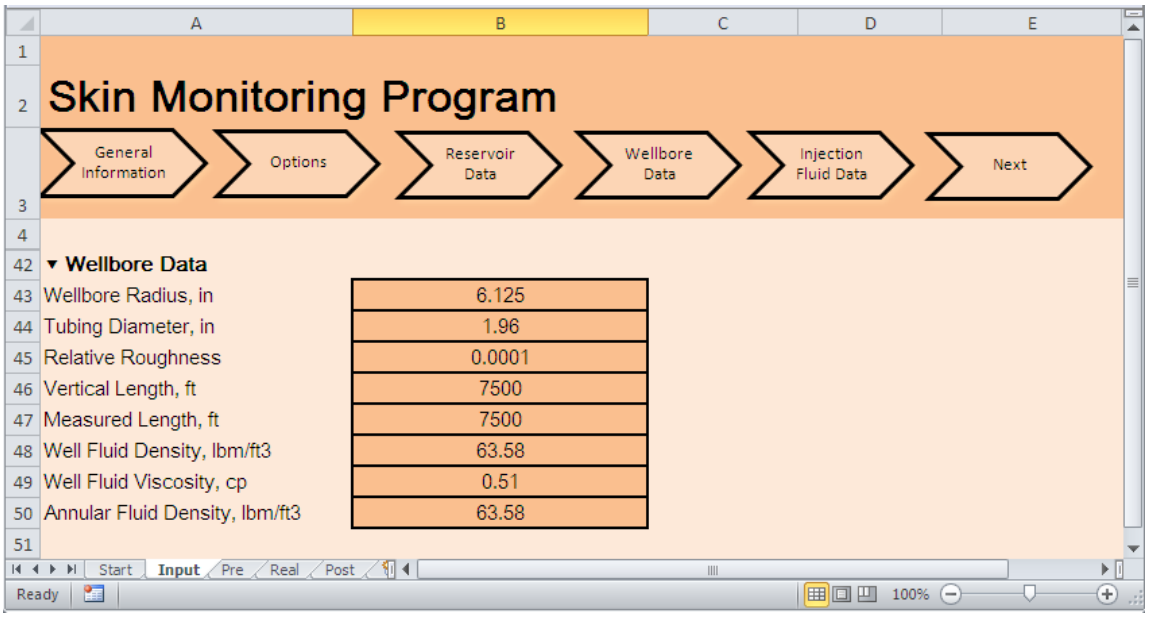

Fig. A7—The wellbore data input panel for vertical wells.

Figs. A8 and A9 represent the input panels if Horizontal Well option is selected.

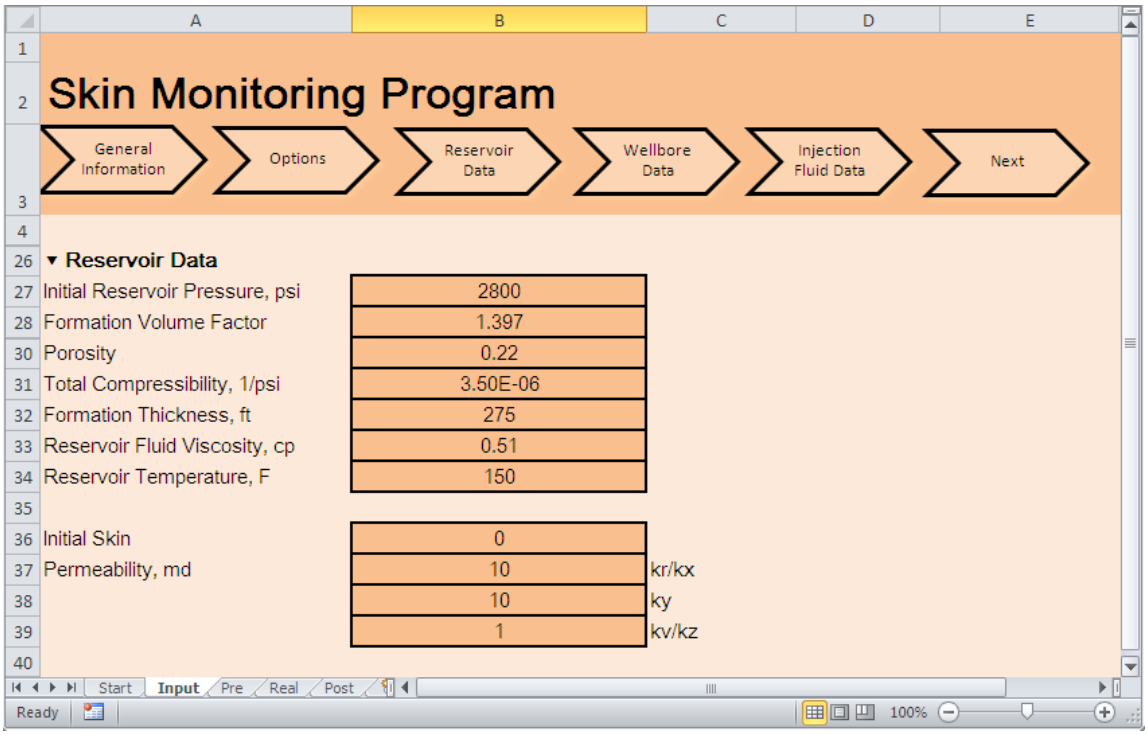

Fig. A8—The reservoir data input panel for horizontal well.

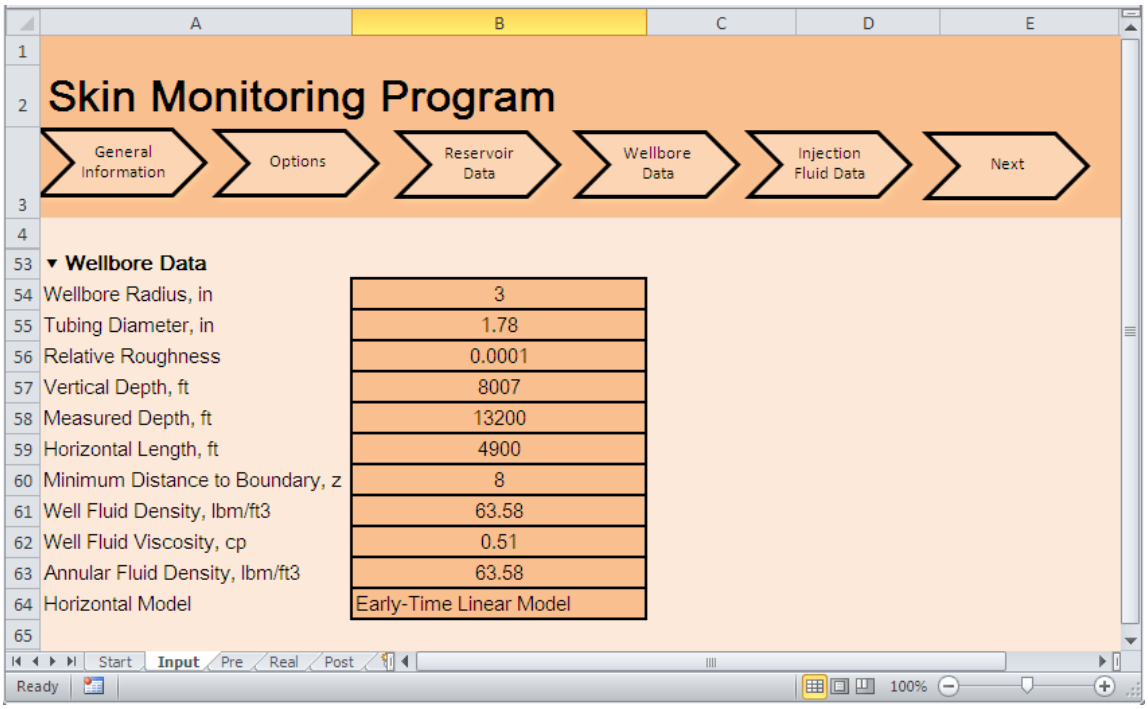

Fig. A9—The wellbore data input panel for horizontal well.

The fluid density and viscosity in the Wellbore Data section are the viscosity and density of the fluid already in the wellbore before the treatment. If a gas well is selected in the options panel, instead of formation volume factor, the user needs to define the compressibility factor Z for the gas.

The Injection button is used to input the injection schedule of fluids in the exactly same order as they are injected during the treatment. **Fig. A10** below shows the input panel for the injection data.

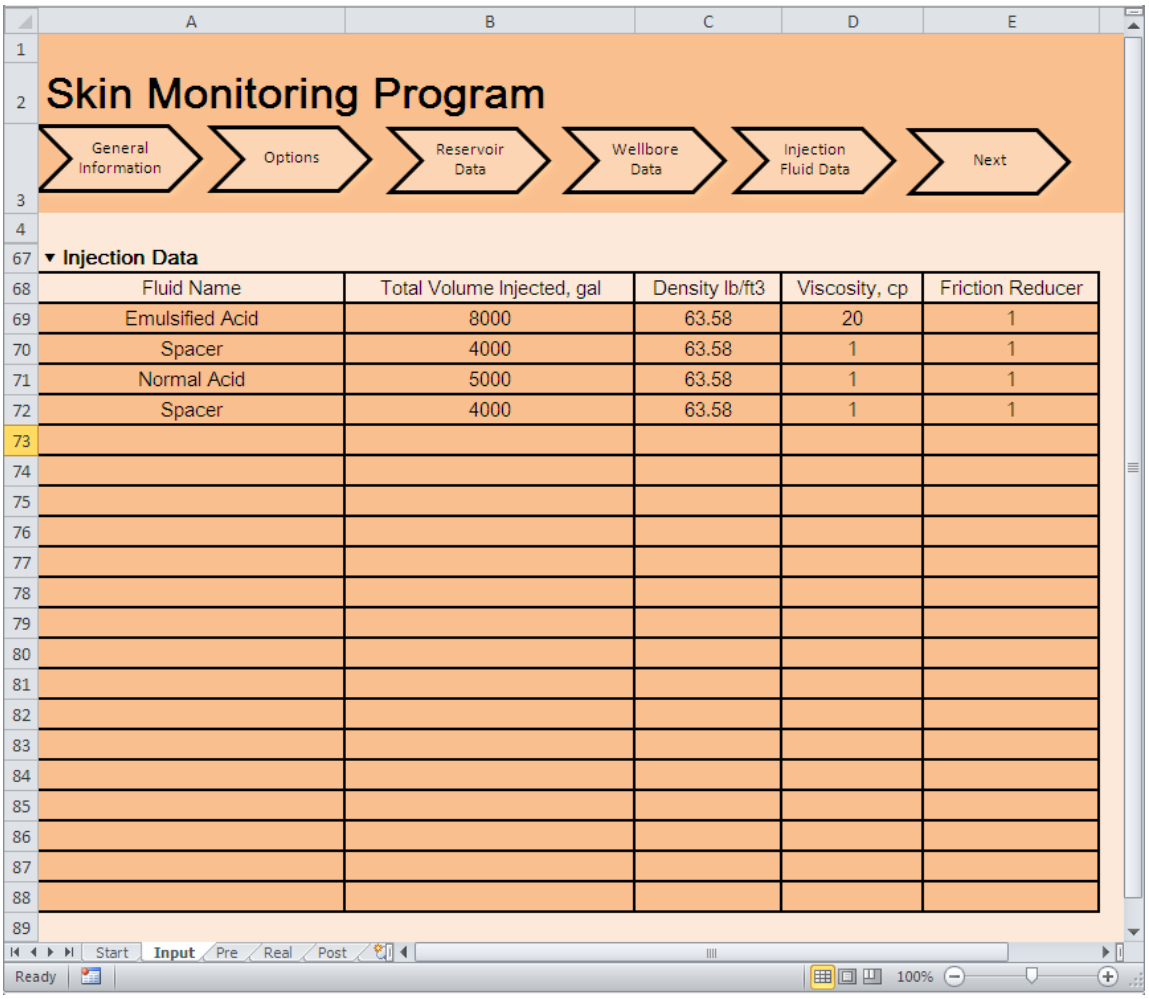

Fig. A10—The injection data input panel.

The fluid properties such as density, viscosity, and friction reducer factor are used to convert surface pressure to bottomhole pressure. Also, the fluid front in the wellbore is tracked and the changes in properties for multiple fluids in the wellbore are accounted.

A3. Pre-Treatment Test Panel

The pre-treatment test is based on the concept of the constant rate injection test analysis to estimate the permeability and initial skin factor of the formation. This

analysis is required when the required reservoir parameters are not known. The measured pressure for the test can either be surface pressure or bottomhole pressure.

If the option of pre-treatment test is selected on the options input panel, the Next button on the input panel will navigate to the panel shown in **Fig. A11.** Furthermore, the permeability and skin factor boxes are hidden on the reservoir input panel. All of the other input data are necessary for the analysis.

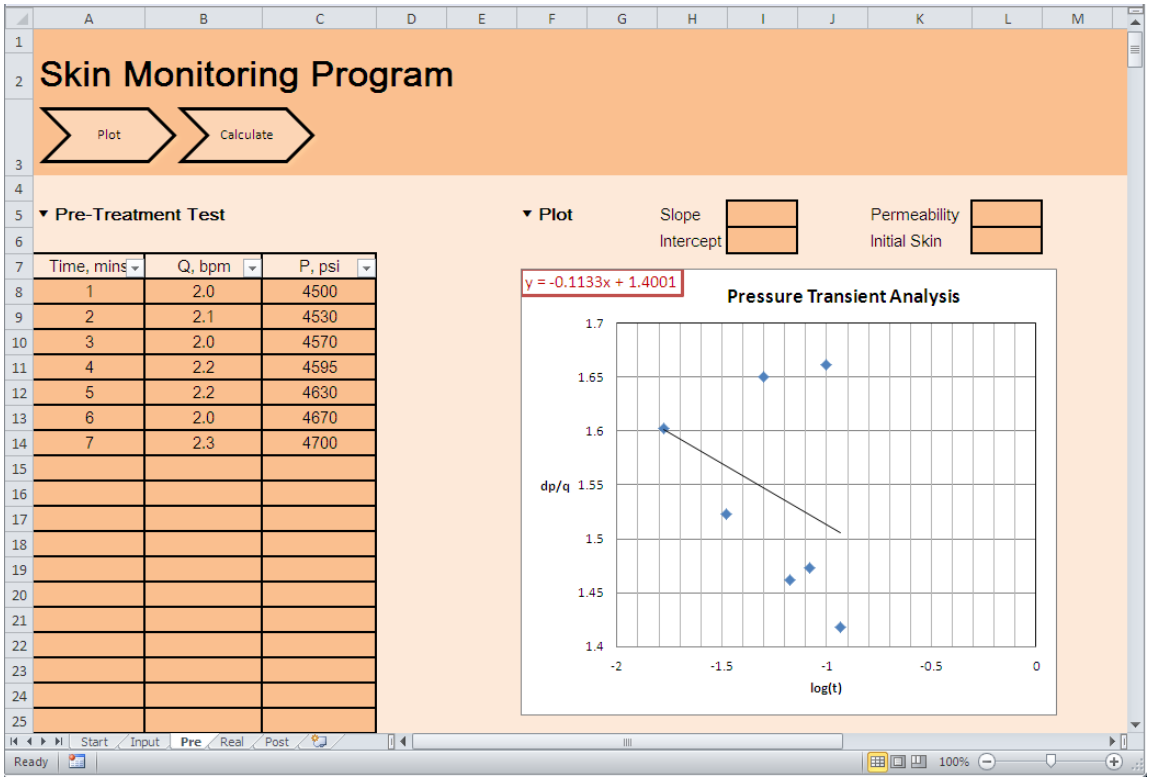

Fig. A11—The pre-treatment test panel.

This panel has three columns; the time is in the first column, the flow rate is in the second column and the pressure is in the third column. The Plot button is used to plot the test data on the inverse injectivity versus log(t) chart. Then, the test data is filtered to pick a straight line with an appropriate slope and intercept to best-fit the test data **(Fig.**

A12). The calculated permeability and initial skin factor from the fitted line will be shown in the corresponding boxes of this panel. This section is available for vertical wells only.

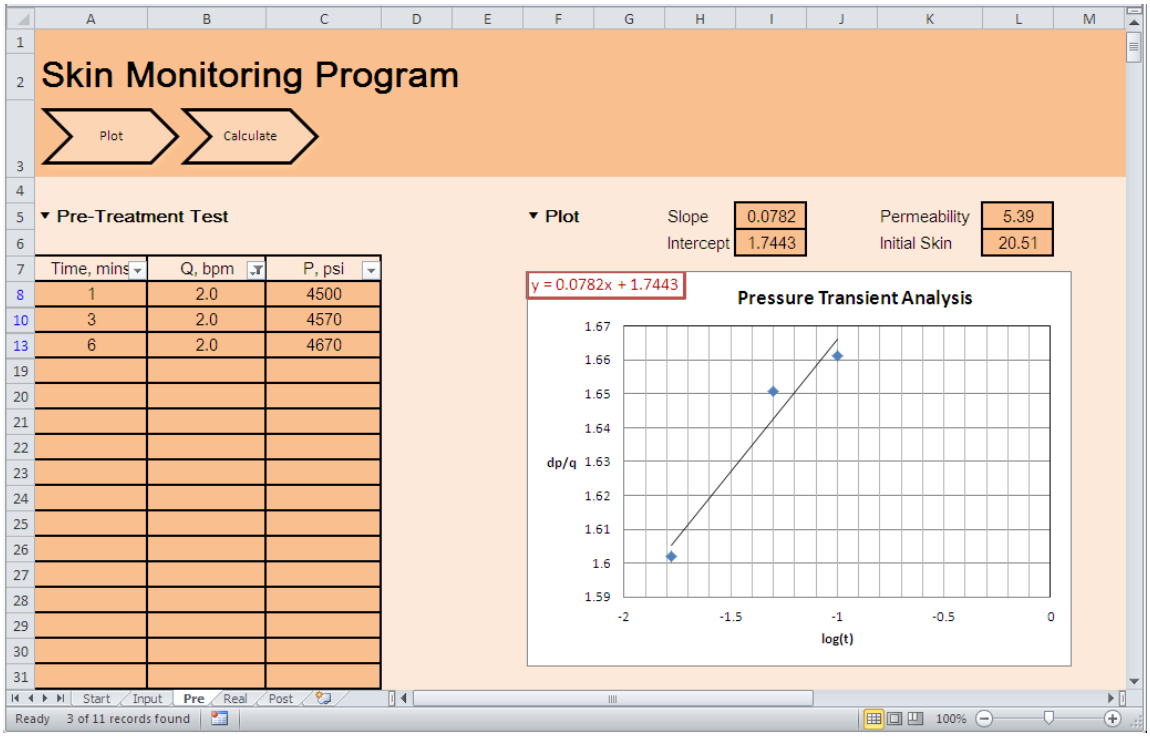

Fig. A12—The filtered data is plotted on the chart.

A4. Real-Time Monitoring Panel

If the option of real-time monitoring is selected on the options input panel, the Next button on the input panel will navigate to the panel shown in **Fig. A13.** All of the input data are necessary for the analysis, including the permeability and the initial skin factor. However, the initial skin factor may be assumed zero if it cannot be accurately determined using the pre-treatment test.

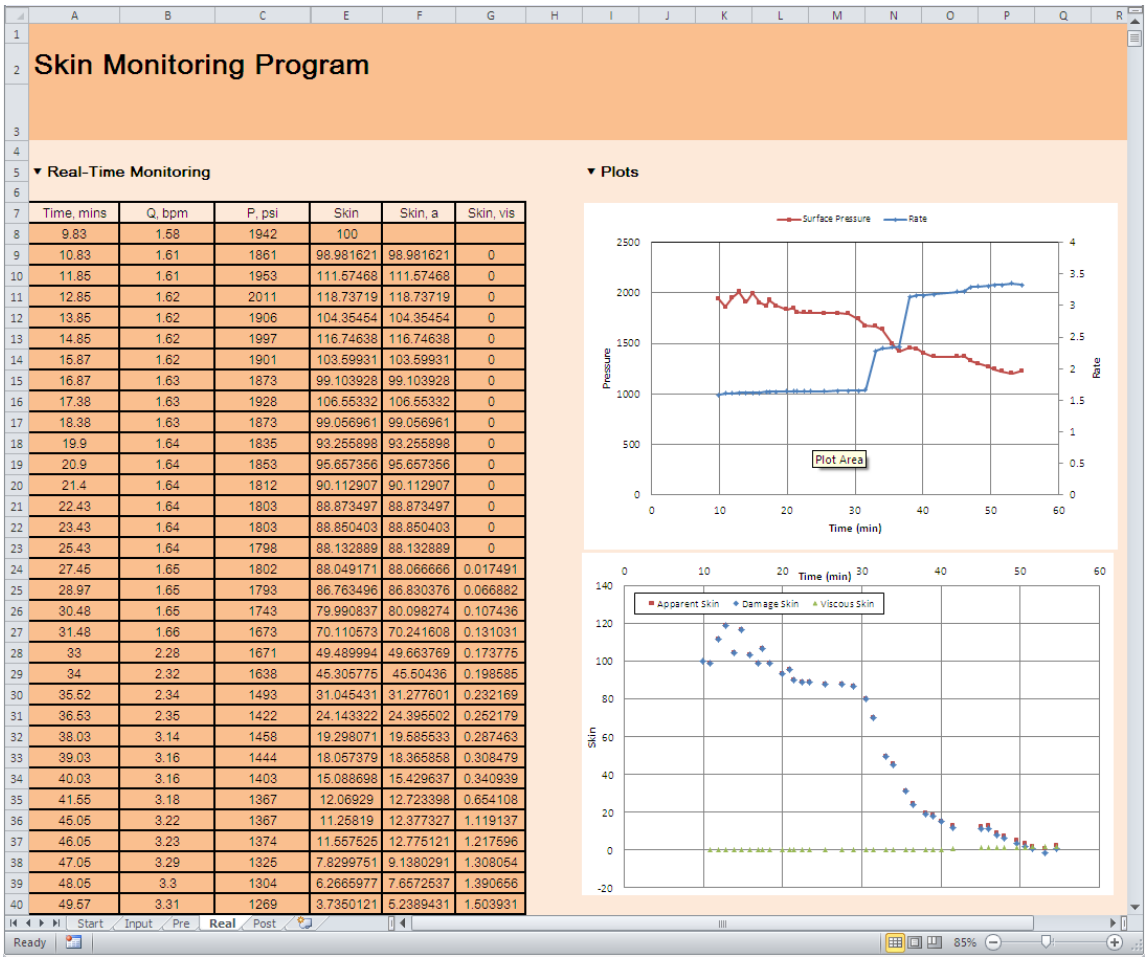

Time, mins	Q, bpm	P, psi	Skin	Skin, a	Skin, vis
9.83	1.58	1942	100		
10.83	1.61	1861	98.981621	98.981621	0
11.85	1.61	1963	111.57468	111.57468	0
12.85	1.62	2011	118.73719	118.73719	0
13.85	1.62	1906	104.35454	104.35454	0
14.85	1.62	1997	116.74638	116.74638	0
15.87	1.62	1901	103.59931	103.59931	0
16.87	1.63	1873	99.103928	99.103928	0
17.38	1.63	1928	106.55332	106.55332	0
18.38	1.63	1873	99.056961	99.056961	0
19.9	1.64	1835	93.255898	93.255898	0
20.9	1.64	1853	95.657356	95.657356	0
21.4	1.64	1812	90.112907	90.112907	0
22.43	1.64	1803	88.873497	88.873497	0
23.43	1.64	1803	88.850403	88.850403	0
25.43	1.64	1798	88.132889	88.132889	0
27.45	1.65	1802	88.049171	88.066666	0.017491
28.97	1.65	1793	86.763496	86.830376	0.066882
30.48	1.65	1743	79.990837	80.098274	0.107436
31.48	1.66	1673	70.110573	70.241608	0.131031
33	2.28	1671	49.489994	49.663769	0.173775
34	2.32	1638	45.305775	45.50436	0.198585
35.52	2.34	1493	31.045431	31.277601	0.232169
36.53	2.35	1422	24.143322	24.395502	0.252179
38.03	3.14	1458	19.298071	19.585533	0.287463
39.03	3.16	1444	18.057379	18.365858	0.308479
40.03	3.16	1403	15.088698	15.429637	0.340939
41.55	3.18	1367	12.06929	12.723398	0.654108
45.05	3.22	1367	11.25819	12.377327	1.119137
46.05	3.23	1374	11.557525	12.775121	1.217596
47.05	3.29	1325	7.8299751	9.1380291	1.308054
48.05	3.3	1304	6.2665977	7.6572537	1.390656
49.57	3.31	1269	3.7350121	5.2389431	1.503931

Fig. A13—The real-time monitoring panel.

In this panel, the measured time is in the first column, the flow rate is in the second column and the pressure is in the third column. The data is acquired into the program by manually typing the data using the keyboard. Once the pressure data is typed in the third column, the program calculates the damage skin factor at the current time in the fourth column. The fifth column is the calculated apparent skin and the sixth column is the calculated viscous skin. If the measured pressures are recorded at the surface, the program converts the surface pressure to bottomhole pressure, and puts the bottomhole

pressure in the fourth column, thereby, shifting the calculated skin factor columns to the right.

Also, the program plots two graphs automatically. The first graph is the treatment data versus time, and the second graph is the skin factor versus time. One requirement for the program is that at least one fluid needs to be input in the injection schedule input panel. If the injection schedule for the treatment is uncertain, it is suggested that the user input a large injection volume for the first fluid that is to be injected to avoid erroneous skin calculations.

A5. Post-Treatment Study Panel

The post-treatment study is done after the acidizing treatment is completed. This study aims at evaluating the treatments to improve future treatment designs. If the option of post-treatment study is selected on the options input panel, the Next button on the input panel will navigate to the panel shown in **Fig. A14.**

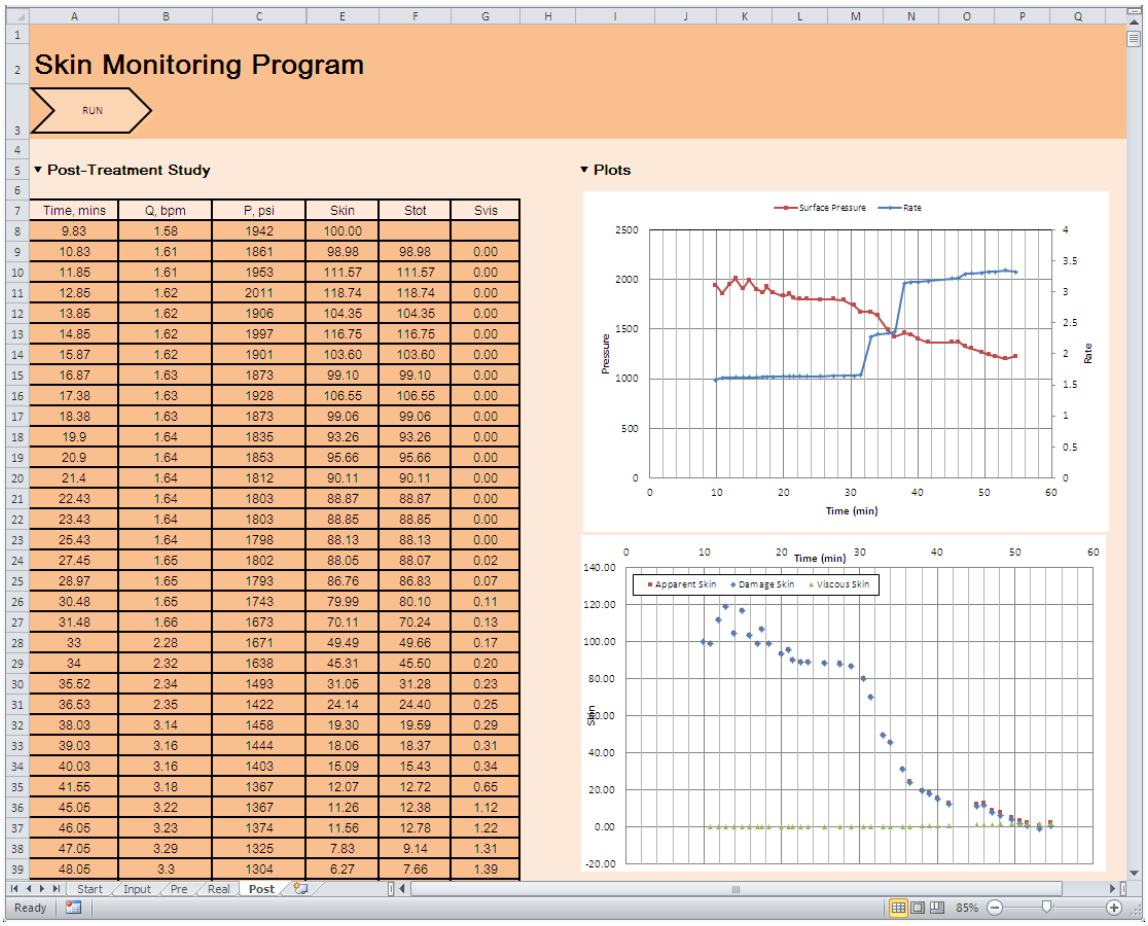

Time, mins	Q, bpm	P, psi	Skin	Stot	Svis
9.83	1.58	1942	100.00		
10.83	1.61	1861	98.98	98.98	0.00
11.85	1.61	1953	111.57	111.57	0.00
12.85	1.62	2011	118.74	118.74	0.00
13.85	1.62	1906	104.35	104.35	0.00
14.85	1.62	1997	116.75	116.75	0.00
15.87	1.62	1901	103.60	103.60	0.00
16.87	1.63	1873	99.10	99.10	0.00
17.38	1.63	1928	106.55	106.55	0.00
18.38	1.63	1873	99.06	99.06	0.00
19.9	1.64	1835	93.26	93.26	0.00
20.9	1.64	1853	95.66	95.66	0.00
21.4	1.64	1812	90.11	90.11	0.00
22.43	1.64	1803	88.87	88.87	0.00
23.43	1.64	1803	88.85	88.85	0.00
25.43	1.64	1798	88.13	88.13	0.00
27.45	1.65	1802	88.05	88.07	0.02
28.97	1.65	1793	86.76	86.83	0.07
30.48	1.65	1743	79.99	80.10	0.11
31.48	1.66	1673	70.11	70.24	0.13
33	2.28	1671	49.49	49.66	0.17
34	2.32	1638	45.31	45.50	0.20
35.52	2.34	1493	31.05	31.28	0.23
36.53	2.35	1422	24.14	24.40	0.25
38.03	3.14	1458	19.30	19.59	0.29
39.03	3.16	1444	18.06	18.37	0.31
40.03	3.16	1403	15.09	15.43	0.34
41.55	3.18	1367	12.07	12.72	0.65
45.05	3.22	1367	11.26	12.38	1.12
46.05	3.23	1374	11.56	12.78	1.22
47.05	3.29	1325	7.83	9.14	1.31
48.05	3.3	1304	6.27	7.66	1.39

Fig. A14—The post-treatment study panel.

Similar to the real-time monitoring panel, the measured time is in the first column, the flow rate is in the second column, and the pressure is in the third column in the above panel. However, the skin factor and bottomhole pressure are calculated by clicking on the Run button. These values are subsequently generated in the other columns as seen in Fig. A14.

APPENDIX B

TREATMENT EVALUATION FOR ADDITIONAL WELLS

B1. Well 1

Treatment Description

This well is a horizontal well with a cased and perforated completion, as seen below in the well diagram. The actual acidizing treatment design comprised of bullheading 22% carbonate emulsion acid (CEA) through coil-tubing followed by fresh water displacement stage.

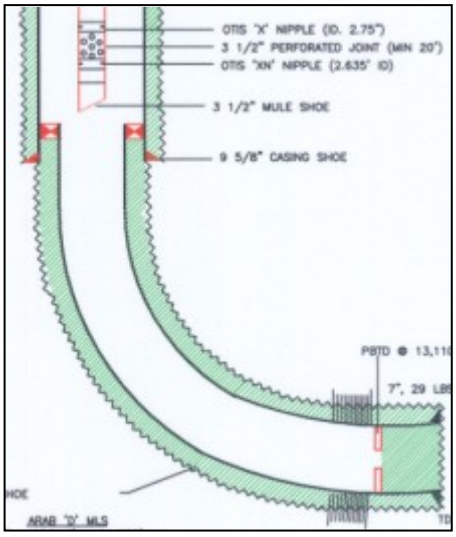

Fig. B1—Well diagram for Well 1.

The data for the reservoir, the wellbore, and the acid injection is shown in the tables below.

Table B1—Reservoir Properties for Well 1

Initial Reservoir Pressure, psi	2600
Formation Volume Factor	1.35
Porosity	0.15
Total Compressibility, 1/psi	3.50E-06
Formation Thickness, ft	435
Reservoir Fluid Viscosity, cp	0.46
Permeability, md	24
Anisotropy	0.1

Table B2—Wellbore Properties for Well 1

Wellbore Radius, in	3.092
Tubing Diameter, in	2.992
Relative Roughness	0.0001
Vertical Depth, ft	7636
Measured Depth, ft	10940
Horizontal Length, ft	2855
Well Fluid Density, lbm/ft3	63.58
Well Fluid Viscosity, cp	1

Table B3—Acid Injection Schedule for Well 1

Fluid Name	Volume Used, gal	Density, lb/ft3	Viscosity, cp	Friction Reducer
Acid	21538	63.18	4	0.7
Water	15550	60.85	1	0.7

Skin Monitoring Results

The surface pressure and injection rate data was measure on-site during the acid job. The figure below plots the measured injection rate, and the measured surface pressure recorded during the acidizing treatment.

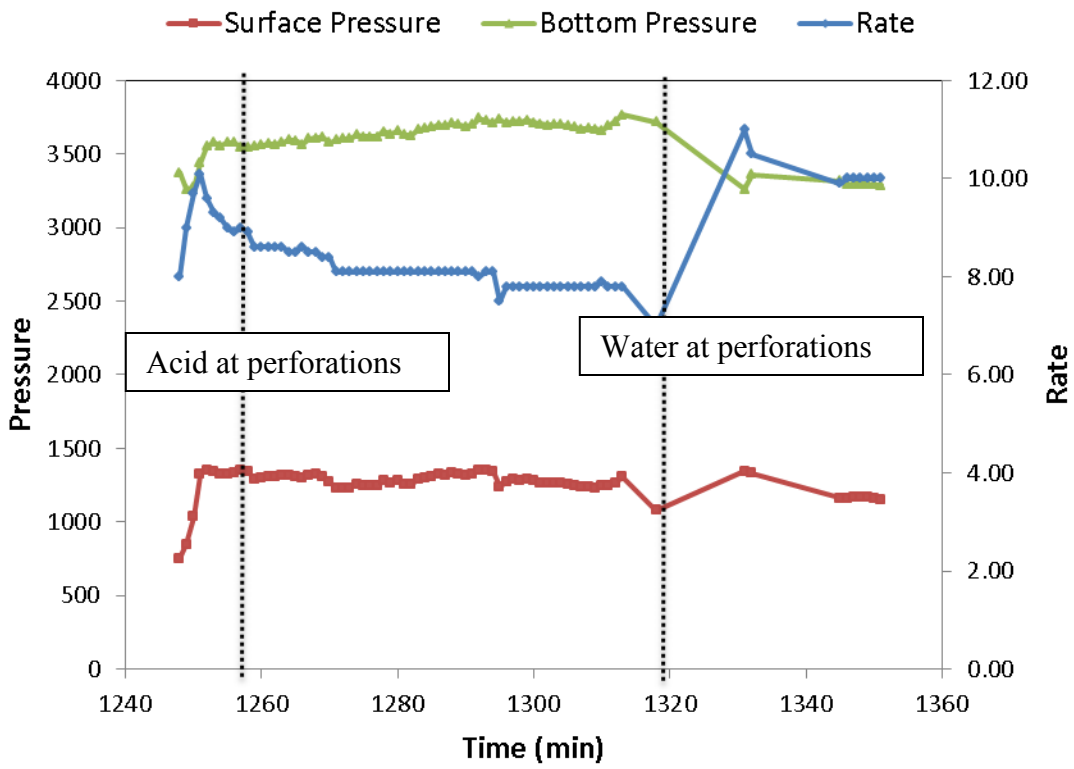

Fig. B2—Treatment data for Well 1.

In the figure above, the bottomhole pressure was calculated from the surface pressure. From the calculated bottomhole pressure and measured injection rate, the skin was calculated at each time step. The skin evolution during the acid job is shown in the figure below.

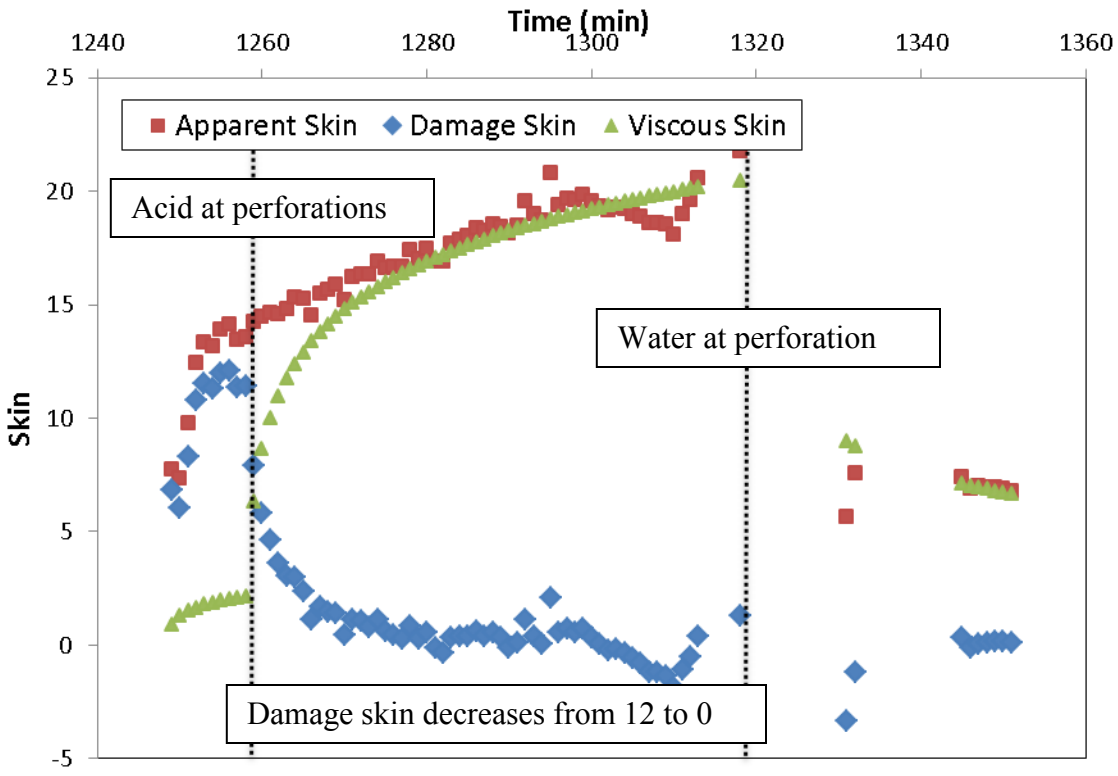

Fig. B3—Skin response for Well 1.

Discussion of Results

In the figure above, viscous effects due to the emulsified acid is clearly evident because the apparent skin begins to increase when the acid front enters the formation. It is observed that the 22% CEA system was effective as a viscous diverter for the stimulation treatment.

The viscous skin was estimated and matched the apparent skin for the CEA stage. The increasing trend of viscous skin factor resulted in a decreasing trend in the damage skin factor. It is noticed that the volume of acid injected was sufficient as the damage skin continues to reduce until the end of the acid injection and remains constant for water injection.

The skin trend was validated using the production test from before and after the well is stimulated. In this case, the production rate of liquids from this well after stimulation increased from 1910 barrels/day to 5557 barrels/day. Therefore, the production test confirms that the acidizing treatment was successful.

B2. Well 2

Treatment Description

This well is a vertical well with a cased and perforated completion, as seen below in the well diagram. The actual acidizing treatment design comprised of two stages: 15% hydrochloric acid (HCL) and 22% carbonate emulsion acid (CEA).

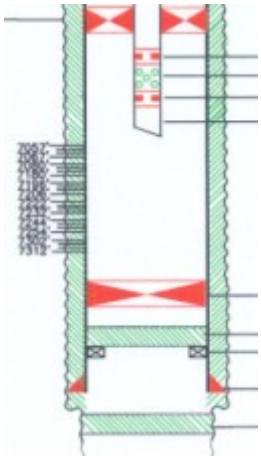

Fig. B4—Well diagram for Well 2.

The data for the reservoir, the wellbore, and the acid injection is shown in the tables below.

Table B4—Reservoir Properties for Well 2

Initial Reservoir Pressure, psi	2200
Formation Volume Factor	1.35
Porosity	0.2
Total Compressibility, 1/psi	3.50E-06
Formation Thickness, ft	321
Reservoir Fluid Viscosity, cp	0.46
Permeability, md	3

Table B5—Wellbore Properties for Well 2

Wellbore Radius, in	3.5
Tubing Diameter, in	1.78
Relative Roughness	0.0001
Vertical Depth, ft	7295
Measured Depth, ft	7360
Well Fluid Density, lbm/ft3	65.62
Well Fluid Viscosity, cp	0.46

Table B6—Acid Injection Schedule for Well 2

Fluid Name	Volume Used, gal	Density, lb/ft3	Viscosity, cp	Friction Reducer
HCl	3000	65.62	0.46	1
CEA	7498	63.19	4	1
Flush	4411	62.71	1	1

Skin Monitoring Results

The surface pressure and injection rate data was measure on-site during the acid job. The figure below plots the measured injection rate, and the measured surface pressure recorded during the acidizing treatment.

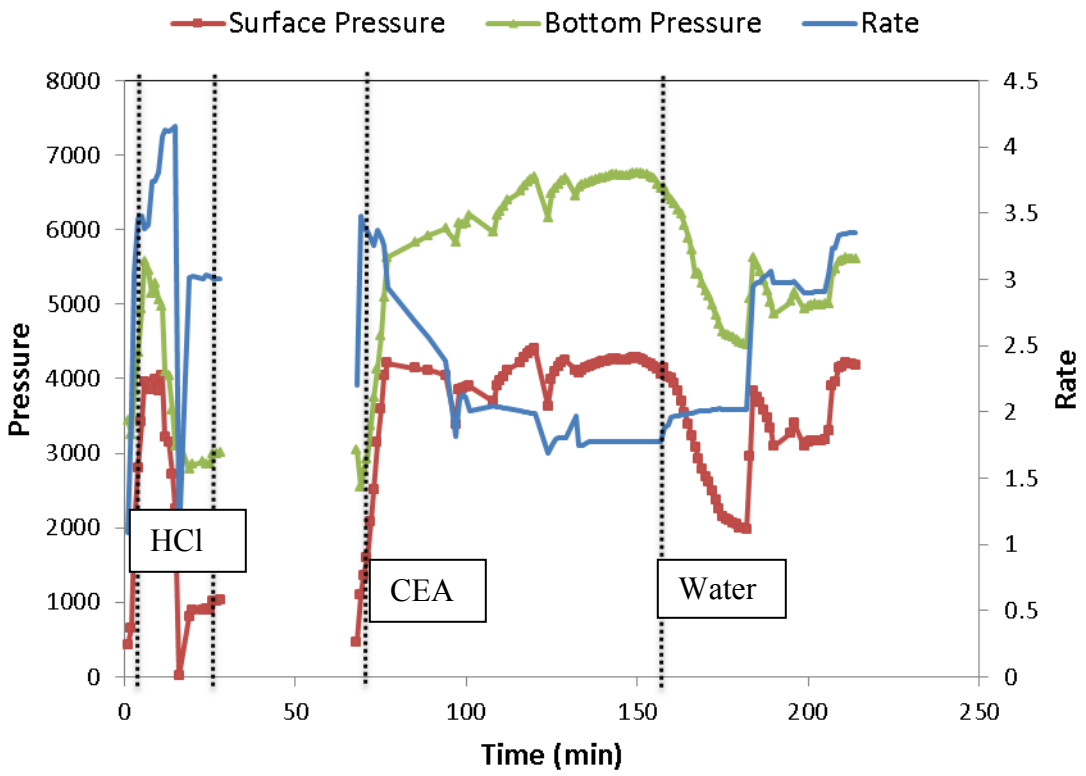

Fig. B5—Treatment data for Well 2.

In the figure above, the bottomhole pressure was calculated from the surface pressure. From the calculated bottomhole pressure and measured injection rate, the skin was calculated at each time step. The skin evolution during the acid job is shown in the figure below.

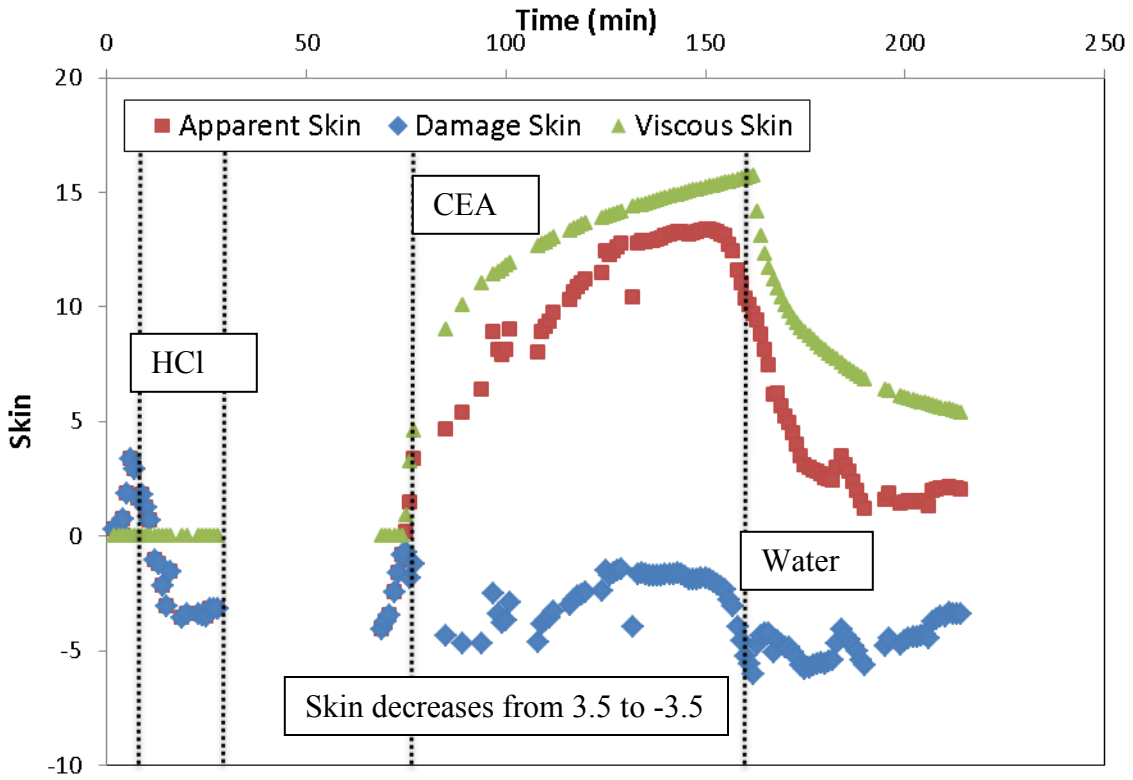

Fig. B6—Skin response for Well 2.

Discussion of Results

In the figure above, the skin value decreases from 3.5 to -3.5 for the entire treatment duration. However, it is inferred that mainly HCl acid system contributed to the skin decline. Furthermore, the viscous effects due to the emulsified acid are clearly evident because the apparent skin begins to increase when the CEA acid front was at the end of the tubing. Therefore, the 22% CEA system was effective as a viscous diverter for the stimulation treatment.

The viscous skin was estimated and matched the apparent skin for the CEA stage. The increasing trend of viscous skin factor resulted in constant flat trend in the damage skin factor. Thus, the damage skin factor remains almost constant after the HCl stage.

The skin trend was validated using the production test from before and after the well is stimulated. In this case, the production rate of oil from this well after stimulation increased from 1530 barrels/day to 1739 barrels/day. Therefore, the production test indicates that the treatment was successful.

B3. Well 3

Treatment Description

This well is a horizontal well with an open-hole lateral, as seen below in the well diagram. The actual acidizing treatment was divided into two parts. The first part consisted of injection of viscoelastic surfactants (VES) followed by injection of mutual solvent solution. And, the second part comprised of alternate injection stages of VES and hydrochloric acid (HCl) followed by displacement with diesel and fresh water.

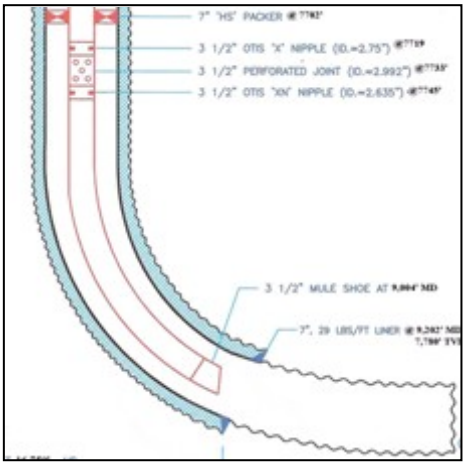

Fig. B7—Well diagram for Well 3.

The data for the reservoir, the wellbore, and the acid injection is shown in the tables below.

Table B7—Reservoir Properties for Well 3

Initial Reservoir Pressure, psi	3000
Formation Volume Factor	1.397
Porosity	0.165
Total Compressibility, 1/psi	3.50E-06
Formation Thickness, ft	16
Reservoir Fluid Viscosity, cp	0.51
Permeability, md	5
Anisotropy	0.1

Table B8—Wellbore Properties for Well 4

Wellbore Radius, in	3
Tubing Diameter, in	1.75
Relative Roughness	0.0001
Vertical Depth, ft	8007
Measured Depth, ft	12800
Horizontal Length, ft	4600
Well Fluid Density, lbm/ft3	63.58
Well Fluid Viscosity, cp	0.51

Table B9—Acid Injection Schedule for Well 3

Stage	Fluid Name	Volume Used, gal	Density, lb/ft3	Viscosity, cp	Friction Reducer
1	VES	16798	63.58	0.51	1
2	Fresh Water	2520	63.58	0.51	1
3	Fresh Water	840	63.58	0.51	1
4	Mutual Solvent	7476	63.58	0.51	1
5	Fresh Water	2310	63.58	0.51	1
6	HCl	8819	63.58	0.51	1
7	VES	2100	63.58	0.51	1
8	HCl	8820	63.58	0.51	1
9	VES	2100	63.58	0.51	1
10	HCl	8820	63.58	0.51	1
11	Diesel	9032	63.58	0.51	1
12	Fresh Water	2312	63.58	0.51	1

Skin Monitoring Results

The figure below plots the measured injection rate, and the measured surface pressure recorded during the acidizing treatment.

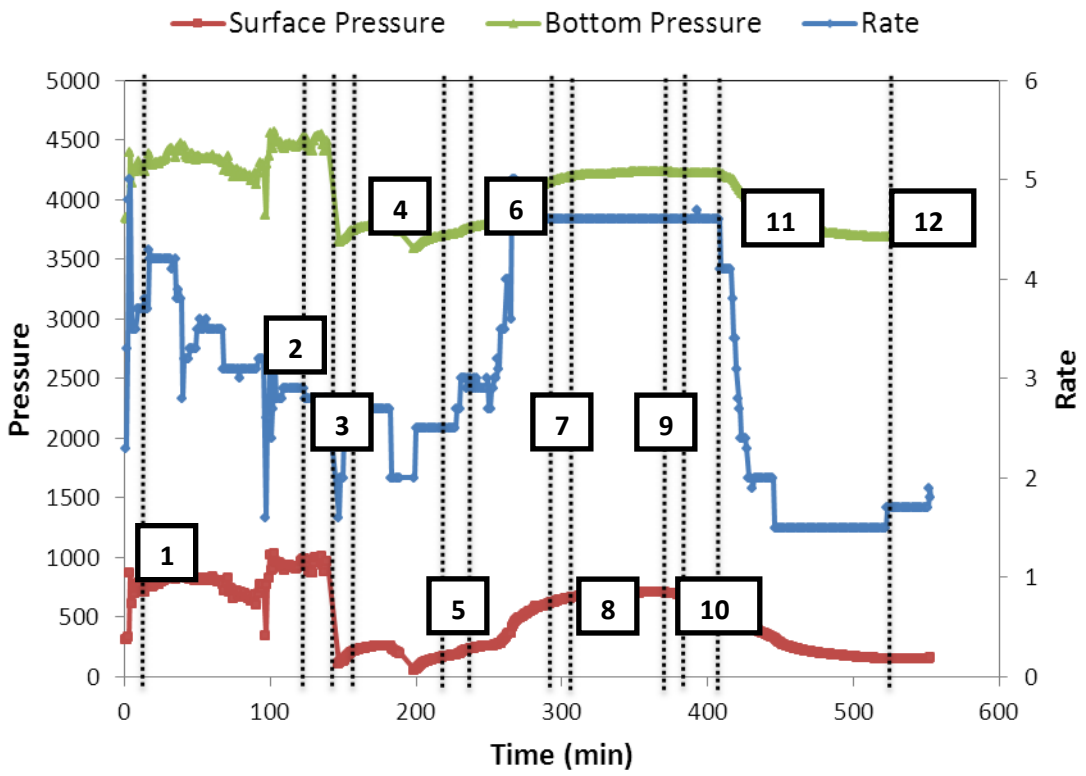

Fig. B8—Treatment data for Well 3.

In the figure above, the bottomhole pressure was calculated from the surface pressure. Also, the numbered flags in the above figure represent the corresponding stage fluid as it enters into the formation. From the calculated bottomhole pressure and measured injection rate, the skin was calculated at each time step. The skin evolution during the acid job is shown in the figure below.

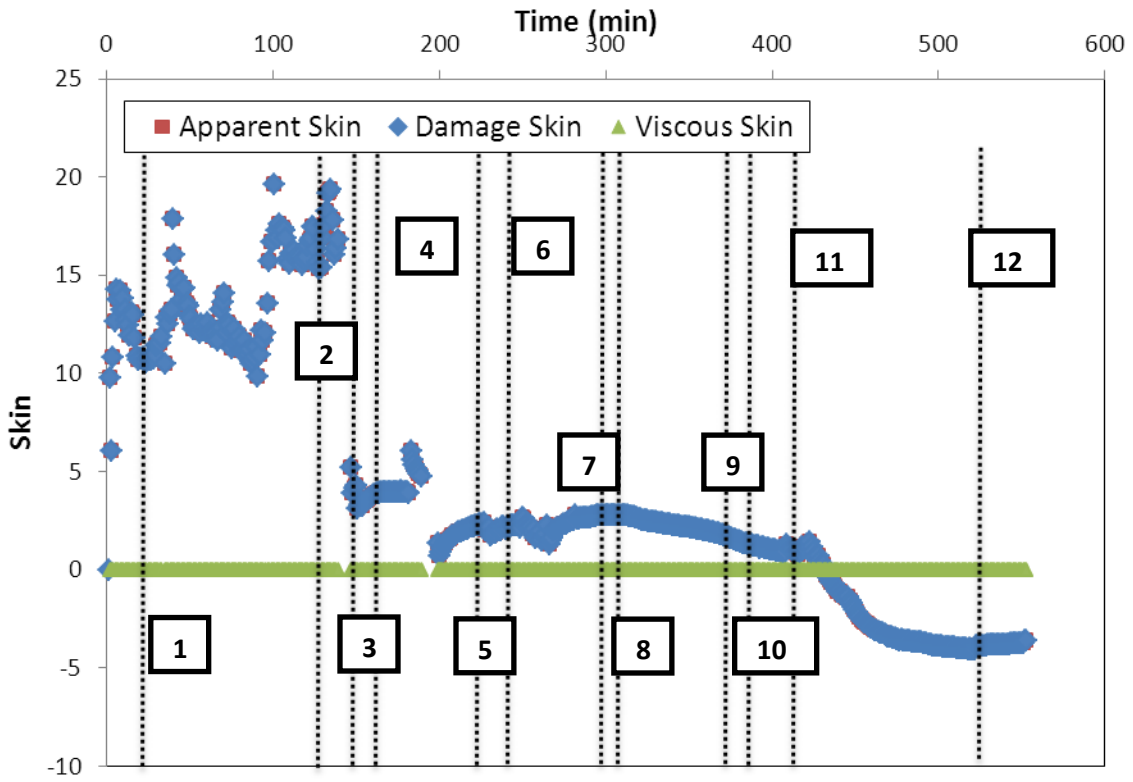

Fig. B9—Skin response for Well 3.

Discussion of Results

In the figures above, typical wavy pressure and skin behaviors are noticed for the first VES injection (stage 1). The injection of mutual solvent (stage 4) decreased the skin, from 15 to 5, by breaking up the viscous polymers and reducing their viscosity of VES in the formation.

The similar wavy behavior was not seen during the alternate injection stages of VES and HCl due to lesser VES volumes. However, the injection of HCl and diesel (stages 6, 8, 10, and 11) resulted in major skin decline from 5 to -4. It is inferred that the volume of acid injected was sufficient as the damage skin continues to reduce until the end of the acid injection and remains constant for water injection.

The skin trend was validated using the production test from before and after the well is stimulated. In this case, the production rate of liquids from this well after stimulation increased from 1471 barrels/day to 2288 barrels/day. Therefore, the production test confirms that the acidizing treatment was.

B4. Well 4

Treatment Description

This well is a horizontal well with an open-hole lateral, as seen in the well diagram below. The actual acidizing treatment design comprised of treating the target interval with 22% carbonate emulsion acid (CEA) using coil-tubing.

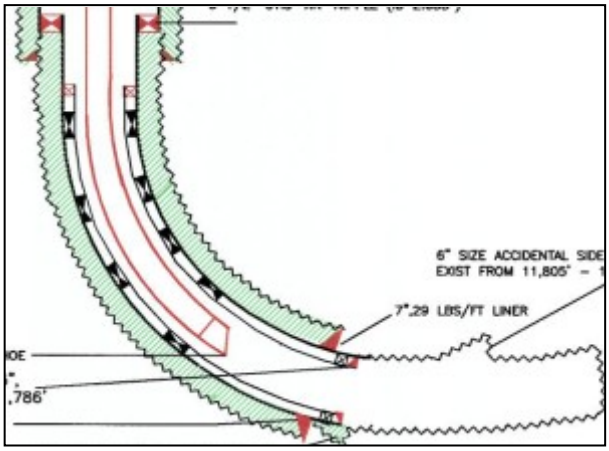

Fig. B10—Well diagram for Well 4.

The data for the reservoir, the wellbore, and the acid injection is shown in the tables below.

Table B10—Reservoir Properties for Well 4

Initial Reservoir Pressure, psi	2500
Formation Volume Factor	1.397
Porosity	0.21
Total Compressibility, 1/psi	3.50E-06
Formation Thickness, ft	40
Reservoir Fluid Viscosity, cp	0.51
Permeability, md	1
Anisotropy	0.1

Table B11—Wellbore Properties for Well 4

Wellbore Radius, in	4.25
Tubing Diameter, in	1.688
Relative Roughness	0.0001
Vertical Depth, ft	7821
Measured Depth, ft	14440
Horizontal Length, ft	4102
Well Fluid Density, lbm/ft3	64.3
Well Fluid Viscosity, cp	0.51

Table B12—Acid Injection Schedule for Well 4

Fluid Name	Volume Used, gal	Density, lb/ft3	Viscosity, cp	Friction Reducer
Flush	414	63.3	0.51	1
CEA	20510	64.3	0.51	1
Flush	2964	62.3	0.51	1

Skin Monitoring Program Results

The surface pressure and injection rate data was measure on-site during the acid job. The figure below plots the measured injection rate, and the measured surface pressure recorded during the acidizing treatment.

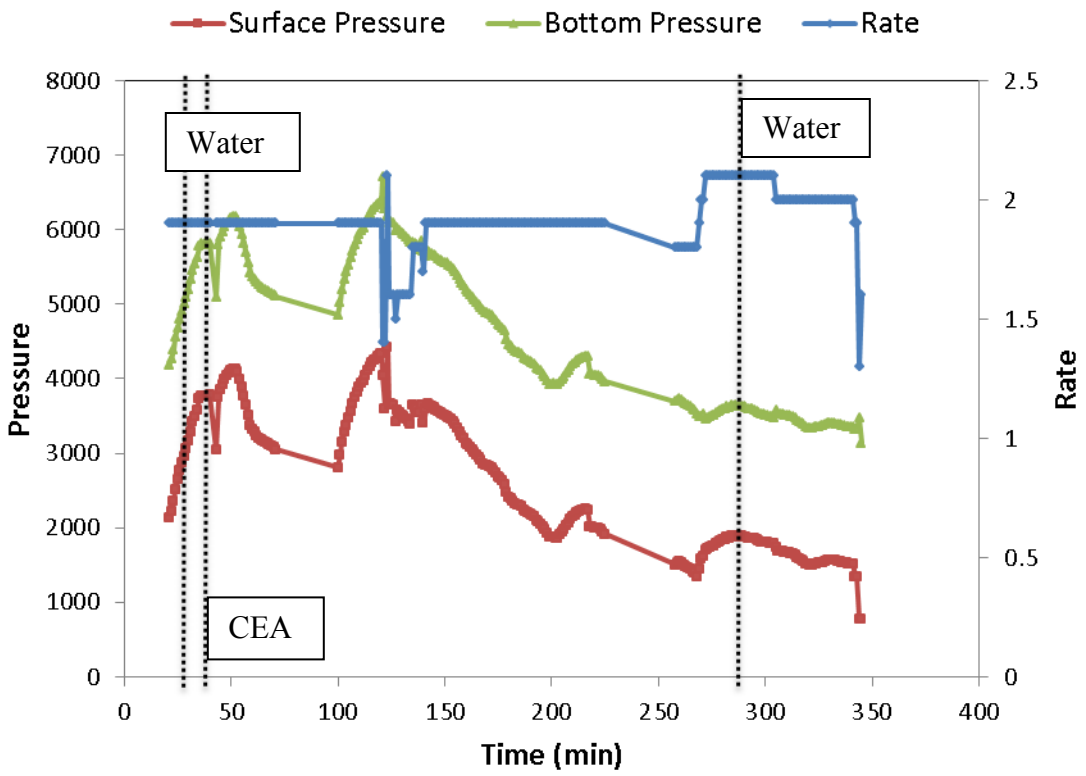

Fig. B11—Treatment data for Well 4.

In the figure above, the bottomhole pressure was calculated from the surface pressure. From the calculated bottomhole pressure and measured injection rate, the skin was calculated at each time step. The skin evolution during the acid job is shown in the figure below.

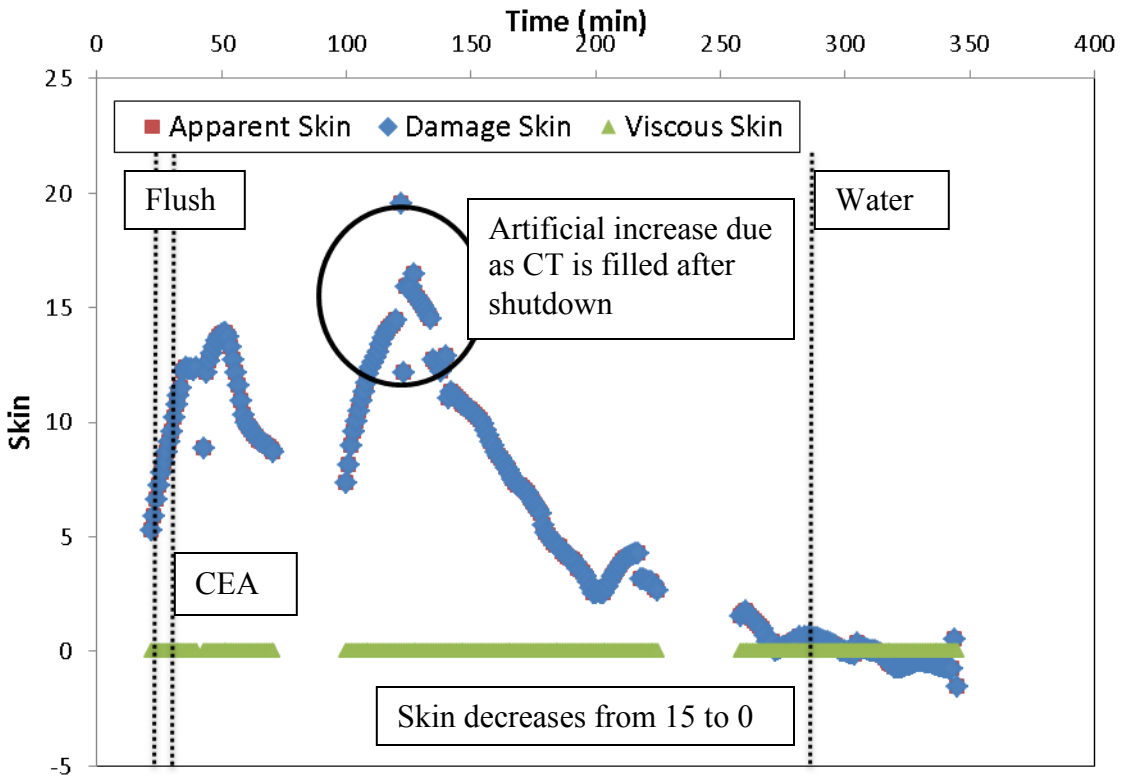

Fig. B12—Skin response for Well 4.

Discussion of Results

In the figure above, the skin begins to decrease when the acid front enters the formation, and the skin value decreases from 15 to 0 by the end of acid injection. It is noticed that the volume of acid injected was sufficient as the skin continues to decrease until the end of the injection. Also, the skin trend flattens during the water injection.

For the most part of the treatment, the emulsified acid did not show any evidence of viscous diversion because no increasing trend in the skin is noticed. However, the small increase in the skin trend may be a result of increase in pressure as the coil-tubing is filled with the acid after the pump shutdown.

The skin trend was validated using the production test from before and after the stimulation process. In this case, the production rate of liquids from this well after stimulation increased from 316 barrels/day to 1400 barrels/day. However, the flowrate decreased to 400 barrels/day within 12 hours of production. The formation damage reported was due to the presence of bitumen (tar) in the formation. Although, the treatment was initially successful in increasing production, the bitumen present in the reservoir returned to lower the productivity of this well.

B5. Well 5

Treatment Description

This well is a horizontal well with an open-hole lateral, as seen in the well diagram below. The actual acidizing treatment design comprised of treating the target interval with 15% hydrochloric acid (HCl) using coil-tubing.

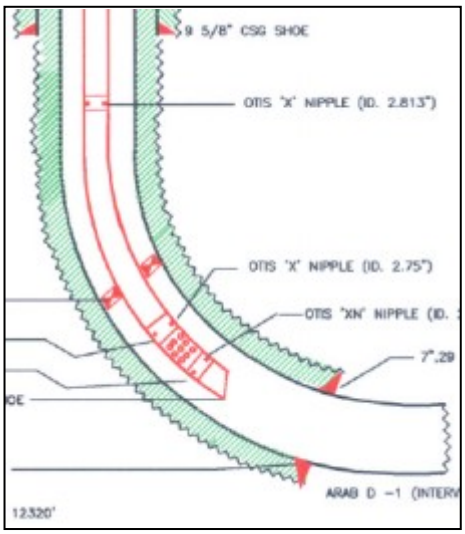

Fig. B13—Well diagram for Well 5.

The data for the reservoir, the wellbore, and the acid injection is shown in the tables below.

Table B13—Reservoir Properties for Well 5

Initial Reservoir Pressure, psi	2500
Formation Volume Factor	1.397
Porosity	0.21
Total Compressibility, 1/psi	3.50E-06
Formation Thickness, ft	40
Reservoir Fluid Viscosity, cp	0.51
Permeability, md	1
Anisotropy	0.1

Table B14—Wellbore Properties for Well 5

Wellbore Radius, in	4.25
Tubing Diameter, in	1.688
Relative Roughness	0.0001
Vertical Depth, ft	7821
Measured Depth, ft	14440
Horizontal Length, ft	4102
Well Fluid Density, lbm/ft3	64.3
Well Fluid Viscosity, cp	0.51

Table B15—Acid Injection Schedule for Well 5

Fluid Name	Volume Used, gal	Density, lb/ft3	Viscosity, cp	Friction Reducer
Flush	414	63.3	0.51	1
CEA	20510	64.3	0.51	1
Flush	2964	62.3	0.51	1

Skin Monitoring Results

The surface pressure and injection rate data was measure on-site during the acid job. The figure below plots the measured injection rate, and the measured surface pressure recorded during the acidizing treatment.

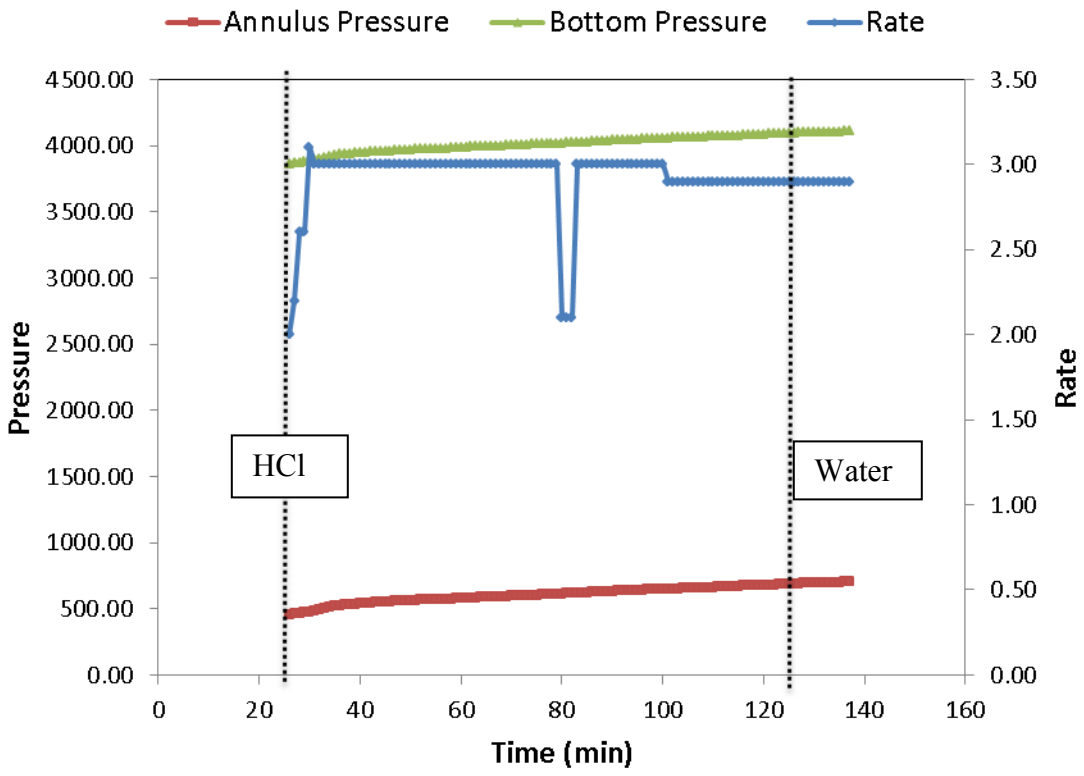

Fig. B14—Treatment data for Well 5.

In the figure above, the bottomhole pressure was calculated from the annulus pressure. From the calculated bottomhole pressure and measured injection rate, the skin was calculated at each time step. The skin evolution during the acid job is shown in the figure below.

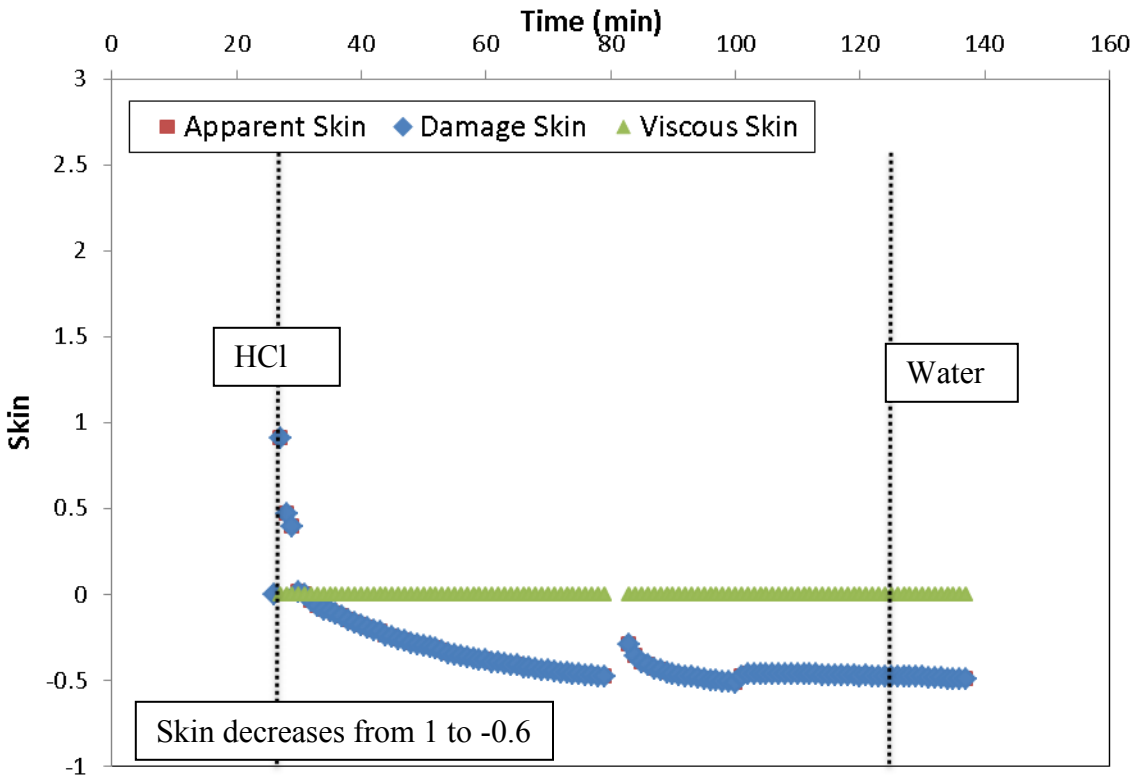

Fig. B15—Skin response for Well 5.

Discussion of Results

In the figure above, the skin begins to decrease when the acid front enters the formation, and the skin value decreases from 1 to -0.6 by the end of acid injection. It is noticed that the designed acid coverage was not sufficient as the skin begins to flatten towards the end of acid injection.

The skin trend was validated using the production test from before and after the stimulation process. In this case, the production rate of liquids from this well after stimulation increased from 2653 barrels/day to 2757 barrels/day. Therefore, the production test confirms the decreasing skin trend.

B6. Well 6

Treatment Description

This well is a vertical well with a cased and perforated completion, as seen below in the well diagram. The actual acidizing treatment design comprised of alternate stages of bullheading 22% carbonate emulsion acid (CEA) and associative polymer solution. Sea water was injected instead of fresh water for the water displacement stage.

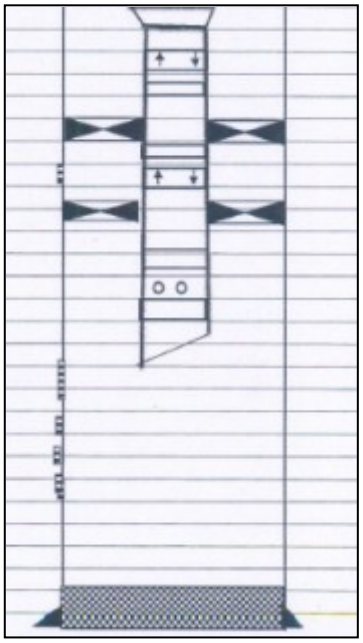

Fig. B16—Well diagram for Well 6.

The data for the reservoir, the wellbore, and the acid injection is shown in the tables below.

Table B16—Reservoir Properties for Well 6

Initial Reservoir Pressure, psi	3200
Formation Volume Factor	1.397
Porosity	0.22
Total Compressibility, 1/psi	3.50E-06
Formation Thickness, ft	421
Reservoir Fluid Viscosity, cp	0.51
Permeability, md	100

Table B17—Wellbore Properties for Well 6

Wellbore Radius, in	6.125
Tubing Diameter, in	4
Relative Roughness	0.0001
Vertical Depth, ft	7500
Measured Depth, ft	7500
Well Fluid Density, lbm/ft3	63.58
Well Fluid Viscosity, cp	0.51

Table B18—Acid Injection Schedule for Well 6

Stage	Fluid Name	Volume Used, gal	Density, lb/ft3	Viscosity, cp	Friction Reducer
1	CEA 22%	2752	62.76	0.51	1
2	Polymer Diverter	4114	62.1	0.51	1
3	CEA 22%	5506	63.84	0.51	1
4	Polymer Diverter	5502	62	0.51	1
5	CEA 22%	5513	64.18	0.51	1
6	Sea Water	10500	63.49	0.51	1

Skin Monitoring Results

The figure below plots the measured injection rate, and the measured surface pressure recorded during the acidizing treatment.

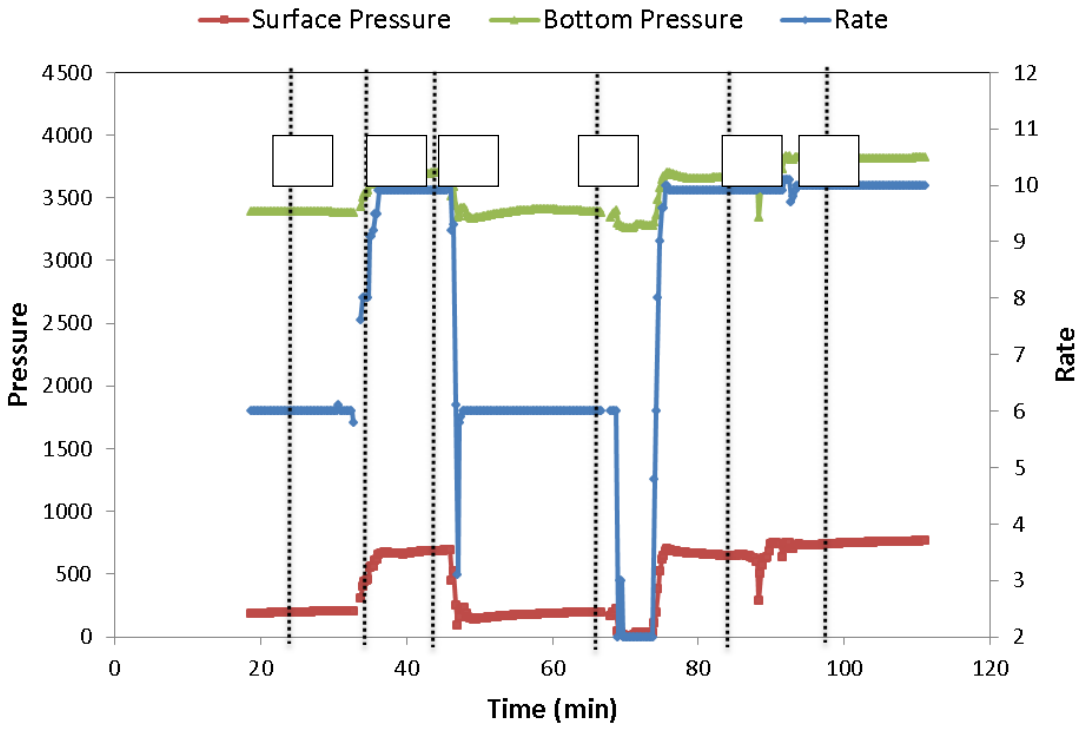

Fig. B17—Treatment data for Well 6.

In the figure above, the bottomhole pressure was calculated from the surface pressure. From the calculated bottomhole pressure and measured injection rate, the skin was calculated at each time step. The numbered flags indicate the time when the corresponding stage fluids hit the formation. The skin evolution during the acid job is shown in the figure below.

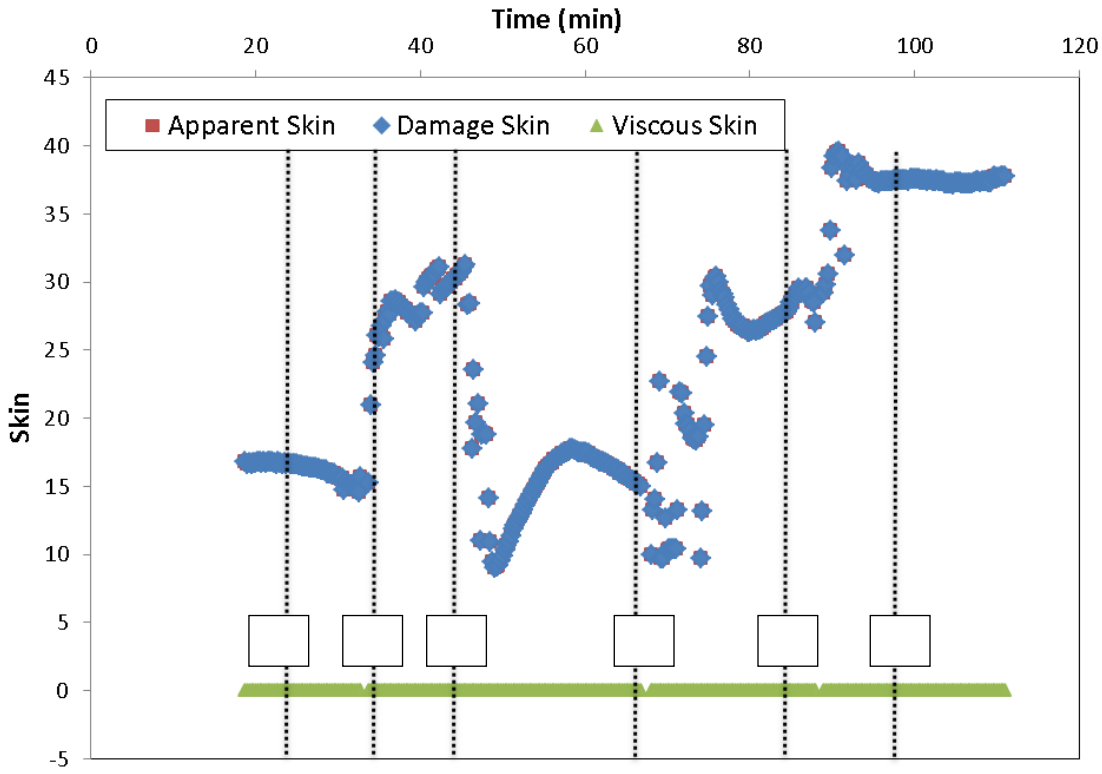

Fig. B18—Skin evolution for Well 6.

Discussion of Results

In the figure above, the skin slightly decreases initially during the injection of first emulsified acid stage (stage 1). During injection of polymer diverter in stage 2, the skin increases due to increase in the viscosity of polymer diverter as it associates with water and spent acid. In stage 3, the hydrocarbon base of the emulsified acid breaks the viscosified solution. Again, the skin increases during the injection of polymer diverter (stage 4).

However, the emulsified acid injection during stage 5 continues to increase skin and is not able to reduce the viscosity of the polymer. Therefore, the volume of

emulsified acid injected during stage 5 was not sufficient. During sea water injection (stage 6), the skin does not decrease and remains constant. Usually, the displacement stage should be comprised of diesel or mutual solvent to break the viscous polymer solution.

The productivity index ratio from the initial and final skin value was estimated to be 0.58, assuming the drainage radius (r_e) of 1000 ft. The skin trend was validated using the production test from before and after the well is stimulated. The production rate of liquids from this well after stimulation decreased from 11400 barrels/day to 4361 barrels/day. However, after the stimulation process, the water cut declined from 75% to 66%. Therefore, the associative polymer acid system reduced production by adding formation damage.

B7. Well 7

Treatment Description

This well is a horizontal well with an open-hole lateral, as seen in the well diagram below. The actual acidizing treatment design comprised of treating the target interval with 15% hydrochloric acid and 22% carbonate emulsion acid (CEA).

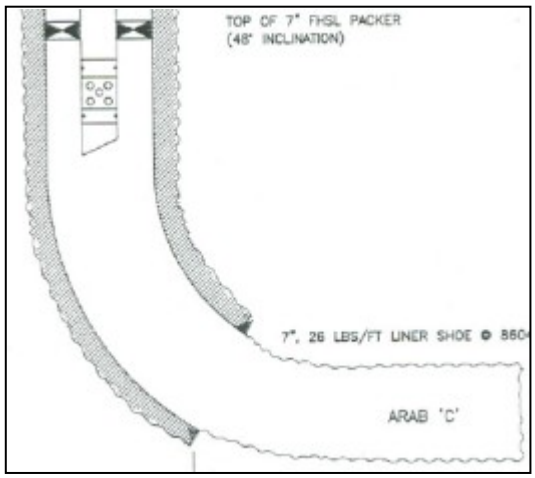

Fig. B19—Well diagram for Well 7.

The data for the reservoir, the wellbore, and the acid injection is shown in the tables below.

Table B 19—Reservoir Properties for Well 7

Initial Reservoir Pressure, psi	2000
Formation Volume Factor	2
Porosity	0.12
Total Compressibility, 1/psi	3.50E-06
Formation Thickness, ft	10
Reservoir Fluid Viscosity, cp	0.21
Permeability, md	0.6
Anisotropy	0.1

Table B20—Wellbore Properties for Well 7

Wellbore Radius, in	3
Tubing Diameter, in	1.688
Relative Roughness	0.0001
Vertical Depth, ft	7842
Measured Depth, ft	10280
Horizontal Length, ft	1673
Well Fluid Density, lbm/ft3	61.11
Well Fluid Viscosity, cp	0.21

Table B21—Acid Injection Schedule for Well 7

Fluid Name	Volume Used, gal	Density, lb/ft3	Viscosity, cp	Friction Reducer
HCl 15%	16791.6	65.82	0.21	0.1
CEA 20%	36141	65.07	0.21	0.1
Flush	7000	62.83	0.21	0.1

Skin Monitoring Results

The figure below plots the measured injection rate, and the measured surface pressure recorded during the acidizing treatment.

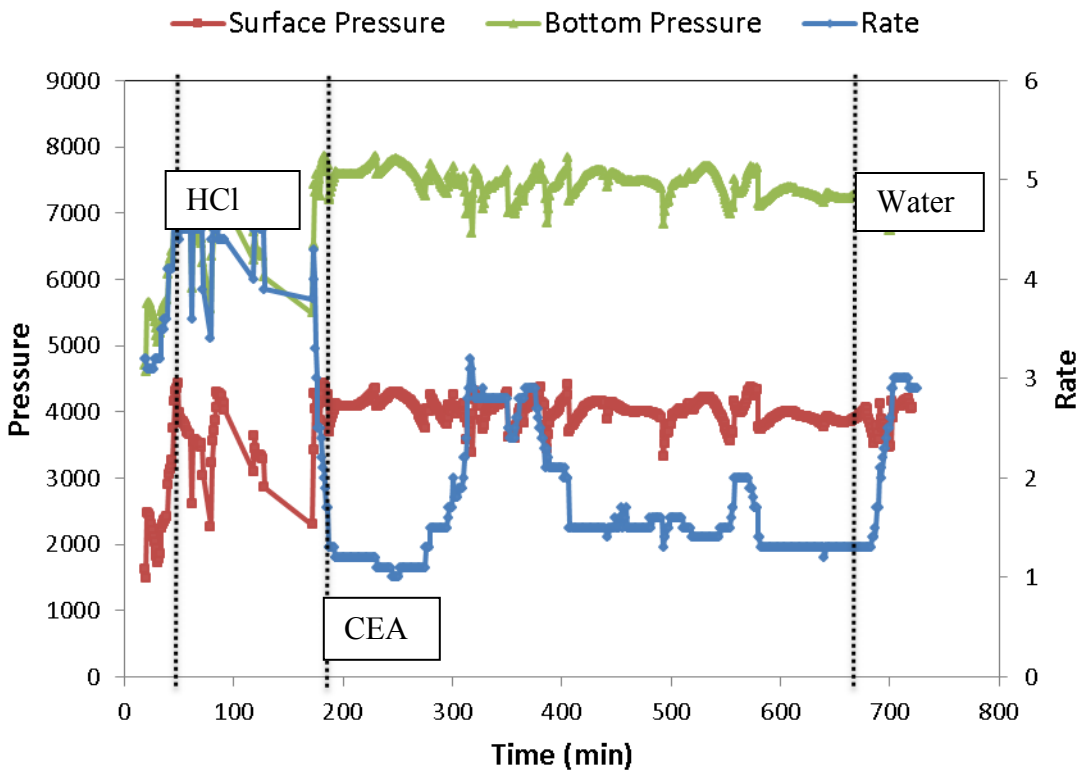

Fig. B20—Treatment data for Well 7.

In the figure above, the bottomhole pressure was calculated from the surface pressure. From the calculated bottomhole pressure and measured injection rate, the skin was calculated at each time step. The skin evolution during the acid job is shown in the figure below.

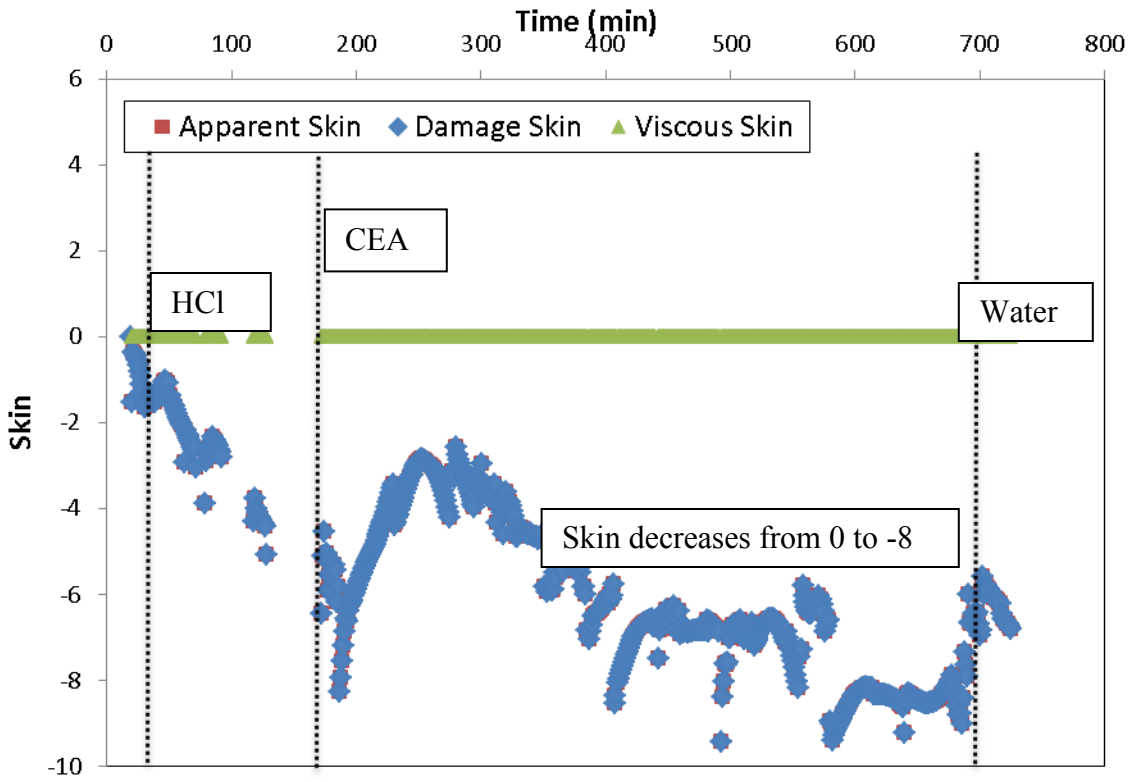

Fig. B21—Skin response for Well 7.

Discussion of Results

In the figure above, the skin begins to decrease during HCl injection, and the skin continues to decrease during CEA injection. It is noticed that the volume of acid injected was sufficient as the skin continues to decrease until the end of the injection. The emulsified acid did not show any evidence of viscous diversion because no increasing trend in the skin is noticed.

The skin trend was validated using the production test from before and after the stimulation process. In this case, the production rate of liquids from this well after stimulation increased from 661 barrels/day to 4105 barrels/day. Therefore, the production test confirms the decreasing skin trend.

B8. Well 8

Treatment Description

This well is a horizontal well with a cased and perforated completion, as seen in the well diagram below. The actual acidizing treatment design was divided into two parts: 1) injection of 15% hydrochloric acid (HCl); and 2) injection of 22% carbonate emulsion acid (CEA). Each of the two parts of the treatments comprised of the acid stage followed by the fresh water displacement stage.

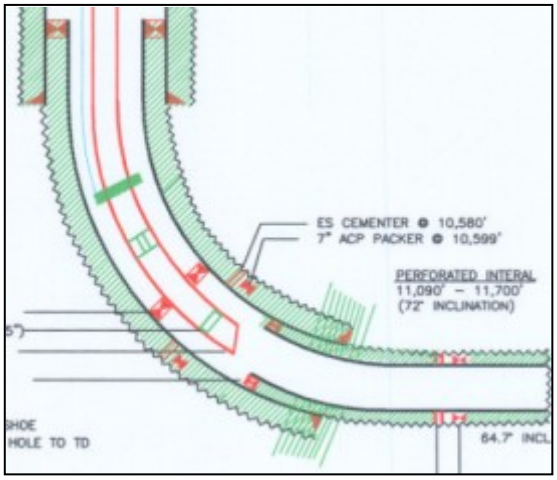

Fig. B22—Well diagram for Well 8.

The data for the reservoir, the wellbore, and the acid injection is shown in the tables below.

Table B22—Reservoir Properties for Well 8

Initial Reservoir Pressure, psi	2500
Formation Volume Factor	1.397
Porosity	0.17
Total Compressibility, 1/psi	3.50E-06
Formation Thickness, ft	161
Reservoir Fluid Viscosity, cp	0.51
Permeability, md	3
Anisotropy	0.1

Table B23—Wellbore Properties for Well 8

Wellbore Radius, in	3
Tubing Diameter, in	2.275
Relative Roughness	0.0001
Vertical Depth, ft	7767
Measured Depth, ft	10600
Horizontal length, ft	610
Well Fluid Density, lbm/ft3	63.58
Well Fluid Viscosity, cp	0.51

Table B24—Acid Injection Schedule for Well 8

Fluid Name	Volume Used, gal	Density, lb/ft3	Viscosity, cp	Friction Reducer
15% HCl	7318	67.3	0.51	0.1
Fresh water	880	63.6	0.51	0.1
22% CEA	18219	64.48	0.51	0.1
Fresh water	7707	63.21	0.51	0.1

Skin Monitoring Results

The figure below plots the measured injection rate, and the measured surface pressure recorded during the acidizing treatment.

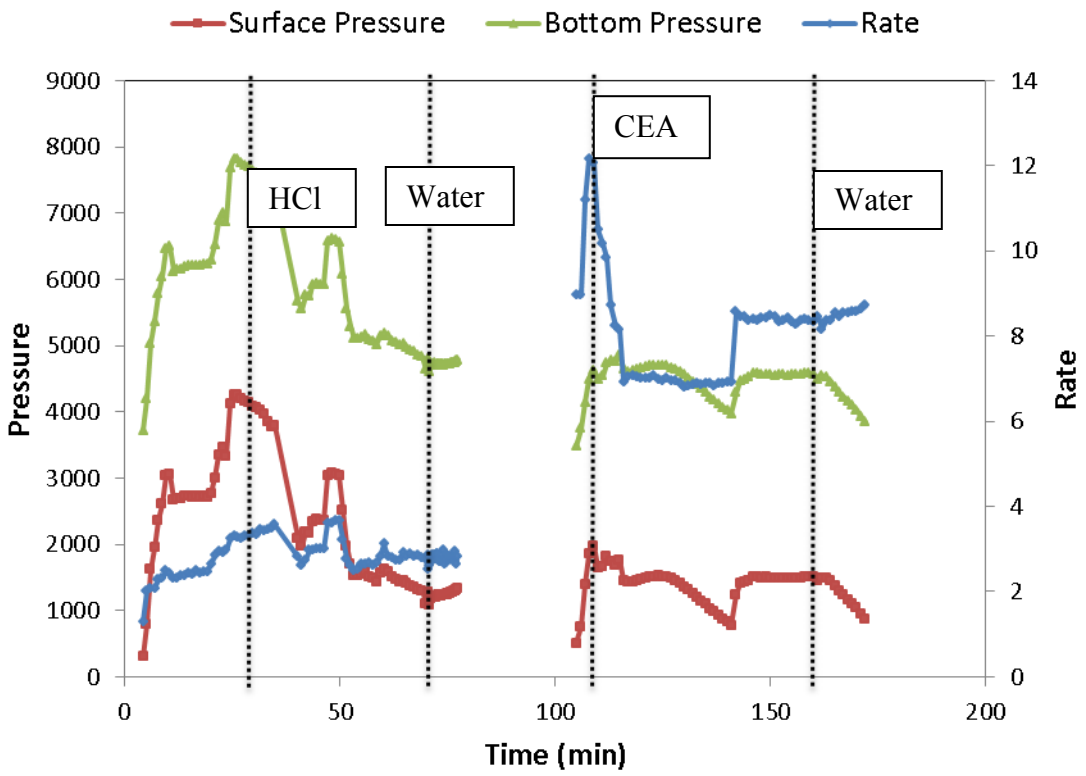

Fig. B23—Treatment data for Well 8.

In the figure above, the bottomhole pressure was calculated from the surface pressure. From the calculated bottomhole pressure and measured injection rate, the skin was calculated at each time step. The skin evolution during the acid job is shown in the figure below.

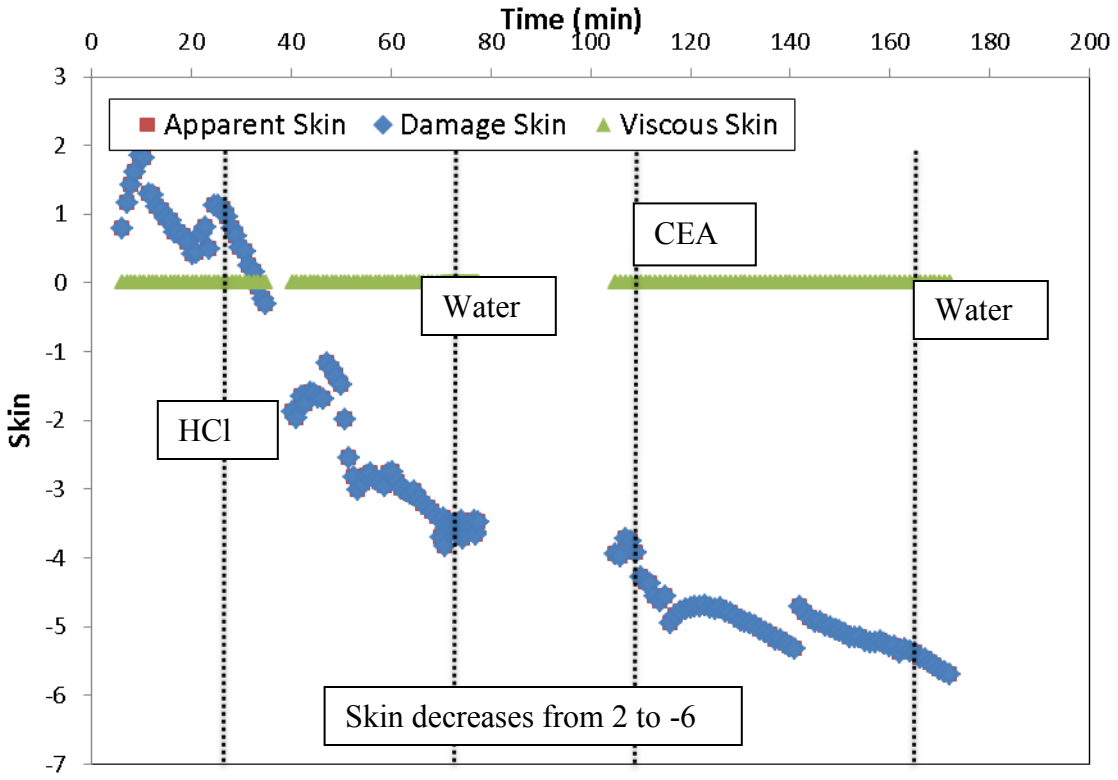

Fig. B24—Skin response for Well 8.

Discussion of Results

In the figure above, the skin begins to decrease from 1 to -4 during HCl injection and from -4 to -6 during CEA injection. It is noticed that CEA system did not contribute significantly to the stimulation process as most of the decline in skin resulted during the HCl injection. The emulsified acid did not show any evidence of viscous diversion because no increasing trend in the skin is noticed.

The skin trend was validated using the production test from before and after the stimulation process. In this case, the production rate of liquids from this well after stimulation increased to 8462 barrels/day.

B9. Well 9

Treatment Description

This well is a horizontal well with an open-hole lateral, as seen in the well diagram below. The actual acidizing treatment design was divided into two parts: 1) pumping 15% hydrochloric acid (HCl) and 22% carbonate emulsion acid (CEA)and through coil-tubing; 2) bullheading 22% carbonate emulsion acid (CEA) through tubing.

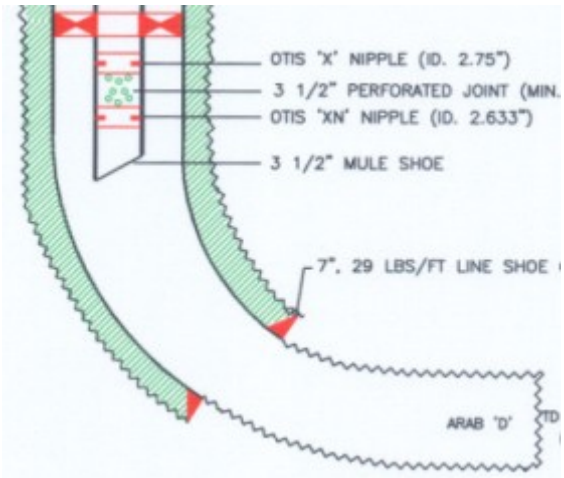

Fig. B25—Well diagram for Well 9.

The data for the reservoir, the wellbore, and the acid injection is shown in the tables below.

Table B25—Reservoir Properties for Well 9

Initial Reservoir Pressure, psi	2900
Formation Volume Factor	1.397
Porosity	0.16
Total Compressibility, 1/psi	3.50E-06
Formation Thickness, ft	50
Reservoir Fluid Viscosity, cp	0.51
Permeability, md	11
Anisotropy	0.1

Table B26—Wellbore Properties for Well 9

Wellbore Radius, in	3
Tubing Diameter, in	1.78
Relative Roughness	0.0001
Vertical Depth, ft	7574
Measured Depth, ft	12650
Horizontal length, ft	2483
Well Fluid Density, lbm/ft3	64.33
Well Fluid Viscosity, cp	0.51

Table B27—Acid Injection Schedule for Well 9

Fluid Name	Volume Used, gal	Density, lb/ft3	Viscosity, cp
15% HCl	49686	66.59	0.51
22% CEA	37500	65.8	0.51
Fresh water	2311	65.8	0.51
22% CEA	36988	65.8	0.51
Fresh water	11360	63.6	0.51

Skin Monitoring Results

The figure below plots the measured injection rate, and the measured pressure recorded during the acidizing treatment.

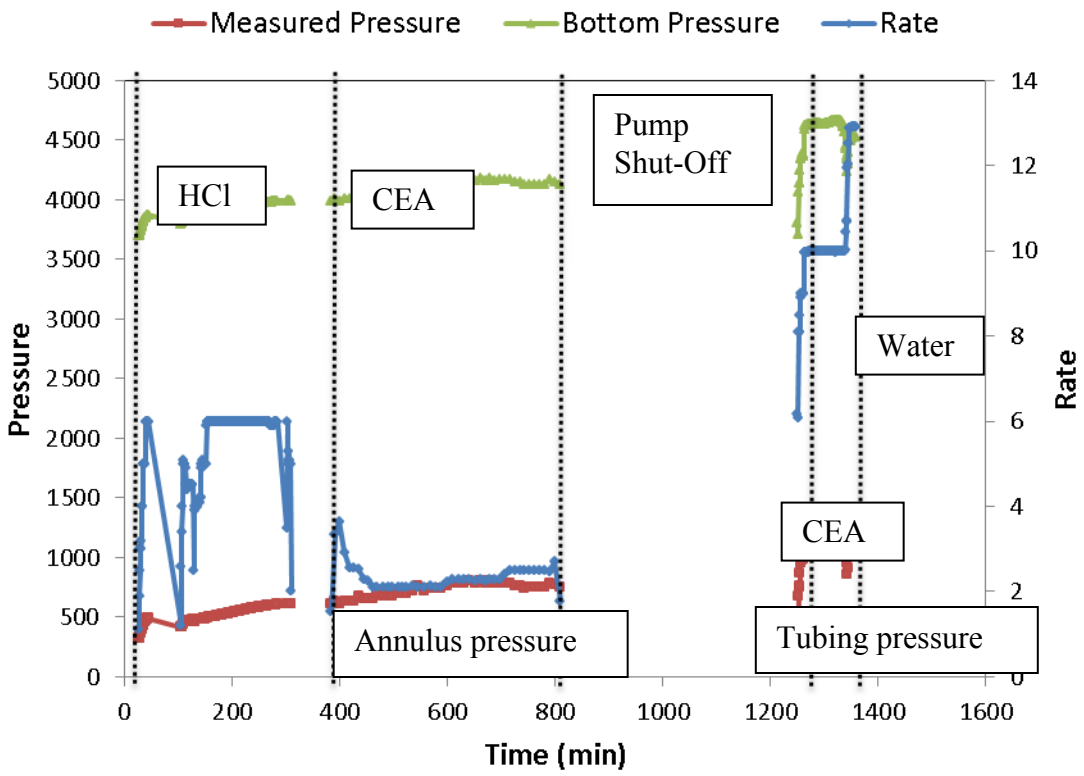

Fig. B26—Treatment data for Well 9.

In the figure above, the bottomhole pressure was calculated from the annulus pressure for the first part and from the tubing pressure for the second part. It is speculated that the pressure for the second part of the treatment may not recorded correctly. From the calculated bottomhole pressure and measured injection rate, the skin was calculated at each time step. The skin evolution during the acid job is shown in the figure below.

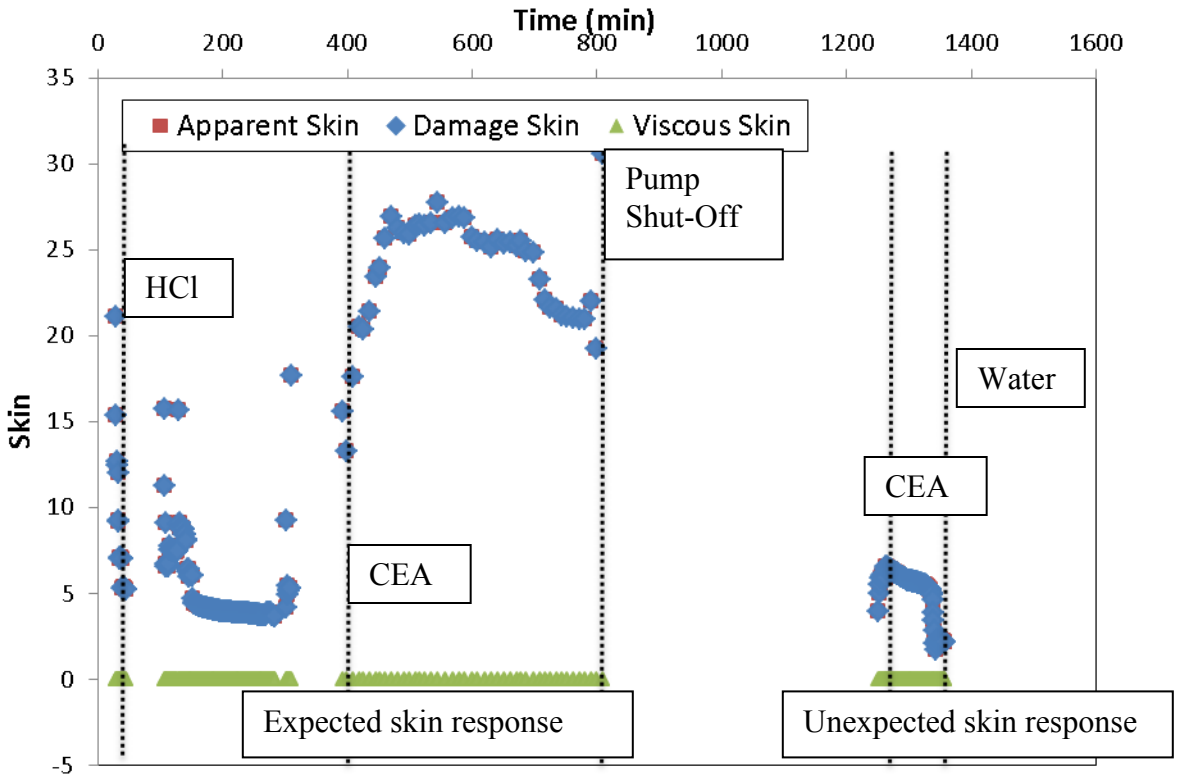

Fig. B27—Skin response for Well 9.

Discussion of Results

In the figure above, the skin begins to decrease during HCl injection, but the skin increases during CEA injection. Although the skin increases during the CEA injection, it was not due to viscous diversion. The CEA may have further damaged the well which is evident as the production rate of liquids from this well after stimulation decreased from 4517 barrels/day to 4225 barrels/day. However, the second part of the treatment with CEA system did not show a similar trend. The declining skin trend for the second part was not expected and may be due to incorrect pressure measurements.

B10. Well 10

Treatment Description

This well is a horizontal well with open-hole completion, as seen below in the well diagram. The actual acidizing treatment design comprised of 15% HCl wash to stimulate intervals between 11670-9814 ft and 9545-8326 ft. The acid was pumped through the coil-tubing while the coil-tubing was moved up and down over the target intervals.

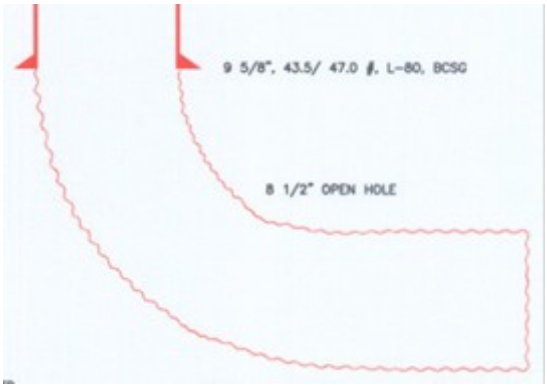

Fig. B28—Well diagram for Well 10.

The data for the reservoir, the wellbore, the acid injection, and the position of the coil-tubing is shown in the tables below.

Table B28—Reservoir Properties for Well 10

Initial Reservoir Pressure, psi	2700
Formation Volume Factor	1.397
Porosity	0.23
Total Compressibility, 1/psi	3.50E-06
Formation Thickness, ft	80
Reservoir Fluid Viscosity, cp	0.51
Permeability, md	10.3
Anisotropy	0.1

Table B29—Wellbore Properties for Well 10

Wellbore Radius, in	4.25
Tubing Diameter, in	1.68
Relative Roughness	0.0001
Vertical Depth, ft	7235
Measured Depth, ft	11530
Horizontal Length, ft	3468
Well Fluid Density, lbm/ft3	63.58
Well Fluid Viscosity, cp	0.51

Table B30—Acid Injection Schedule for Well 10

Fluid Name	Volume Used, gal	Density, lb/ft3	Viscosity, cp	Friction Reducer
HCl	54810	63.58	0.51	0.25

Table B31—Events with coil-tubing positions for Well 10

#	Event	Measured Depth, ft
1	Start Pump	11420
2	POOH	11135
3	POOH	9814
4	POOH	9545
5	POOH	8326
6	RIH	9545
7	RIH	9814
8	Stop Pump	11420

Skin Monitoring Results

The figure below plots the measured injection rate, and the measured surface pressure recorded during the acidizing treatment.

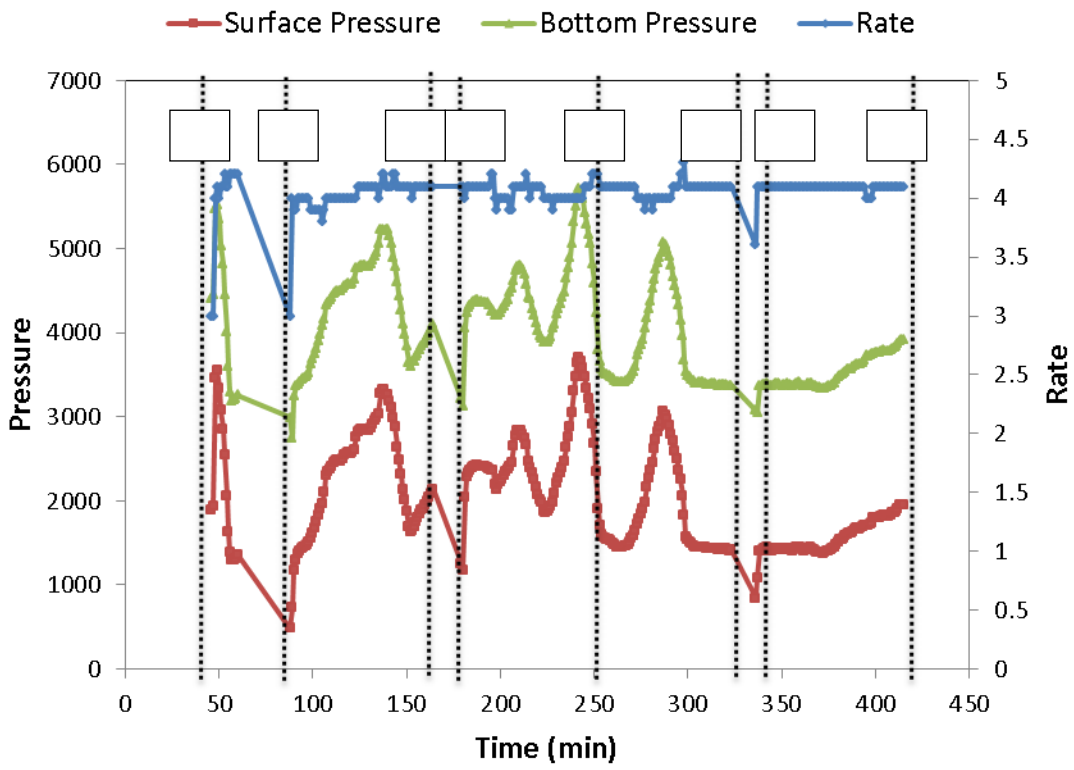

Fig. B29—Treatment data for Well 10.

In the figure above, the bottomhole pressure was calculated from the surface pressure. From the calculated bottomhole pressure and measured injection rate, the skin was calculated at each time step. Also, the numbered flags in the above figure represent the position of the coil-tubing in the wellbore as the acid is being pumped. The skin evolution during the acid job is shown in the figure below.

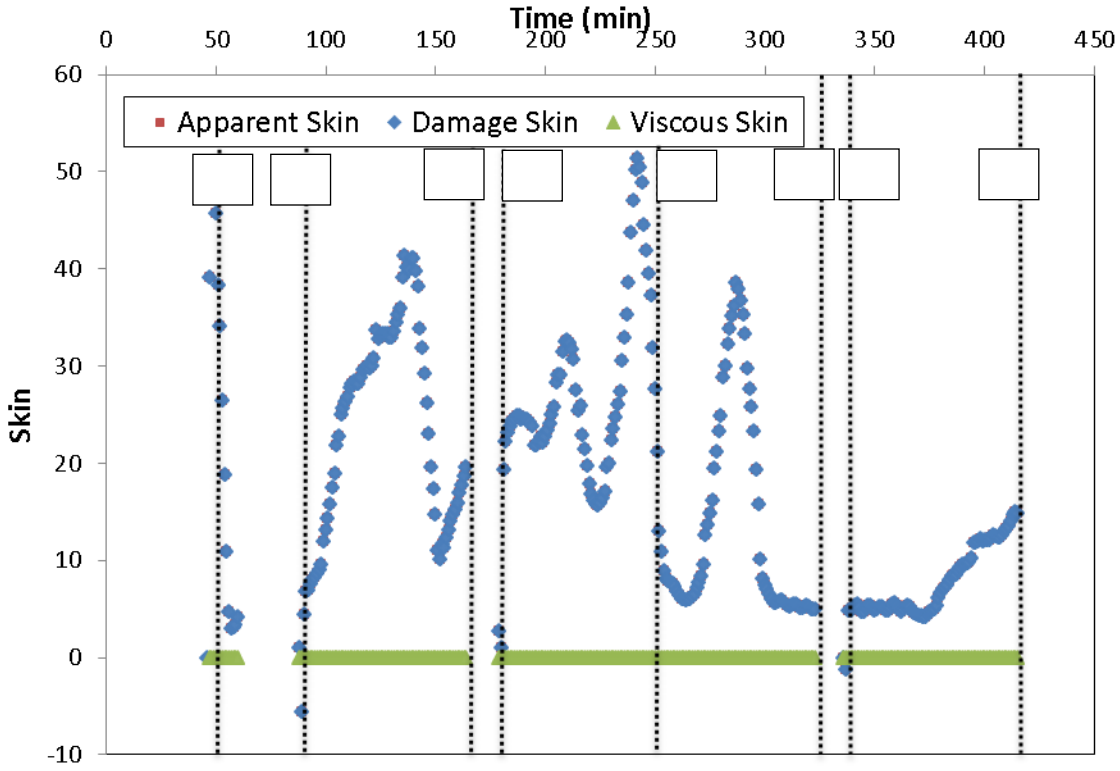

Fig. B30—Skin response for Well 10.

Discussion of Results

In the figure above, a very uncharacteristic wavy behavior of the skin factor is noticed. It is noticed that the pressure response to the injection rate is very undulating. The wavy skin behavior may be due the undulating pressure response recorded during

the treatment. This unexpected trend could be due to changes in frictional pressure drop and the movement of the coil-tubing.

The production rate of liquids from this well after stimulation increased from 1554 barrels/day to 2484 barrels/day. Although the production test confirms that the acidizing treatment was successful, the skin monitoring method was not able to capture the skin response correctly.

B11. Well 11

Treatment Description

This well is a horizontal well with an open-hole lateral, as seen below in the well diagram. The actual acidizing treatment design comprised of one injection stage of foamed acid through coil-tubing. Foamed acid is made up of hydrochloric acid in liquid phase and nitrogen in gas phase.

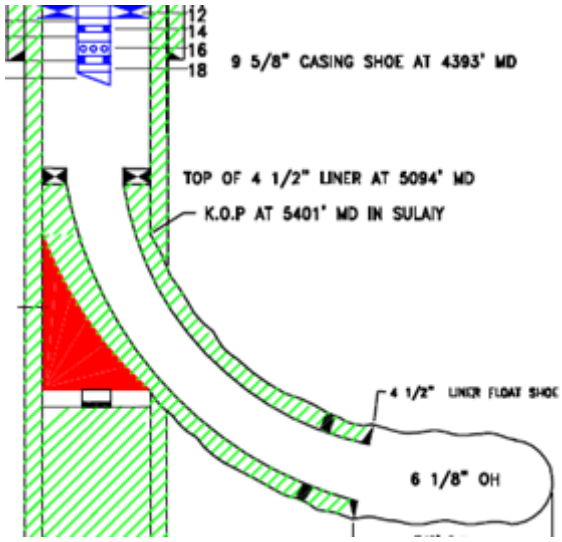

Fig. B31—Well diagram for Well 11.

The data for the reservoir, the wellbore, and the acid injection is shown in the tables below.

Table B32—Reservoir Properties for Well 11

Initial Reservoir Pressure, psi	3000
Formation Volume Factor	1.405
Porosity	0.13
Total Compressibility, 1/psi	3.50E-06
Formation Thickness, ft	32
Reservoir Fluid Viscosity, cp	0.47
Permeability, md	15
Anisotropy	1.5

Table B33—Wellbore Properties for Well 11

Wellbore Radius, in	3
Tubing Diameter, in	1.688
Relative Roughness	0.0001
Vertical Depth, ft	6227
Measured Depth, ft	7282
Horizontal Length, ft	754
Annulus Fluid Density, lbm/ft3	63.58
Well Fluid Viscosity, cp	0.47

Table B34—Acid Injection Schedule for Well 11

Fluid Name	Volume Used, gal	Density, lb/ft3	Viscosity, cp
Foamed Acid	19801.83	63.58	0.47
Water	1449.00	63.58	0.47

Skin Monitoring Results

The figure below plots the measured injection rate, and the measured annulus pressure recorded during the acidizing treatment.

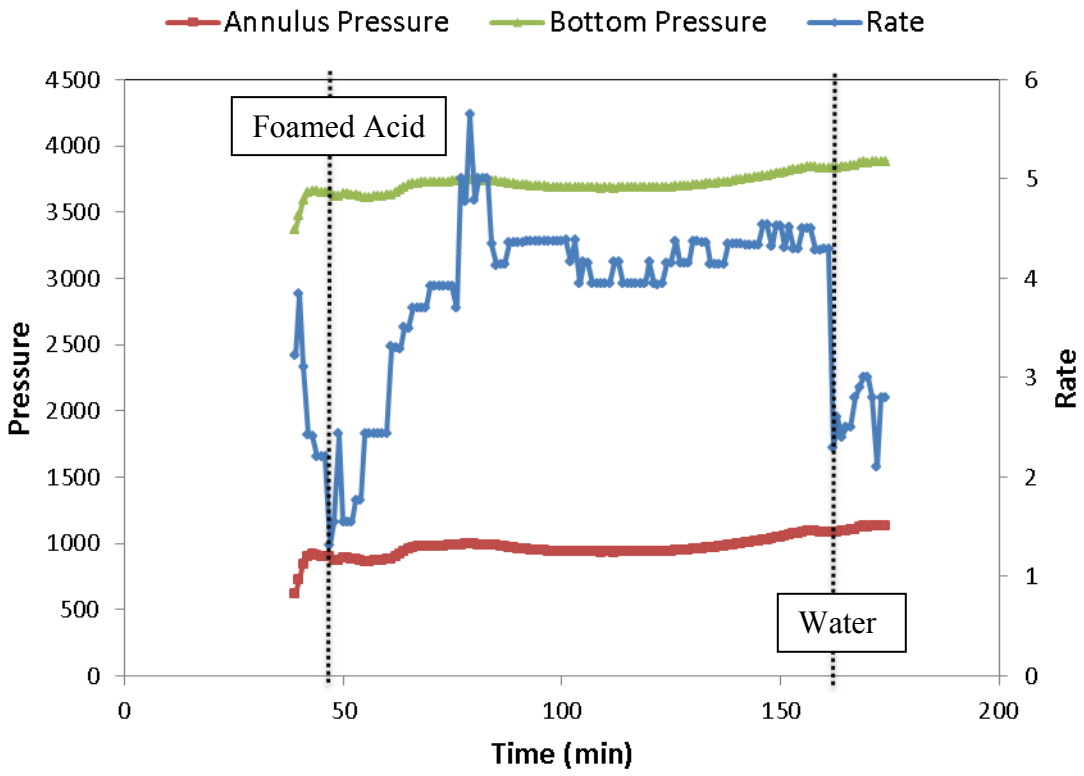

Fig. B32—Treatment data for Well 11.

In the figure above, the bottomhole pressure was calculated from the annulus pressure. For the foamed acid, the injection rate is calculated as the sum of liquid acid and nitrogen gas rates. The average foam quality was 46%. From the calculated bottomhole pressure and injection rate, the skin was calculated at each time step. The skin evolution during the acid job is shown in the figure below.

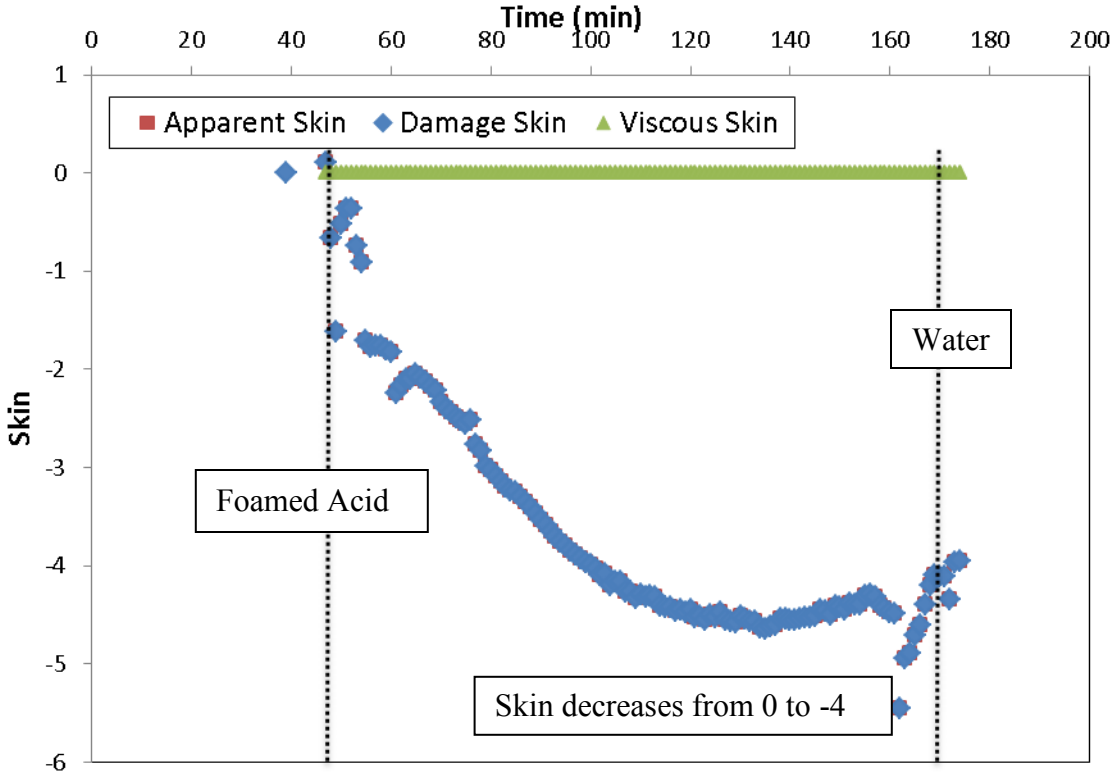

Fig. B33—Skin response for Well 11.

Discussion of Results

In the figure above, the skin begins to decrease when the foamed acid front enters the formation, and the skin value decreases from 0 to -4 by the end of acid injection. It is inferred that the volume of acid injected was sufficient as the skin continues to decrease until the end of the injection. The foamed acid did not show any evidence of viscous diversion as increasing trend in the skin is not noticed.

The skin trend was validated using the production test from before and after the stimulation process. In this case, the production rate of liquids from this well after stimulation increased to 1234 barrels/day. Therefore, the production test confirms the decreasing skin trend and it is clear that the acidizing treatment was successful.

B12. Well 12

Treatment Description

This well is a vertical well with cased and perforated completion, as seen below in the well diagram. The actual acidizing treatment design comprised of one injection stage of foamed acid through coil-tubing. Foamed acid is made up of hydrochloric acid in liquid phase and nitrogen in gas phase.

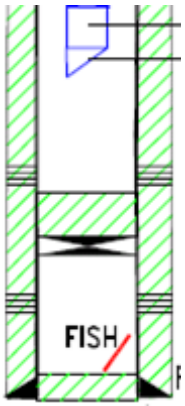

Fig. B34 —Well diagram for Well 12.

The data for the reservoir, the wellbore, and the acid injection is shown in the tables below.

Table B35—Reservoir Properties for Well 12

Initial Reservoir Pressure, psi	2500
Formation Volume Factor	1.546
Porosity	0.17
Total Compressibility, 1/psi	3.50E-06
Formation Thickness, ft	76
Reservoir Fluid Viscosity, cp	0.28
Permeability, md	3

Table B36—Wellbore Properties for Well 12

Wellbore Radius, in	6.366
Tubing Diameter, in	1.25
Relative Roughness	0.0006
Vertical Depth, ft	6420
Measured Depth, ft	6465
Well Fluid Density, lbm/ft3	63.5
Well Fluid Viscosity, cp	0.28

Table B37—Acid Injection Schedule for Well 12

Fluid Name	Volume Used, gal	Density, lb/ft3	Viscosity, cp
Foamed Acid	2293.2	63.5	0.28
Water	1407	63.5	0.28

Skin Monitoring Results

The figure below plots the measured injection rate, and the measured annulus pressure recorded during the acidizing treatment.

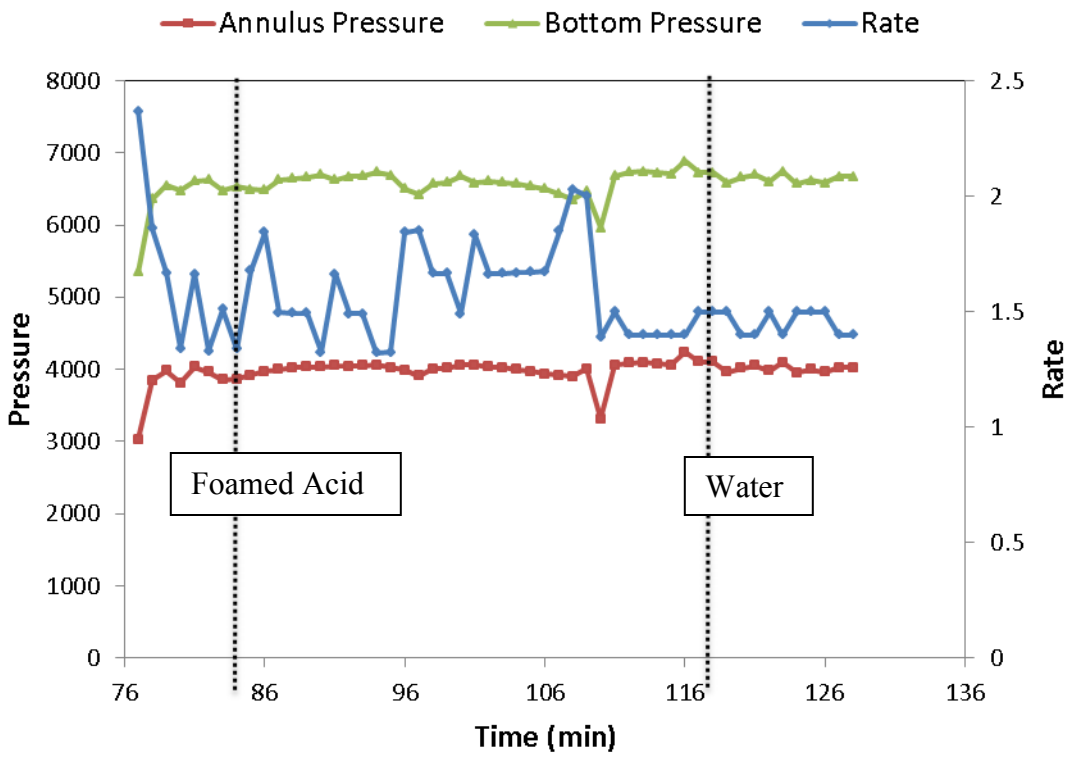

Fig. B35—Treatment data for Well 12.

In the figure above, the bottomhole pressure was calculated from the annulus pressure. For the foamed acid, the injection rate is calculated as the sum of liquid acid and nitrogen gas rates. The average foam quality was 59%. From the calculated bottomhole pressure and injection rate, the skin was calculated at each time step. The skin evolution during the acid job is shown in the figure below.

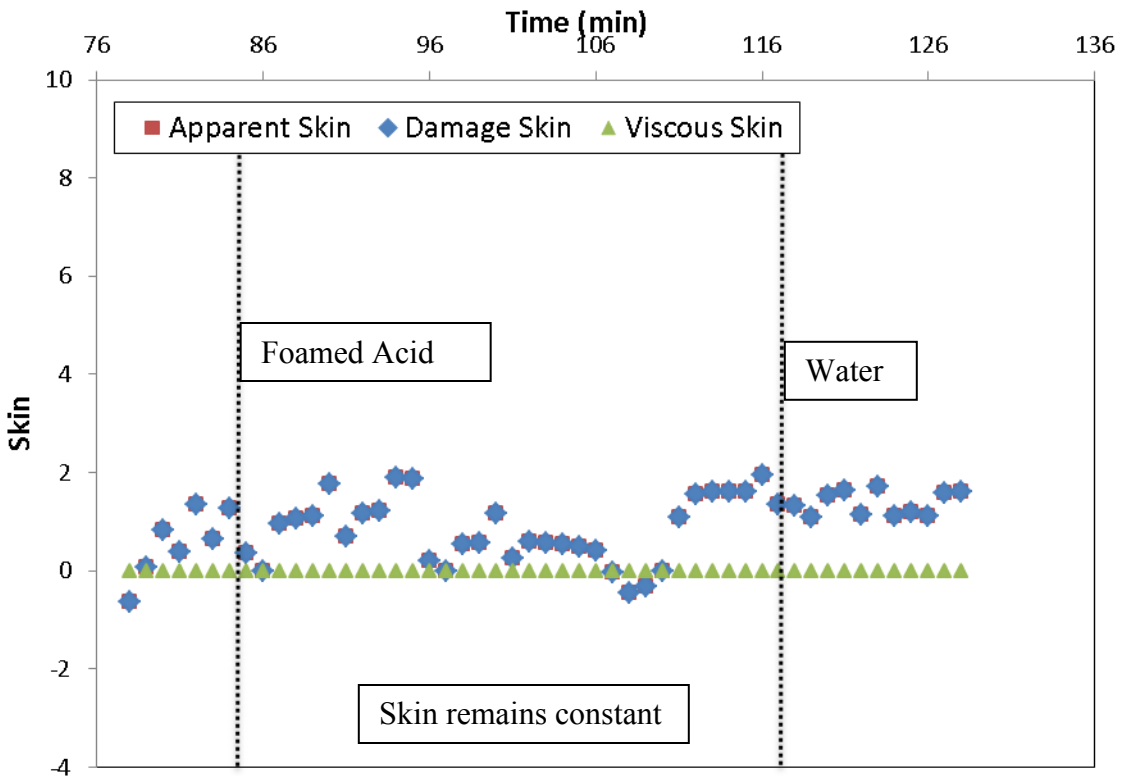

Fig. B36—Skin response for Well 12.

Discussion of Results

In the figure above, the skin remains almost constant throughout the treatment. The foamed acid was injected only for 30 minutes and therefore, the acid volume injected was not sufficient to stimulate the well. Furthermore, the foamed acid did not show any evidence of viscous diversion as increasing trend in the skin is not noticed.

In this case, the production rate of liquids from this well after stimulation increased to only 20 barrels/day. Therefore, the production test indicates that the acidizing treatment was not very beneficial.

.

B13. Well 13

Treatment Description

This well is a horizontal well with an open-hole lateral, as seen below in the well diagram. The actual acidizing treatment design comprised of injection of 15% hydrochloric acid followed by injection of foamed acid through coil-tubing. Foamed acid is made up of hydrochloric acid in liquid phase and nitrogen in gas phase.

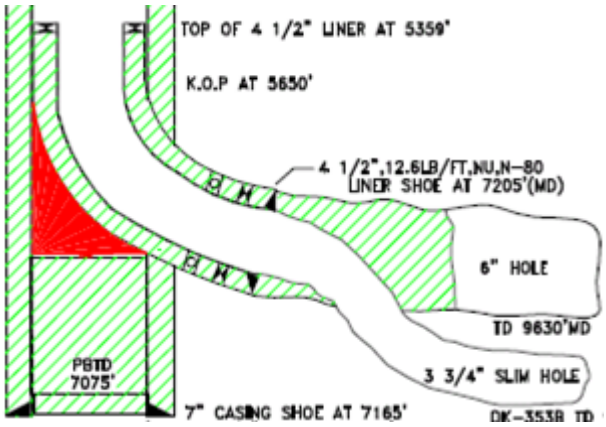

Fig. B37—Well diagram for Well 13.

The data for the reservoir, the wellbore, and the acid injection is shown in the tables below.

Table B38—Reservoir Properties for Well 13

Initial Reservoir Pressure, psi	2500
Formation Volume Factor	1.405
Porosity	0.13
Total Compressibility, 1/psi	3.50E-06
Formation Thickness, ft	28
Reservoir Fluid Viscosity, cp	0.47
Permeability, md	3
Anisotropy	0.1

Table B39—Wellbore Properties for Well 13

Wellbore Radius, in	1.875
Tubing Diameter, in	1.688
Relative Roughness	0.0001
Vertical Depth, ft	7165
Measured Depth, ft	9626
Horizontal Length, ft	2404
Well Fluid Density, lbm/ft3	63.58
Well Fluid Viscosity, cp	0.47

Table B40—Acid Injection Schedule for Well 13

Fluid Name	Volume Used, gal	Density, lb/ft3	Viscosity, cp
15% HCl	24078.60	63.58	0.47
Foamed Acid	20655.60	63.58	0.47

Skin Monitoring Results

The figure below plots the measured injection rate, and the measured annulus pressure recorded during the acidizing treatment.

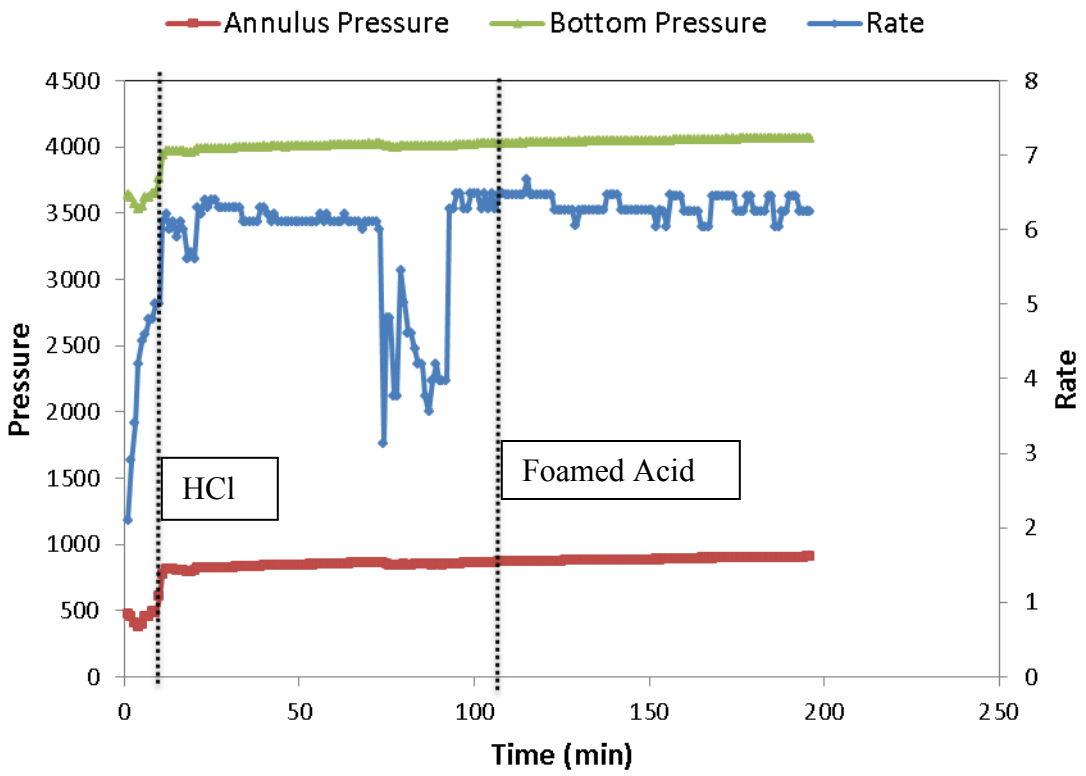

Fig. B38—Treatment data for Well 13.

In the figure above, the bottomhole pressure was calculated from the annulus pressure. For the foamed acid, the injection rate is calculated as the sum of liquid acid and nitrogen gas rates. The average foam quality was 48%. From the calculated bottomhole pressure and injection rate, the skin was calculated at each time step. The skin evolution during the acid job is shown in the figure below.

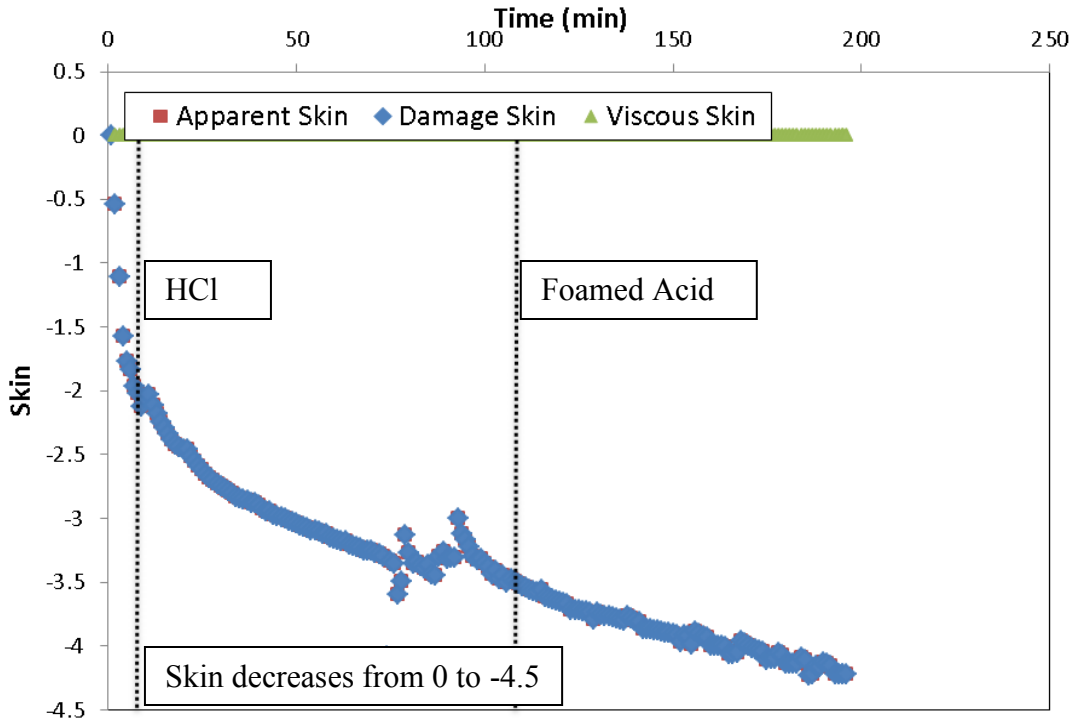

Fig. B39—Skin response for Well 13.

Discussion of Results

In the figure above, the skin begins to decrease during the HCl acid injection, and continues to decrease during the foamed acid injection. The skin value decreases from 0 to -4.5 by the end of treatment. It is noticed that the volume of acid injected was sufficient as the skin continues to decrease until the end of the injection. However, the foamed acid did not show any evidence of viscous diversion as increasing trend in the skin is not noticed.

The skin trend was validated using the production test from before and after the stimulation process. In this case, the production rate of liquids from this well after stimulation increased 107 to 1327 barrels/day. Therefore, the production test confirms the decreasing skin trend and it is clear that the acidizing treatment was successful.

B14. Well 14

Treatment Description

This well is a horizontal well with an open-hole lateral, as seen below in the well diagram. The actual acidizing treatment design comprised of injection of 15% hydrochloric acid followed by injection of foamed acid through coil-tubing. Foamed acid is made up of hydrochloric acid in liquid phase and nitrogen in gas phase.

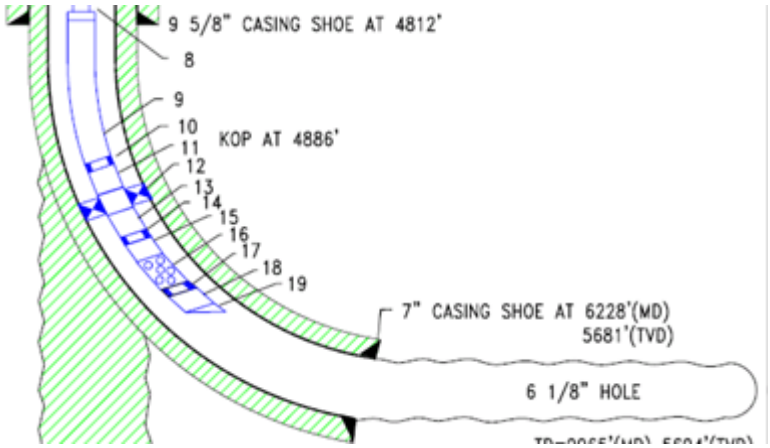

Fig. B40—Well diagram for Well 14.

The data for the reservoir, the wellbore, and the acid injection is shown in the tables below.

Table B41—Reservoir Properties for Well 14

Initial Reservoir Pressure, psi	1400
Formation Volume Factor	1.405
Porosity	0.13
Total Compressibility, 1/psi	3.50E-06
Formation Thickness, ft	26
Reservoir Fluid Viscosity, cp	0.47
Permeability, md	2
Anisotropy	0.1

Table B42—Wellbore Properties for Well 14

Wellbore Radius, in	3
Tubing Diameter, in	1.688
Relative Roughness	0.0001
Vertical Depth, ft	5694
Measured Depth, ft	6228
Horizontal Length, ft	3876
Well Fluid Density, lbm/ft3	63.58
Well Fluid Viscosity, cp	0.47

Table B43—Acid Injection Schedule for Well 14

Fluid Name	Volume Used, gal	Density, lb/ft3	Viscosity, cp
15% HCl	58401.00	63.58	0.47
Foamed Acid	66287.13	63.58	0.47
Water	697.20	63.58	0.47

Skin Monitoring Results

The figure below plots the measured injection rate, and the measured annulus pressure recorded during the acidizing treatment.

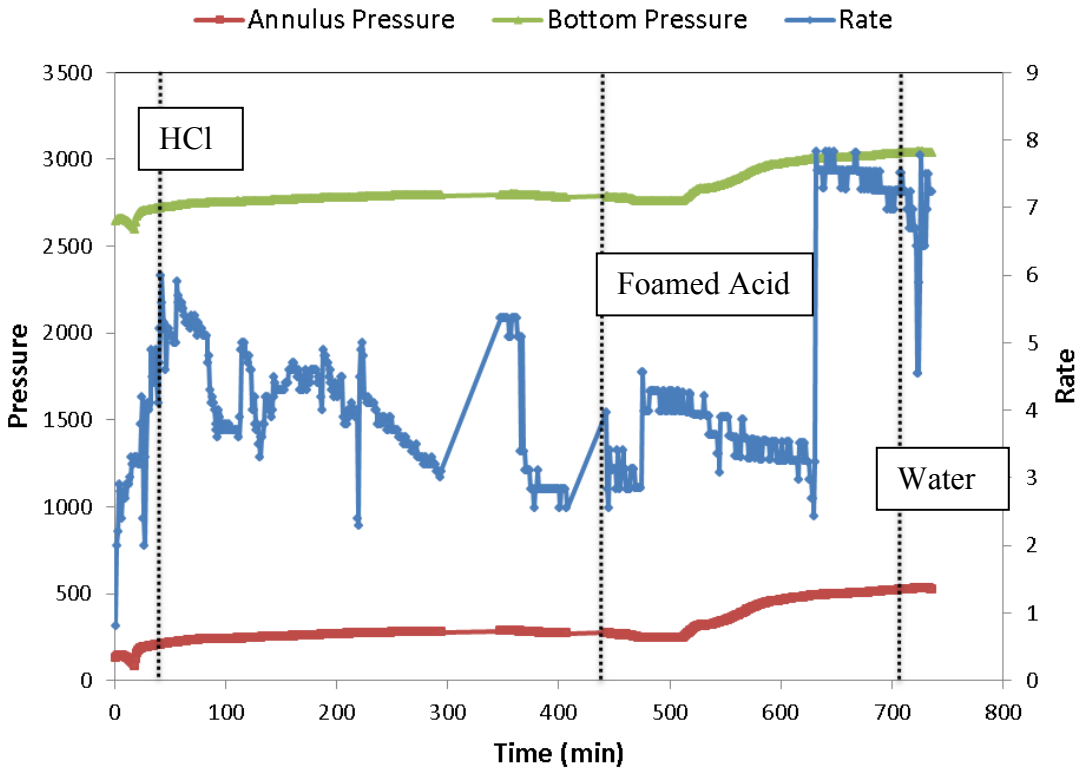

Fig. B41—Treatment data for Well 14.

In the figure above, the bottomhole pressure was calculated from the annulus pressure. For the foamed acid, the injection rate is calculated as the sum of liquid acid and nitrogen gas rates. The average foam quality was 36%. From the calculated bottom-hole pressure and injection rate, the skin was calculated at each time step. The skin evolution during the acid job is shown in the figure below.

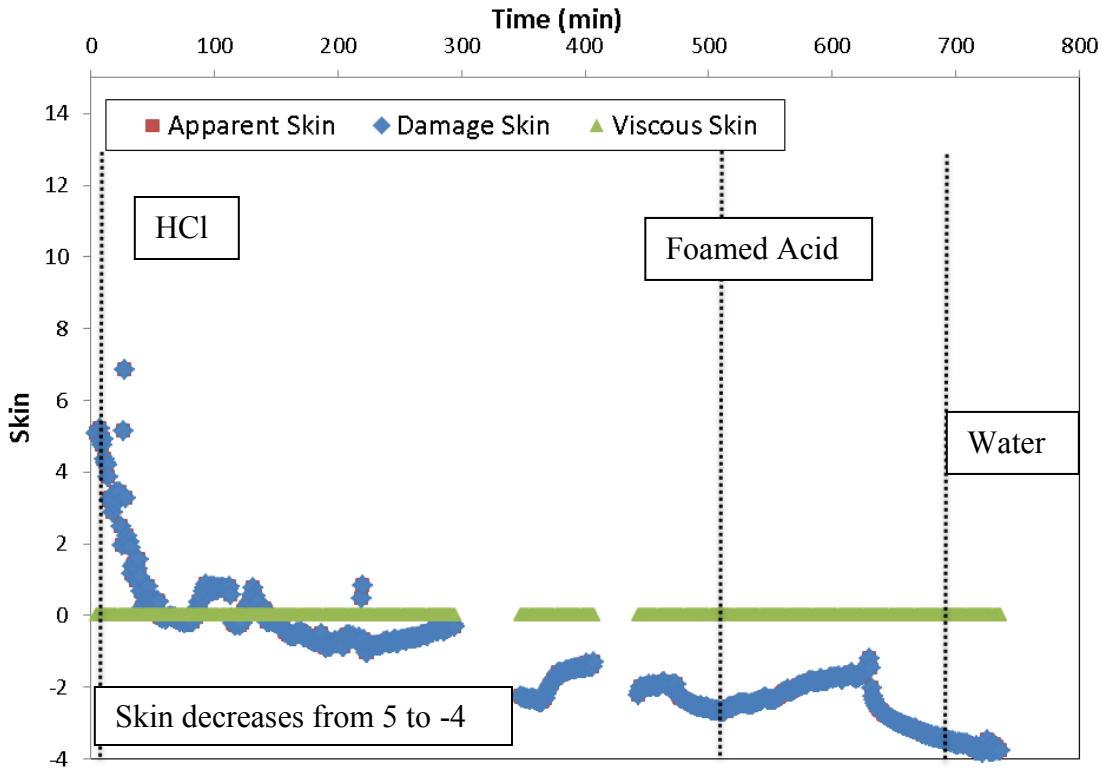

Fig. B42—Skin response during for Well 14.

Discussion of Results

In the figure above, the skin begins to decrease during the HCl acid injection, but flattens during the foamed acid injection. The skin value decreases from 5 to -4 by the end of acid injection. It is noticed that the stimulation is mostly contributed by injection of HCl. The foamed acid did not show any evidence of viscous diversion or stimulation.

The skin trend was validated using the production test from before and after the stimulation process. In this case, the production rate of liquids from this well after stimulation increased 2682 to 3162 barrels/day. Therefore, the production test confirms the decreasing skin trend.

APPENDIX C

CALCULATION FOR EXAMPLE CASE

For the example case, the well is assumed to be a vertical well. The wellbore properties, reservoir properties, and pump schedule are shown in **Tables C1 through C3.**

Table C1—Reservoir Properties for Example Case

Initial Reservoir Pressure, psi	3200
Formation Volume Factor	1
Porosity	0.18
Total Compressibility, 1/psi	3.50E-06
Formation Thickness, ft	306
Reservoir Fluid Viscosity, cp	0.51
Permeability, md	100

Table C2—Wellbore Properties for Example Case

Wellbore Radius, in	2
Tubing Diameter, in	2.99
Relative Roughness	0.0001
Vertical Depth, ft	5000
Measured Depth, ft	5000
Annulus Fluid Density, lbm/ft3	64.35
Well Fluid Viscosity, cp	0.51

Table C3—Acid Injection Schedule for Example Case

Fluid Name	Volume Used, gal	Density, lb/ft3	Viscosity, cp
Spacer	2478	65	0.51

The tubing in the wellbore is initially filled with acid. The acid is pushed into the formation and being displaced in the tubing by an inert fluid (spacer) that is being pumped. The initial skin factor is assumed to be 30. The treatment data, the calculated bottomhole pressure, and the calculated skin factors are shown below in **Table C4.**

Table C4—Treatment Data and Result for Example Case

Time (min)	Rate (bpm)	Surface Pressure (psi)	Bottom Pressure (psi)	Damage Skin	Apparent Skin	Viscous Skin
1	3.36	1436	3579.3	30.00		
2	3.39	1421	3564.5	25.57	25.57	0.00
3	2.00	1200	3401.1	22.93	22.93	0.00
4	3.43	1342	3486.3	18.27	18.27	0.00
5	3.48	1341	3484.2	17.60	17.60	0.00

The following equations indicate the calculation steps required to estimate the skin factors and the bottomhole pressure at point 5 (time = 5 minutes).

Bottomhole Pressure Calculation

The total acid volume injected for 5 minutes is given by

$$V_{total} = \sum_{i=2}^{5} (q_i \times (t_i - t_{i-1}))$$

$$= \left[3.39 \times (2-1) + 2 \times (3-2) + 3.43 \times (4-3) + 3.48 \times (5-4)\right] \times 5.615$$

$$= 69.065 \ \ ft^3 . \quad \text{.....(C1)}$$

The length of the column of the new injected fluid in the tubing is

$$Length_{new} = \frac{V_{total} \times 144 \times 4}{\pi \times (d_{tube})^2} = \frac{69.065 \times 144 \times 4}{\pi \times (2.992)^2}$$

$$= 1414.221 \ ft . \ \ldots\ldots\ldots\ldots\ldots\ldots\ldots\ldots\ldots\ldots\ldots\ldots\ldots\ldots\ldots\ldots\ldots\ldots(C2)$$

and the length of the column of the existing wellbore fluid is

$$Length_{old} = TVD - Length_{new} = 5000 - 1414.398 \ = 3585.779 \ \ ft . \ \ldots\ldots\ldots\ldots(C3)$$

Therefore, the hydrostatic pressure in the tubing is given by

$$\Delta P_{PE} = \frac{g}{g_c} \times (\rho_{new} \times Length_{new} + \rho_{old} \times Length_{old})$$

$$= 0.006939 \times (65.00 \times 1414.221 + 64.35 \times 3585.779)$$

$$= 2239.001 \ \ psi . \ \ldots\ldots\ldots\ldots\ldots\ldots\ldots\ldots\ldots\ldots\ldots\ldots\ldots\ldots\ldots\ldots\ldots\ldots(C4)$$

In order to calculate the frictional pressure drop, the Reynolds number is calculated first to understand the flow regime and estimate the frictional factor. The Reynolds number for the injected fluid in the tubing is

$$N_{RE} = \frac{1.48 \times \rho \times q}{\mu \times d_{tube}}$$

$$= \frac{1.48 \times 65 \times (3.48 \times 1440)}{0.51 \times 2.992}$$

$$= 315925.8 . \ \ldots\ldots\ldots\ldots\ldots\ldots\ldots\ldots\ldots\ldots\ldots\ldots\ldots\ldots\ldots\ldots\ldots\ldots\ldots\ldots(C5)$$

Similarly, the Reynolds number for the wellbore fluid is 312766.5. Since the Reynolds numbers are greater than 2000, the flow in the tubing is turbulent. The friction factor is calculated by

$$f_f = \left[-4\log\left\{ \frac{0.0001}{3.7065} - \frac{5.0452}{315925.8}\log\left[\frac{0.0001^{1.1098}}{2.8257} + \left(\frac{7.149}{315925.8} \right)^{0.8981} \right] \right\} \right]^{-2}$$

$$= 3.84 \times 10^{-3}. \quad \text{.....(C6)}$$

Similarly, the friction factor for the wellbore fluid is 3.86×10^{-3}. Therefore, the frictional pressure drop is

$$\Delta P_f = \frac{7.355 \times 10^{-7} \times q^2 \times \left(\rho_{new} \times Length_{new} \times f_{fn} + \rho_{old} \times Length_{old} \times f_{fo} \right)}{d_{tube}^5}$$

$$= \left(65.00 \times 1414.221 \times 3.84 \times 10^{-3} + 64..35 \times 3585.779 \times 3.86 \times 10^{-3} \right)$$

$$\times \frac{7.355 \times 10^{-7} \times (3.48 * 1440)^2}{(2.992)^5}$$

$$= 95.799 \ psi. \quad \text{.....(C7)}$$

Therefore, the bottomhole pressure is

$$p_{wf} = p_{sf} + \Delta p_{PE} - \Delta p_f$$

$$= 1341 + 2239 - 95.8$$

$$= 3484.2 \ psi. \quad \text{.....(C8)}$$

Apparent Skin Calculation

The slope of the inverse injectivity and superposition time function line is calculated by

$$m = \frac{162.6 \cdot B \cdot \mu}{k \cdot h}$$

$$= \frac{162.6 \times 1 \times 0.51}{100 \times 306}$$

$$= 0.00271. \quad \text{.....(C9)}$$

and the superposition time function is given by

$$\Delta t_{\text{sup}} = \sum_{j=1}^{N} \frac{q_j - q_{j-1}}{q_N} \cdot \log\left(t_N - t_{j-1}\right)$$

$$= \frac{3.36}{3.48}\log\left(\frac{5}{60}\right) + \frac{3.39-3.36}{3.48}\log\left(\frac{5-1}{60}\right)$$

$$+ \frac{2.00-3.39}{3.48}\log\left(\frac{5-2}{60}\right) + \frac{3.43-2.00}{3.48}\log\left(\frac{5-3}{60}\right)$$

$$+ \frac{3.48-3.43}{3.48}\log\left(\frac{5-4}{60}\right)$$

$$= -1.165. \quad \text{.....(C10)}$$

Therefore, the intercept is given by

$$b = \frac{p_{wf} - p_i}{q_i} - m \cdot \Delta t_{\text{sup}}$$

$$= \frac{3484.2 - 3200}{3.48 \times 1440} - 0.00271 \times (-1.165)$$

$$= 0.0599. \quad \text{.....(C11)}$$

and the apparent skin factor is

$$s_{Apparent} = \frac{1}{0.868}\left(\frac{b}{m} - \log\left(\frac{k}{\phi \cdot \mu \cdot c_t \cdot r_w^2}\right) + 3.23\right)$$

$$= \frac{1}{0.868}\left(\frac{0.0599}{0.00271} - \log\left(\frac{100}{0.18 \cdot 0.51 \cdot 3.5 \times 10^{-6} \cdot \left(\frac{2}{12}\right)^2}\right) + 3.23\right)$$

$$= 17.60. \quad \text{.....(C12)}$$

Viscous Skin Calculation

The radius of penetration of acid is

$$r_i = \sqrt{\frac{V_i}{\pi \cdot \phi \cdot h} + r_w^{\ 2}}$$

$$= \sqrt{\frac{69.065}{\pi \cdot 0.18 \cdot 306} + \left(\frac{2}{12}\right)^2}$$

$$= 0.654 \ \ ft \, . \ \ldots\ldots\ldots\ldots\ldots\ldots\ldots\ldots\ldots\ldots\ldots\ldots\ldots\ldots\ldots\ldots\ldots\ldots\ldots\ldots\ldots \text{(C13)}$$

and the viscous skin is

$$s_{viscous} = \sum_{i=1}^{n} \frac{\mu_i}{\mu_{res}} \ln\left(\frac{r_i}{r_{i-1}}\right) - \ln\left(\frac{r_n}{r_0}\right)$$

$$= \frac{0.51}{0.51} \ln\left(\frac{0.654}{2/12}\right) - \ln\left(\frac{0.654}{2/12}\right)$$

$$= 0.00 \, . \ \ldots\ldots\ldots\ldots\ldots\ldots\ldots\ldots\ldots\ldots\ldots\ldots\ldots\ldots\ldots\ldots\ldots\ldots\ldots\ldots\ldots \text{(C14)}$$

Damage Skin Calculation

Therefore, the damage skin is given by

$$s_{damage} = s_{apparent} - s_{viscous}$$

$$= 17.60 - 0.00$$

$$= \ 17.60 \, . \ \ldots\ldots\ldots\ldots\ldots\ldots\ldots\ldots\ldots\ldots\ldots\ldots\ldots\ldots\ldots\ldots\ldots\ldots\ldots \text{(C15)}$$

VITA

Name:	Nimish Dinesh Pandya
Address:	3116 Texas A&M University – 714 Richardson Building, College Station, TX 77843-3116
Email Address:	nimishpandya@gmail.com
Education:	M.S., Petroleum Engineering, Texas A&M University, 2012 B.S., Chemical Engineering, Georgia Institute of Technology, 2007

This thesis was typed by the author.